SURROGATE FORMULATION BASED ON CHEMICAL FUNCTIONAL GROUP ANALYSIS

by

Stuart Nates

Bachelor of Science
University of South Carolina

Submitted in Partial Fulfillment of the Requirements

For the Degree of Master of Science in

Mechanical Engineering

College of Engineering and Computing

University of South Carolina

2019

Accepted by:

Sang Hee Won, Director of Thesis

Tanvir Farouk, Reader

Cheryl L. Addy, Vice Provost and Dean of the Graduate School

ACKNOWLEDGEMENTS

I'd like to thank my advisor Dr Sang Hee Won for continuously funding this research through the long process of discovering the best method for developing this approach. This work would not have been possible without my family, friends, coworkers, and everyone who has acted as a sounding board and helped me determine how to overcome several issues that were overcome while developing this approach.

ABSTRACT

Chemical kinetic characteristics of real fuels exhibit high-dimensional complexity due to the excessive number of molecules and molecular classes. As a method of projecting this high-dimensional complexity, which is pertinent to real fuels, to the low-dimensional description, either a surrogate approach or detailed experiments have been utilized, can guide the construction of chemical kinetic models for real fuel. Although the validity of the surrogate approach has been extensively demonstrated by a wide range of canonical experiments for whole fuel/air mixtures, the use of empirical fuel property indicators still worries whether or not the surrogate mixture truly captures the more complex chemical behaviors coupled with fuel physical properties (e.g. distillation). Particularly, a recent experiment has shown that the near-limit combustion behaviors (e.g. lean blow off in gas turbine combustor) are strongly governed by the chemical characteristics of the front (light) end in fuel boiling characteristics. Thus, it is of importance to develop an alternative approach, which can fundamentally characterize fuel chemical properties along the fuel distillation curve. Using Nuclear Magnetic Resonance (NMR) spectra, it is possible to quantify the specific chemical functional groups present in a sample. To demonstrate the applicability of chemical functional group approach in conjunction with NMR spectra interpretation, a surrogate formulation approach based on NMR spectra is demonstrated by using a 12-component model fuel and a known fuel and comparing the synthetic NMR spectra between target fuels and surrogate mixtures.

TABLE OF CONTENTS

LIST OF TABLES

LIST OF FIGURES

LIST OF SYMBOLS

A	The A coefficient from Antoine's Equation
B	The B coefficient from Antoine's Equation
C	The C coefficient from Antoine's Equation
C_i	Synthetic 13C NMR Spectra of each component
Cn	Synthetic 13C NMR Spectra
CI	Integrated Synthetic 13C NMR Spectra.
CIo	Integrated 13C NMR Spectra of the Target Fuel
Co	13C NMR Spectra of the Target Fuel
eq1-6	Residual of each NMR spectra and distillation temperatures
G	Total residual
H	Synthetic 1H NMR Spectra
H_i	Synthetic 1H NMR Spectra of each component
HI	Integrated Synthetic 1H NMR Spectra
HIo	Integrated 1H NMR Spectra of the Target Fuel
Ho	1H NMR Spectra of the Target Fuel
Pv	Vapor pressure of mixture
Pvap	Vapor pressure of each component
Ptotal	Total pressure
P_i	Partial pressure of each component
T	Temperature at which to determine vapor pressure

T10 Temperature at which 10% of the liquid fuel has boiled

T20 Temperature at which 20% of the liquid fuel has boiled

T50 Temperature at which 50% of the liquid fuel has boiled

T90 Temperature at which 90% of the liquid fuel has boiled

T10a Measured temperature at which 10% of the liquid target fuel has boiled

T20a Measured temperature at which 20% of the liquid target fuel has boiled

T50a Measured temperature at which 50% of the liquid target fuel has boiled

T90a Measured temperature at which 90% of the liquid target fuel has boiled

x_i Mole fraction of i^{th} component

xg_i Gas phase mole fraction of each component

LIST OF ABBREVIATIONS

CN .....Cetane Number

CPT.....Combustion Property Target

DCN..... Derived Cetane Number

FP ..... Flash Point

H/C .....Hydrogen to Carbon Ratio

LBO ..... Lean Blow Out

MW.....Molecular Weight

NMR.....Nuclear Magnetic Resonance

TSI.....Threshold Sooting Index

CHAPTER 1

INTRODUCTION

For the past 100 years, the combustion of fossil fuels have been the dominate source of the worlds energy. [1] Fossil fuels is the overarching term that has been given to many non-renewable sources of fuels which include coal, petroleum, and natural gas. Figure 1.1 shows a chart of how the US has historically generated energy and it is clear since the very beginning that combustion has been the primary source.[1] As the US shifted from wood to various fossil fuels, it enabled a large increase of the amount of energy generated.

But as fossil fuels became more widespread, depletion became a concern for many. The world has a limited supply of fossil fuels and fossil fuels produce greenhouse gases which contribute to climate change therefore societies started searching for alternative sources to meet the demand for energy. This interest in alternative and renewable fuels have led to several major methods of producing energy such as biofuel, solar, wind, tidal, geothermal, nuclear, and hydroelectric methods. The chart in Figure 1.2 shows a breakdown of U.S. energy consumption by energy source in 2017. Roughly 80% of all of the energy consumed in the US that year was from of fossil fuels.[2] This amount is not predicted to decrease anytime in the next several decades. Because such a large portion of the US energy comes from fossil fuels, there is a significant need to understand and improve upon how fossil fuels are used.

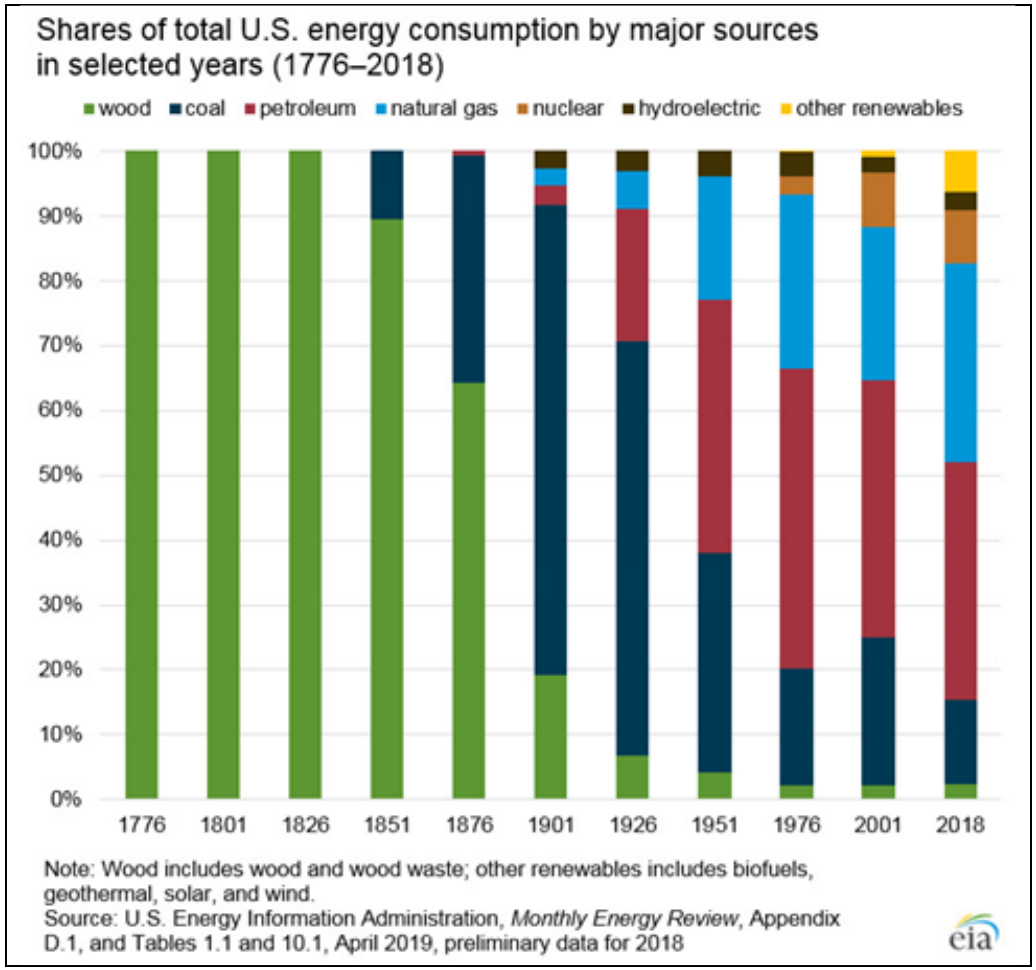

Figure 1.1: History of How the US Has Generated Energy

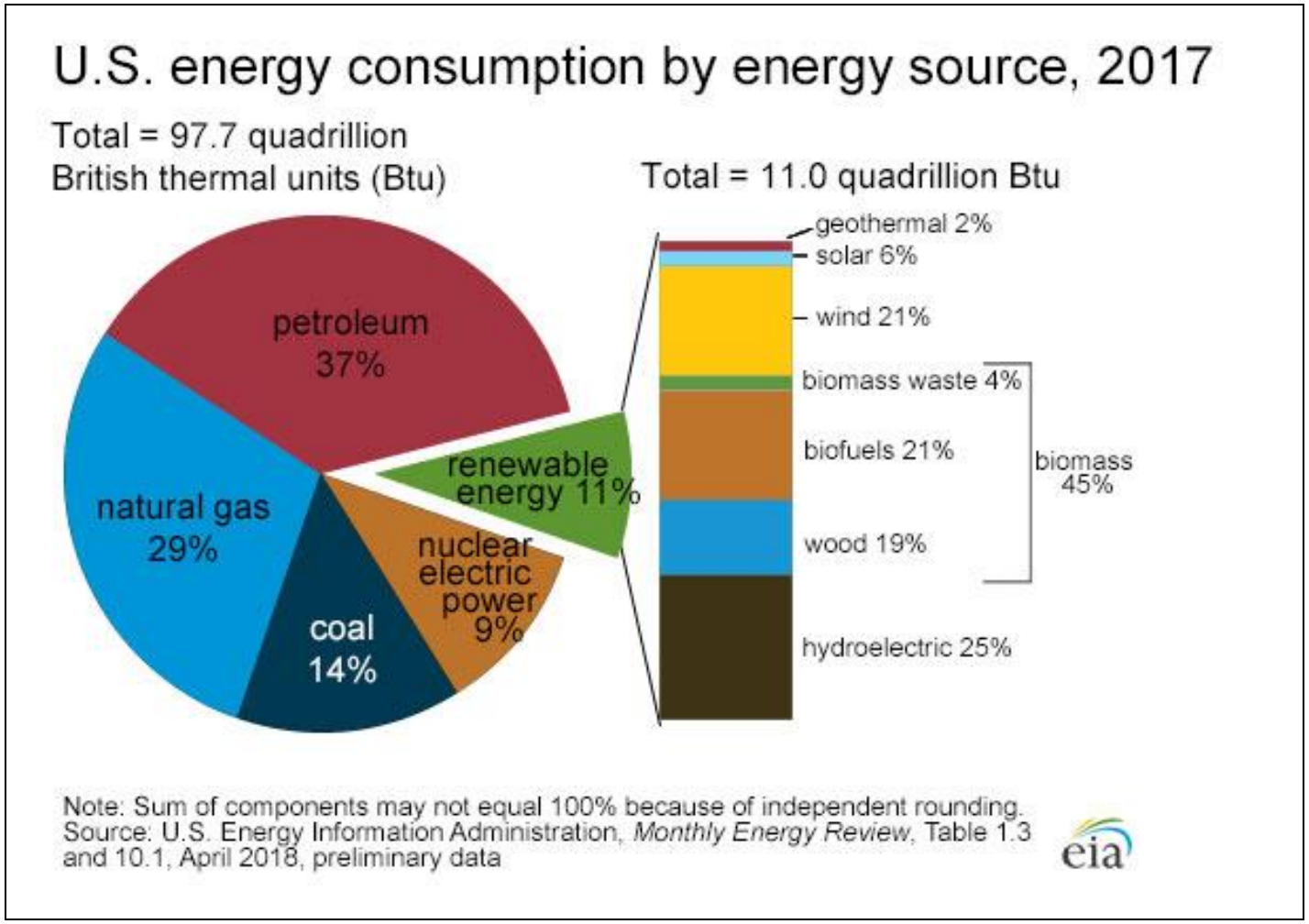

Figure 1.2: How the US Currently Generates Energy

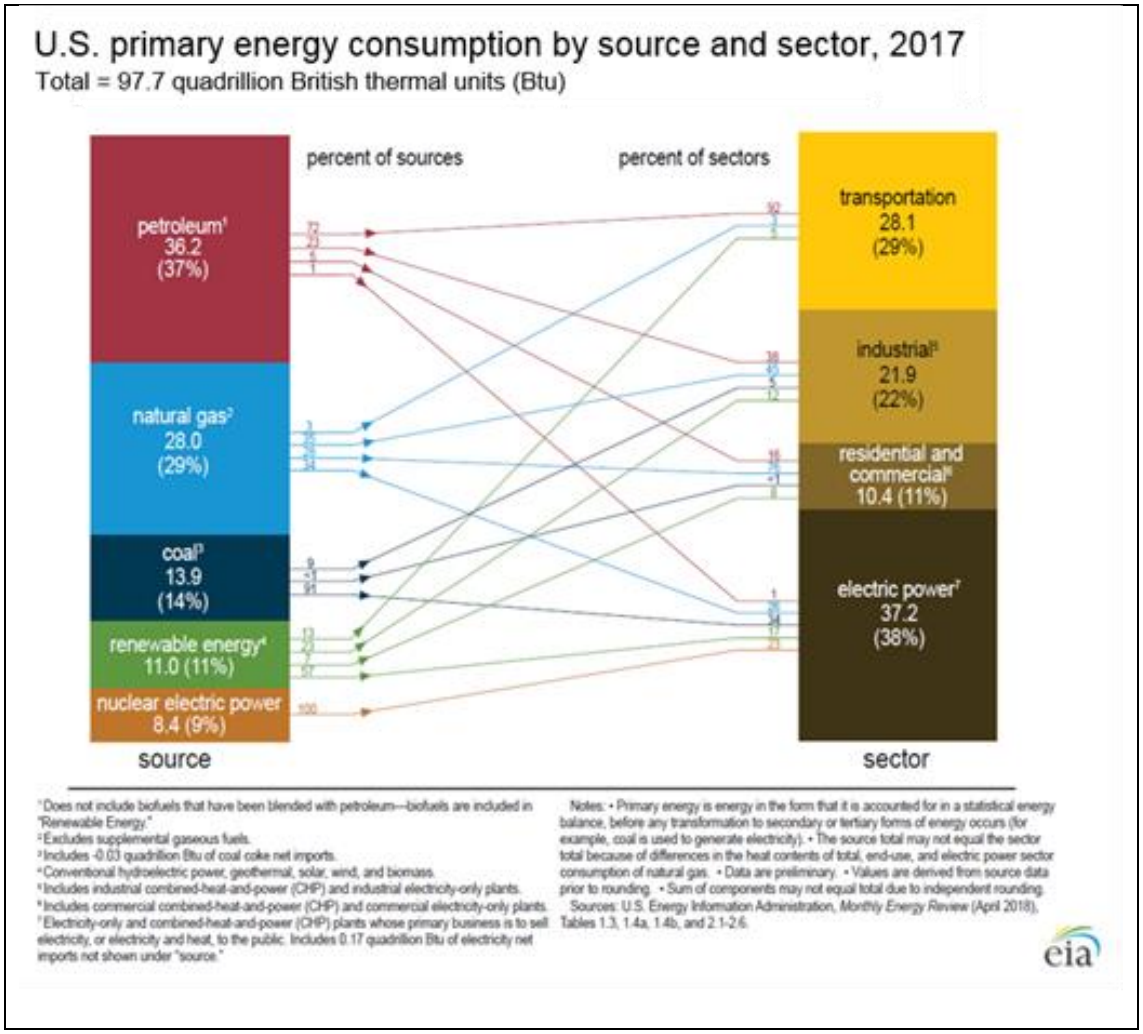

Figure 1.3: How the US Uses Energy

The bar graph shown in Figure 1.3 shows how much energy each sector of society is using as well as which methods of energy generation they use. Certain sectors severely limited by which methods they can use such as transportation. Of all the energy used by the transportation industry, 96% comes from petroleum products.[2]

As much of the infrastructure and operating devices in the US are designed to use fossil fuels in the combustion process, there is interesting in switching to biofuels they use the existing infrastructure while decreasing the fossil fuel consumption rates. Biofuel falls somewhere in between renewable energy and fossil fuels, so it is better classify them as an alternative fuel. Biofuel is the product of producing fuels from the biological waste of many different products such as corn husks or used frying oil.

Renewable energy sources such as solar, wind, and tidal energy all rely on converting the Earth's energy directly to electrical energy using solar panels, or wind/sea turbines. While these methods may produce renewable energy, currently they cannot replace all fossil fuel usage as their ability to generate energy fluxgates with the weather patterns. Geothermal energy, on the other hand, uses the heat from the Earth's crust to produce steam for a turbine plant. Geothermal plants can produce very consistent levels of energy but are limited by suitable location. Similarly, hydroelectric methods can generate significant amounts of electricity at very consistent levels but cause substantial changes to the ecosystem. Nuclear energy can meet the demand for electricity with a significant environmental impact, long term storage of nuclear waste. These are alternatives to fossil fuels that can meet energy needs in very specific ways but none of them are substantial alone and are best used in tandem with fossil fuels.

The issues with renewable energy sources mean that fossil fuels will continue to be used for a large portion of our energy needs for the foreseeable future.[1] Fossil fuels do have their own issues, which consist of emissions, cost, efficiency, and their limitations. Emissions from fossil fuels can have a major impact on the environment contributing to climate change, smog, and acid rain. In the ideal combustion process, the only products are Carbon Dioxide (CO_2) and Water (H_2O). Carbon Dioxide is a contributor to climate change as it is a greenhouse gas that traps heat in the atmosphere warming the environment. In the real-world applications, there are other particulates that are produced such as Carbon Monoxide (CO), Nitric Oxide (NO), and Nitrogen Dioxide (NO_2). Carbon Monoxide is poisonous and can contribute to the production of stronger greenhouse gases. Nitric Oxide and Nitrogen Dioxide are very reactive and are major contributors to acid rain. Very strict regulations have been implemented to release as few of these particulates as possible because of these chemicals and soot. Even though fossil fuels are the cheap for the consumer, they are still expensive because of the refining process. The large cost associated with generating energy is still a very important factor driving innovation to look for cheaper solutions with more efficiency. Just like the rest of the methods of energy generation, fossil fuels have their own limitations. Some of these limitations include strict operating conditions for engines and that the vehicle must carry all the fuel needed.

Most motor vehicles, including airplanes, are powered by fossil fuels and rely on many different types of petroleum derived fuel. In Figure 1.3 shown previously, the transportation sector primarily uses petroleum and natural gas with a slight portion of the energy coming from various renewable sources. Even for electric vehicles, the primary source of energy comes from the fossil fuel methods as they are the largest producer of

energy in the US. These electric vehicles generally have very similar effects on the environment as the traditional internal combustion engine vehicles do. This is due to the fact that the electrical grid is primarily fossil fuel powered and unless renewable energy power generation is increased these vehicles will continue to essentially be powered by fossil fuels.

After the engine has been designed and produced there is little that can be done to adjust the operating envelope other than changing the properties of the fuel used in the engine. The process for certifying new fuels for the highly complex aircraft and turbine engines is extremely expensive and extensive.[3] Due to this high cost, it is preferred to model the fuels and engines first to determine the performance and emissions in order to get a first judgement.

Modeling fuels with engines is a practical way to predict whether a design should be reworked or tested as it requires substantially less time and money to model than to experimentally test. While modeling is strongly preferred, it has limitations due to chemical complexity, the limitations of modern computing, and the fact that many of the chemical properties are linked to mechanical properties. A chemical kinetic model is a list of all chemical reactions and how they occur for every molecule in the fuel and is what is used in the modeling process. Real petroleum derived fuels are extremely chemically diverse and contain thousands of unique chemical species. The chemical kinetic models of these fuels are extremely large due to the enormous number of reactions that can happen.

These large chemical kinetic models are extremely taxing on the computational resources and are often much to massive to use the entire kinetic model. Typically, these

chemical kinetic models are used to generate what are called reduced kinetic models which only consist of the most important reactions to drastically reduce the size. These reduced kinetic models are still large and can be a significant drain on computational power. Because these reduced kinetic models still use such a large amount of computer resources, there is a substantial interest in decreasing the sizes of these models. One way that this has been done is through compact kinetic models which typically only consist of the most dominant molecules in the fuel. One issue with modeling fuels using the compact kinetic model approach is that many of the chemical properties are coupled with mechanical ones. The fact that they are coupled means that once the mechanical properties change, the chemical properties changes as well. This coupling leads to problems with the compact kinetic models replicating all the properties especially when physical environment can change.

Chemical and mechanical coupling along with needing smaller sizes of chemical kinetic models have led to new solutions, one promising method is surrogate fuels. Surrogate fuels are specific mixtures of a few chemicals that accurately reproduce targeted properties of the real fuel of interest.[4-21] They can be created with as few as one component which means the chemical kinetic models generated from them are useable sizes and can be formulated to consider the mechanical and chemical coupling effects. [10]

CHAPTER 2

THEORY

Surrogate fuels are mixtures of chemicals that reproduce the selected behaviors of real-world fuels.[4-21] These are extremely useful when modeling multi-component fuels such as petroleum derived fuels. The kinetic models of multi-component fuels are larger than those of single component fuels as there are more species that need to be considered. The interactions between components in mixtures are important to representing the behavior of real fuels in a model. When compact kinetic models are created, some of these interactions can be lost which can result in slightly different combustion behaviors. [20]

When formulating surrogate fuels, multiple components are used to match the combustion behaviors of interest.[4-22] The fact that these mixtures consist of multiple components allows for the interactions between different chemicals to occur and can better represent the target fuel than a single component representation . The chemical kinetic models for these multi-component surrogate fuels are significantly smaller than those of real fuels. This major reduction in size of chemical kinetic models comes from the fact that real fuels are extremely chemically diverse and contain hundreds if not thousands of different chemical species that all interact with each other to form new species that must be considered in the full-size kinetic model.

All these chemical species that are present in real fuels can be sorted into categories of types of chemicals. The main categories are known as n-alkanes, iso-alkanes, cyclo-

alkanes, and aromatics or phenol groups. There are a handful of others that are not nearly as prevalent and have been excluded. Out of these chemical types, n-alkanes are the most understood and consist of a linear chain of carbon atoms with hydrogen filling in the rest of the bonds. Iso-alkanes are branching chains of carbon atoms that are surrounded by hydrogen atoms. Aromatics and phenol groups are well understood and consist of anything with at least one benzene like ring in the molecule. The last major group of chemicals are what is known as cyclo-alkanes. Cyclo-alkanes are made up of rings of carbon atoms that all have single bonds. Cyclo-alkanes are not understood very well and have widely been ignored in previous research due to reduce reactivity of the cyclo-alkanes compared to that of n-alkanes.[23] Many of the new specialized jet fuels have larger quantities of cyclo-alkane structures and which generate a need to better understand cyclo-alkanes.[20, 23] When formulating surrogate fuels, it is important to have components that can represent each of these groups as they all have special attributes that may need to be accounted for. All these chemical structures can be broken down further to what are known as chemical functional groups. Functional groups are the categories which categorize specific groups of atoms within molecules and describe how the individual atoms in a molecule are bonded. It is known that the same functional group will undergo very similar reactions no matter what molecule it is part of.

Surrogate fuels use only a handful of chemical species to reproduce the combustion behaviors and as such this significantly simplifies the chemistry from extremely complex real fuels to manageable for the surrogate fuels. Many of the very complex chemical structures that are present in real fuels react in similar manners and because of this, the chemistry can be reconstructed using simpler models that will react the

same.[8-11, 21-23] There are many different methods of formulating surrogate fuels with a large majority of them being highly empirically based. These empirical methods test the real fuel for what are known as Combustion Property Targets (CPT's) and then rely on the developer to determine which ones are the most important to be matched for the situation.[4-21]

There are many different groups using these CPT methods with some of the various CPT's being flash point (FP), various ignition and extinction characteristics, sooting propensity using a variety of methods, and various emissions profiles.[4, 5, 7-21, 24] Many of these methods only used one or two CPT's and found that even though their surrogate fuels match the specified CPT's, they tend to not match other CPT's as well. Past work from Won et. Al used these CPT methods as well but chose to use four CPT's to better represent the overall target fuel.[7-9, 11, 21, 25] One of the major issues with the CPT method of surrogate formulation is they typically reproduce the chemical properties or the physical properties of the target fuel but fall short when both are evaluated together. The surrogate fuels that only account for the chemical properties can still correctly predict the reaction mechanisms of the real fuel under the correct circumstances.

A common assumption during the modeling process is to assume that the fuel is completely vaporized before reacting in which case the physical properties of the fuel are negligible. Recent research has shown this assumption of the fuel being prevaporized does not always hold true, especially when in the near limit operating conditions[26-28]. Furthermore, research also suggests that some of these near limit conditions, such as lean blow-out (LBO), are governed by preferential vaporization.[10] Preferential vaporization occurs in real fuels that are injected in liquid state and is due to the components of the fuel

having substantially different vapor pressures which causes some components to vaporize sooner. Figure 2.1 shows the impact that preferential vaporization can have on DCN for several real fuels. These real fuels were separated into 20% bins or cuts by distilling so that the extent of preferential vaporization could be seen. This variance in DCN for each fuel was than analyzed by taking the maximum difference between bins and dividing them by the DCN for the overall fuel which can be seen in Figure 2.2. From Figures 2.1 and 2.2, it is very clear that preferential vaporization can have monuments impacts on the fuels but not all fuels experience the same impacts of preferential vaporization.

The CPT's that were chosen by Won et. Al are the derived cetane number (DCN), sooting propensity measured through the threshold sooting index (TSI), the molecular weight (MW), the Hydrogen to Carbon ratio (H/C), and parts of the distillation curve (T10, T50, T90) so that the surrogates adequately capture the combustion behaviors of the target fuel.[7-9, 11, 21, 23, 25] When the DCN, MW, H/C and TSI are all used in conjunction the chemical properties of the fuel are correctly reproduced but the physical properties are not. The distillation curve needs to be considered to account for the volatility and preferential vaporization of the fuel which will enable the replication of the physical properties.

While investigating the potential surrogate fuels that fit all these constraints, it was seen that the number of CPT's used limits the combinations for the chemical functional group distribution. It is known that chemical functional groups react the same no matter what molecule they are part of, and because of this, they dictate the values of CPT's. Naturally, this begs to question is it possible to formulate a surrogate from the chemical functional group distribution? The first step to answering this question is to decide how to determine the chemical functional groups of the target fuel.

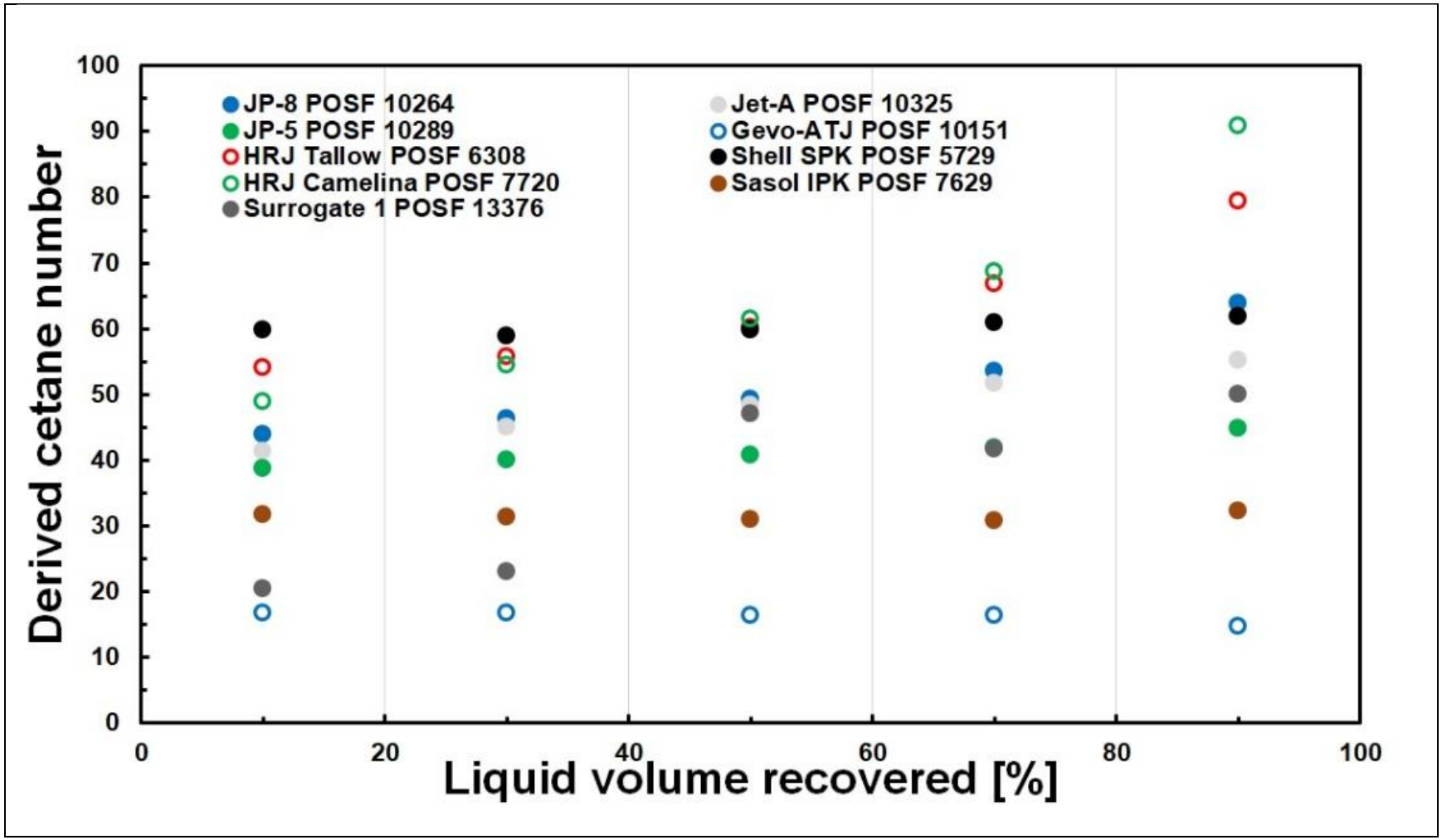

Figure 2.1: Effects of Preferential Vaporization on DCN

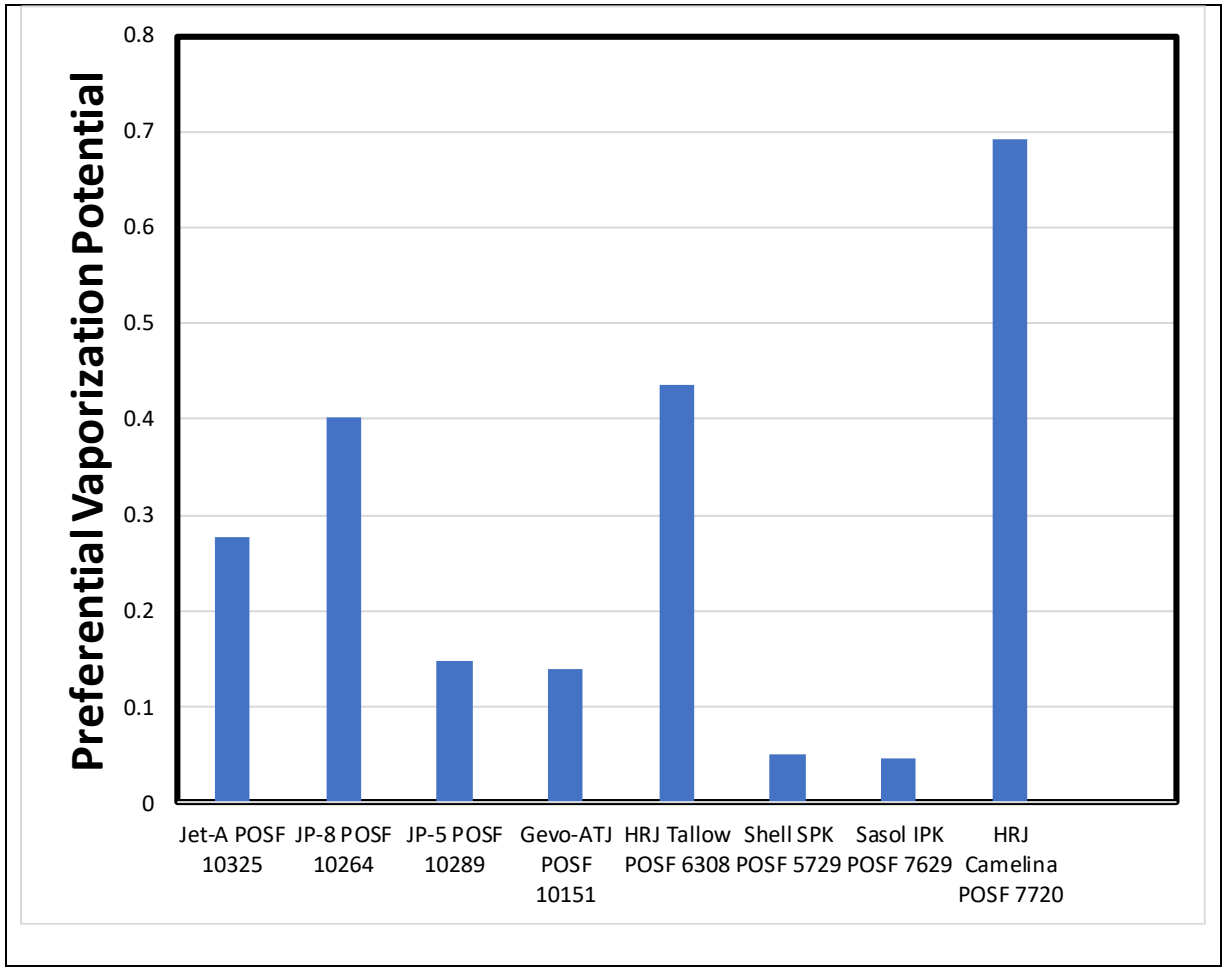

Figure 2.2: Preferential Vaporization Potential

There are several different ways that the functional groups can be determined using direct and indirect methods. Cooney et. Al used a decomposition method to determine the surrogate components and extrapolate the functional group distribution from the components[5]. The method that they used is further modified in a hybrid-based scheme to account for preferential vaporization using a chemical surrogate and a physical surrogate that are combined. Another more direct method of determining the functional group distribution is with Nuclear Magnetic Resonance (NMR). [22, 24, 29-31]

Nuclear Magnetic Resonance is a method of determining the chemical functional groups that are present in a mixture. Traditionally NMR operates using a liquid sample that is exposed to a high strength electromagnetic field. When the electromagnetic field is activated, certain atomic nuclei align with or against the direction of the field. The reaction of the nuclei is then recorded and analyzed to determine the functional groups. Atoms are made of protons, neutrons, and electrons and have respective electrical charges of positive, neutral, and negative. The actual charge depends on what chemical element the atom is with certain elements being more electronegative.

Elements and atoms that are more electronegative are more likely to attract a bonding pair of electrons. This electronegativity is also influenced by if and how the individual atoms are bonded. If an atom with a small degree of electronegativity is bonded to an atom with high electronegativity, the electronegativity of the first atom will be influenced. In the presence of a magnetic field the direction that the nuclei align is relative to the electronegativity of the nuclei. Because the chemical functional groups are defined by the local atomic bonds, each type of functional group has its own electronegativity and responds to the electromagnetic field uniquely. When the functional group responds to the

field, the electronegativity of the group determines the strength of the reaction which can be characterized by the NMR analysis to determine the different functional groups.

NMR is typically used in a qualitative manner to determine what functional groups are present but not necessarily how much of each group are there. However, when ran under certain parameters, the NMR analysis can take quantitative readings to accurately measure the functional group distribution. Because NMR excites the atomic nuclei, the probe can detect only one element at a time, which means the machine can measure either the functional groups from the 1H, or Hydrogen perspective, or the 13C, or Carbon perspective.

Lyu et. Al uses 1H NMR to measure the chemical functional group distribution to produce a single molecule which matches the average functional group distribution of the fuel.[24] This method of producing surrogates would extremely simplify the complex chemistry issues of real fuels, but it would require a new chemical kinetic model for every fuel as every fuel would have a unique molecule. This method would also fail to match the physical properties of the fuel and could neglect the mechanical chemical coupling behaviors, such as preferential vaporization, that are prevalent.

This has led to our group investigating the use of the distillation curve along with the chemical functional group distribution being used to formulate surrogate fuels. Because the chemical functional groups all react the same regardless of the molecule, and the CPT's being a function of the reaction pathways, the functional group distribution should be enough to recreate the chemical properties of the fuel. Using the distillation curve in conjunction with the chemical functional group distribution will account for the chemical

properties, and the mechanical chemical coupling effects of the real fuel. To measure the chemical functional groups distribution using NMR the 1H spectrum is not enough as there can be slightly different functional groups that exhibit similar responses in the 1H spectrum so the 13C spectrum must be considered simultaneously. Using both the 13C and 1H spectra together allows for an adequate description of the chemical functional group distribution which enables all the functional groups of interest can be identified. By using a variety of simple components, the distillation curve can be reproduced as well as the chemical functional group distribution. Using simple components that have known chemical kinetic models allows for a combination of these models to represent the kinetic model of the target fuel. Using the NMR analysis to calculate the chemical functional group distribution also requires a very small sample, as little as 1 mL, to predict how the target fuel will react. This significant reduction in quantity needed to test the fuel allow for a significant cost reduction in the testing and certification of the target fuel.

NMR spectra can be simulated extremely well for simple components and are completely quantitative and will be referred to as synthetic NMR spectra. The NMR spectra of a mixture are a function of the mole fraction of the components because the response is based on the number of moles present. To predict the NMR spectra of a known mixture, the spectra of the individual components can be weighted by their respective mole fraction to reproduce the spectra of the mixture. Using this knowledge, a surrogate fuel can be formulated that optimizes the mole fractions of chosen components to best reproduce the measured NMR spectra of the target fuel from the synthetic spectra of the components. The fact that this method can reproduce the chemical functional group distribution by optimizing the mole fractions of the mixture is beneficial because the distillation curve can

be found by using bubble temperature calculation which is dependent on the initial mole fractions of the mixture. The bubble temperature calculation and the matching of the NMR spectra by using synthetic spectra allows the optimization to determine the best mole fractions.

As beneficial as surrogate fuels can be, the current methods have serious limitations with what they can predict and how well they can be modeled. This is because none of the current generation of surrogate formulation methods account for preferential vaporization. Another issue with the current generation of surrogate formulation methods is that the number of components that are used vary significantly.[4-21, 26, 28] The magnitude of the kinetic model for the surrogate fuel is largely dependent on the number of components. When formulating surrogates for many of the alternative or unique fuels the components will need to be changed, or tailored, to better suit the target fuel, but this is not a major issue if appropriate and well understood components are chosen.

CHAPTER 3

METHOD

During this study, we used NMR to measure the chemical functional group distribution of the target fuel. NMR is typically operated qualitatively to detect what chemical functional groups are present in a sample, without consideration for the quantitative amount of each functional group present. Under certain conditions NMR analysis can obtain quantitative results and determine exactly how much of each functional group is present. A study that was published on NMR analysis of Diesel fuels from 2013 performed quantitative NMR measurements on various diesel fuels and got results that were accurate within 2% of Carbon aromaticity.[29] The acquisition time for quantitative 1H spectra was 3 seconds with an 8 second relaxation delay. For the 13C spectra, Chromium (III) acetylacetonate ($CR(acac)_3$) was added as a relaxation agent to reduce the relaxation delay time to 5 seconds with a 3 second acquisition time. The $CR(acac)_3$ was added until it reached 0.05 molarity in the sample. The solvent for this method is deuterated Chloroform, Chloroform-D or $CDCl_3$ and is referenced at 77.20 ppm for the 13C spectrum and 7.26 ppm for the 1H spectrum. [29]

To calculate the distillation curve of a mixture, the bubble temperature can be determined. The bubble temperature is the temperature at which the mixture begins to boil. To calculate the bubble temperature, the vapor pressure of the individual components needs

to be known and this can be found using Antoine's equation which can be seen in Equation 10. The vapor pressure of the components can be multiplied by their respective mole fractions in the mixture and summed to determine the vapor pressure of the mixture. The mixture is said to be at the bubble temperature when the vapor pressure of the mixture is equal to the atmospheric pressure.

An optimization algorithm was used to determine a surrogate mixture that would reproduce the both the 1N and 13C NMR spectra and the distillation curve, for a best fit solution. One issue that needed to be addressed was the chemical diversity in real fuels. This diversity plays a large role in real fuels which create resolution issues that come from experimental measurements that result in a substantially loss of sharpness in the NMR spectra. This factor was mitigated by taking the cumulative integral across the domain of each spectra resulting in a significantly closer continuous curve. Using the cumulative integrated approach for both the synthetic component and measured spectra for the target fuels gives results which can be compared. All the cumulative integrated spectra were normalized to give the same location and height so that they could be fairly compared. The cost function for this optimization method is defined as:

$$G = \sum|eq1| + |eq2| + |eq3| + |eq4| + |eq5| + |eq6| \quad (1)$$

Where

$$eq1 = \sum|HIo - HI| * HIo \quad (2)$$

$$eq2 = \sum|CIo - CI| * CIo \quad (3)$$

$$eq3 = \frac{T10 - T10a}{T10a} \quad (4)$$

$$eq4 = \frac{T20 - T20a}{T20a} \tag{5}$$

$$eq5 = \frac{T50 - T50a}{T50a} \tag{6}$$

$$eq6 = \frac{T90 - T90a}{T90a} \tag{7}$$

The terms in the above equations, HIo and CIo are the cumulative integrated 1H and 13C NMR spectra, respectfully, of the target fuel. HI and CI are the cumulative integrated synthetic spectra for the generated mixture where the original spectra can be computed using the below formulas where the Hi and Ci are the synthetic spectra of the individual components.

$$H = x_i H_i \tag{8}$$

$$C = x_i C_i \tag{9}$$

The method of calculating the distillation curve through the bubble temperatures used Antoine's equation, Raoult's Law, and Dalton's Law. Antoine's equation was used to calculate the vapor pressure of each component and can be found from Equation 10

$$Pvap = e^{A + \frac{B}{T+C}} \tag{10}$$

Raoult's Law allows for the calculation of the vapor pressure of the mixture which was said to bubble once the vapor pressure was equal to the atmospheric pressure. Raoult's Law which is shown in Equation 11 states that the vapor pressure of a mixture is equal to the sum of the vapor pressure of each component multiplied by their respective mole fractions.

$$Pv = \sum x_i Pvap_i \tag{11}$$

Lastly, Dalton's Law is used to calculate the gas phase mole fractions of the vapor above the liquid at the bubble temperature. The equation, shown in Equation 12, is used to determine how much of each component has vaporized and is defined as following:

$$P_{total} = \sum P_i \tag{12}$$

All these different pieces fit into the cost function G and the value for the number of moles of each component is determined using a minimax optimization approach. Several different optimization algorithms were investigated throughout this study and the minimax approach was selected due to this approach finding a significantly smaller error than other methods. This makes sense as the primary goal of the minimax algorithm is to minimize the maximum error of the cost function where many of the other methods solve for local minima and may not be the best approach when dealing with non-smooth error surfaces. A flowchart of this method can be seen for convenience in Figure 3.1.

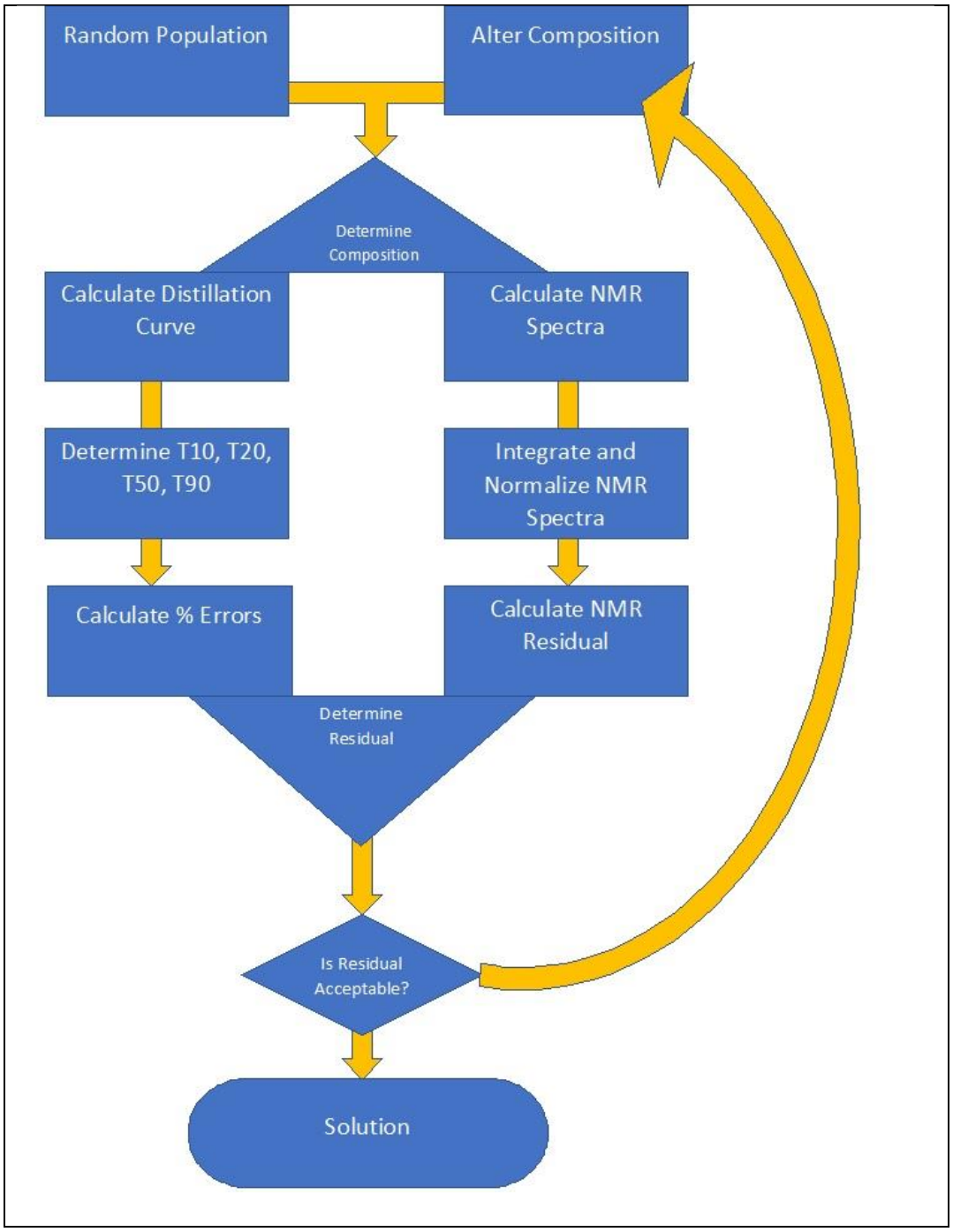

Figure 3.1: Flowchart of Optimization Method

CHAPTER 4

RESULTS

To verify that this method could work, a known 12-component fuel was used to generate a synthetic 1H NMR spectrum and compute the distillation curve. This new spectrum and distillation curve were used as the target fuel in the optimization method to determine if it could be reproduced. It was determined that this "target fuel" could be reproduced exactly using this method but both the 1H NMR spectrum and the distillation curve were needed to create a unique solution since multiple mixtures were found to reproduce the NMR spectrum. Once this mixture was correctly matched, it was tested using Jet-A POSF 10325 and the mixture could not be properly replicate the CPT values of the real fuel. This lack of ability to constrain the mixture led to the inclusion of the 13C NMR spectra as one of the optimization targets.

After the 13C spectra was added, this method was used on multiple fuels consisting of several petroleum derived real fuels and various alternative jet fuels. The first fuels tested were the alternative jet fuels that exhibit low preferential vaporization potential and lacked chemical diversity to evaluate the validity of this method. Next the alternative jet fuels that have substantially higher chemical diversity, but they still had significantly less diversity than petroleum derived fuels and varying amounts of preferential vaporization potential. The last fuels that were tested were the petroleum derived fuels as they have the

highest chemical diversity. This was done to determine the validity of this method and how well it can capture the larger number of species and preferential vaporization potential.

The first fuel tested was Surrogate 1 which was calculated by Won et al. [21] and mixed by the Air Force Research Lab as POSF 13376 so the exact mixture was known. The results of the optimization can be seen in Figures 4.1 and 4.2 which show the integrated NMR spectra of the generated mixture compared to that of Surrogate 1. Both integrated spectra were matched but because this is the cumulated integrated spectra, functional groups that occur near each other can be lost so the actual NMR spectra must be checked.

The last target for the surrogate generation is the distillation curve which is shown in Figure 4.3. The distillation curve is calculated for the generated mixture then compared to the known temperatures of the real fuel. Because the only temperatures that are known for the target fuel are T10, T20, T50, and T90, they are represented as specific points as to get a truer representation. Both 1H and 13C NMR spectra for the generated mixture and Surrogate 1 are shown in Figures 4.4 and 4.5. The proton spectrum of the real fuel is reproduced very well with a 0.067 percent difference. All the key functional groups that are of interest are well matched as well.

Figure 4.5 shows the carbon spectrum of Surrogate 1 and the formulated surrogate mixture. While it is not reproduced as well, 2.31 % error, it still clearly captures the chemical functional groups present. The paraffinic groups are all very well reproduced along with most of the aromatic carbons present. The major differences between the target spectrum and the simulated spectrum are due to the limitations of real-world tests. In the real fuel spectrum, not all the quaternary aromatic carbons are observed as both carbon

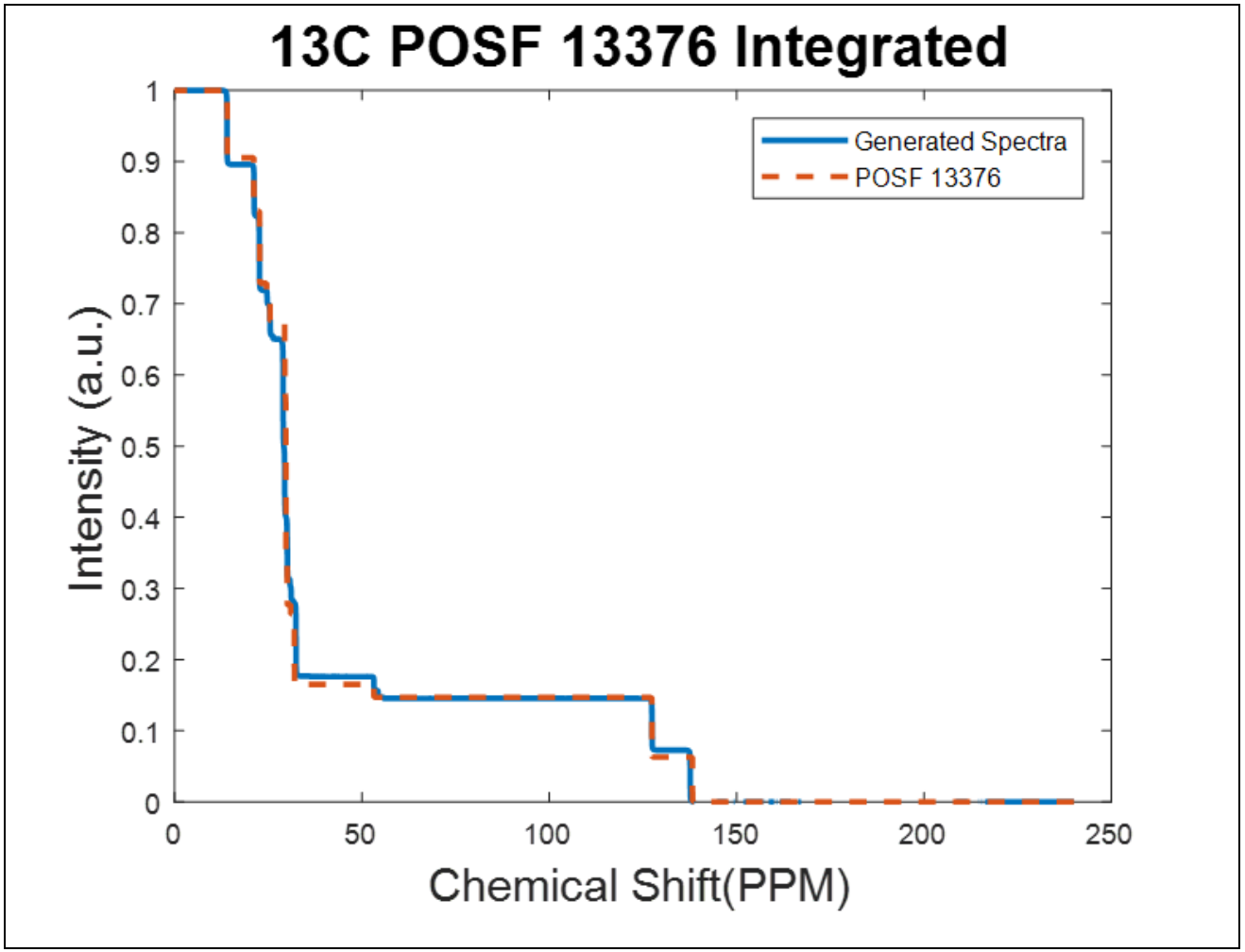

Figure 4.1: Integrated 13C NMR Spectra of Surrogate 1

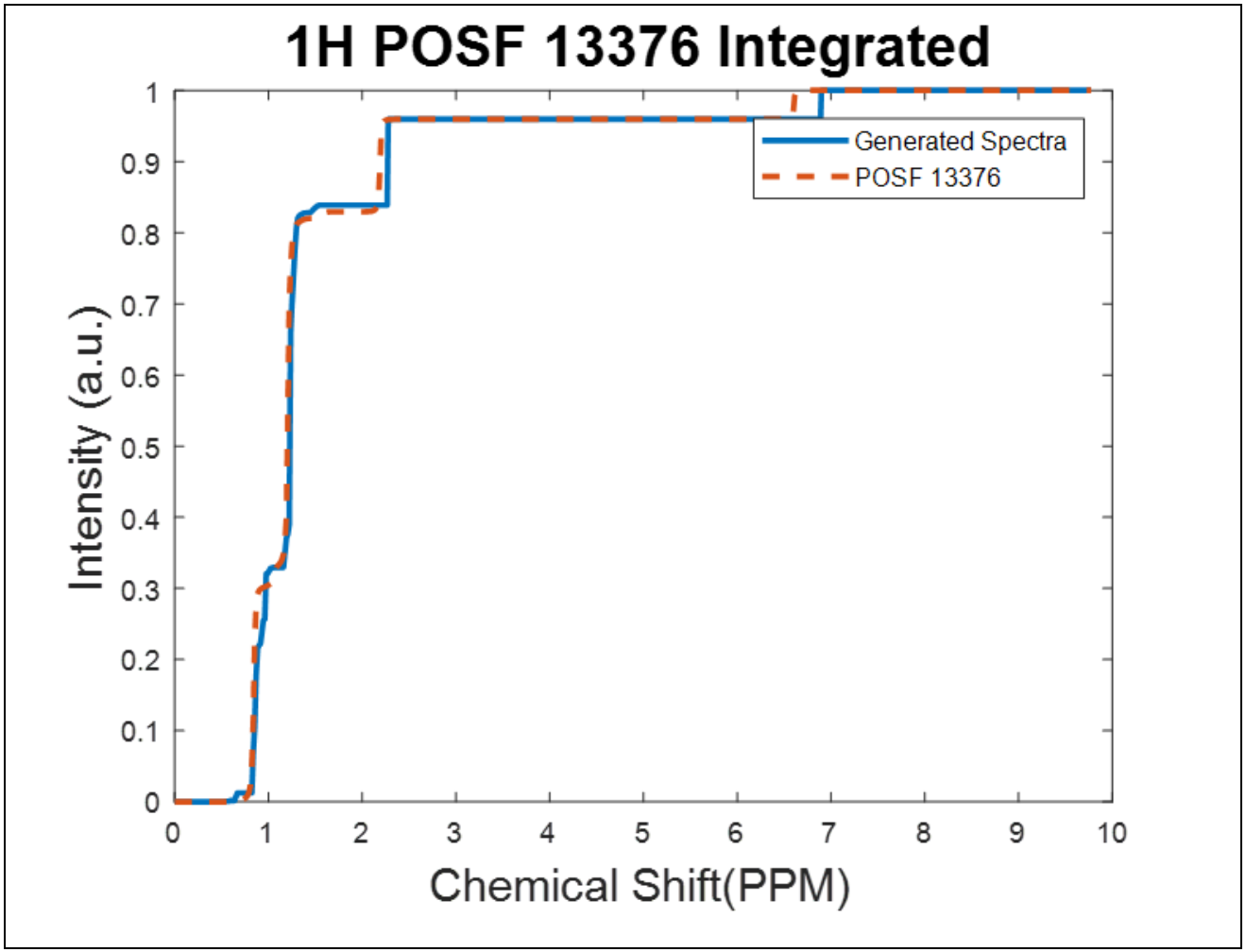

Figure 4.2: Integrated 1H NMR Spectra of Surrogate 1

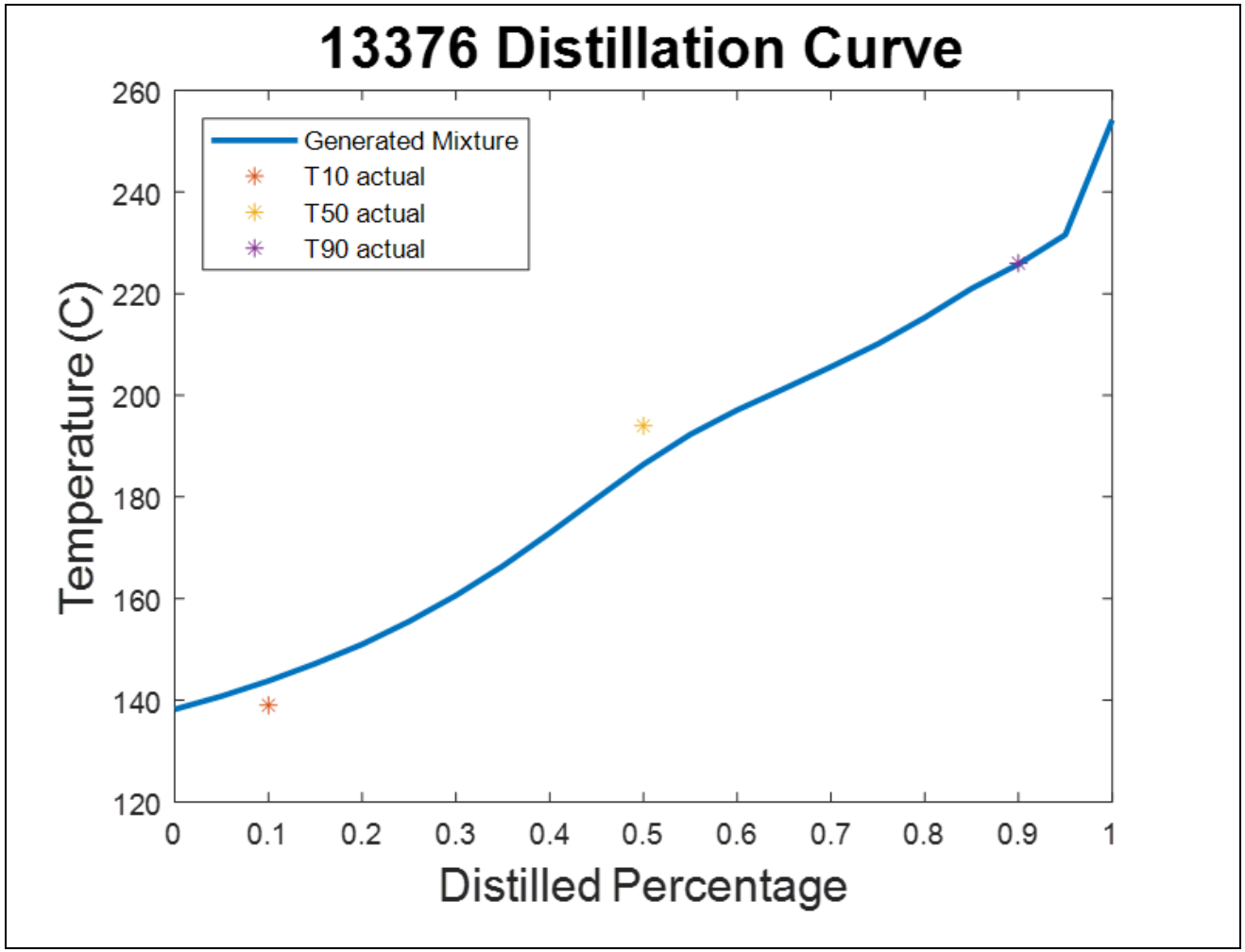

Figure 4.3: Distillation Curve of Surrogate 1

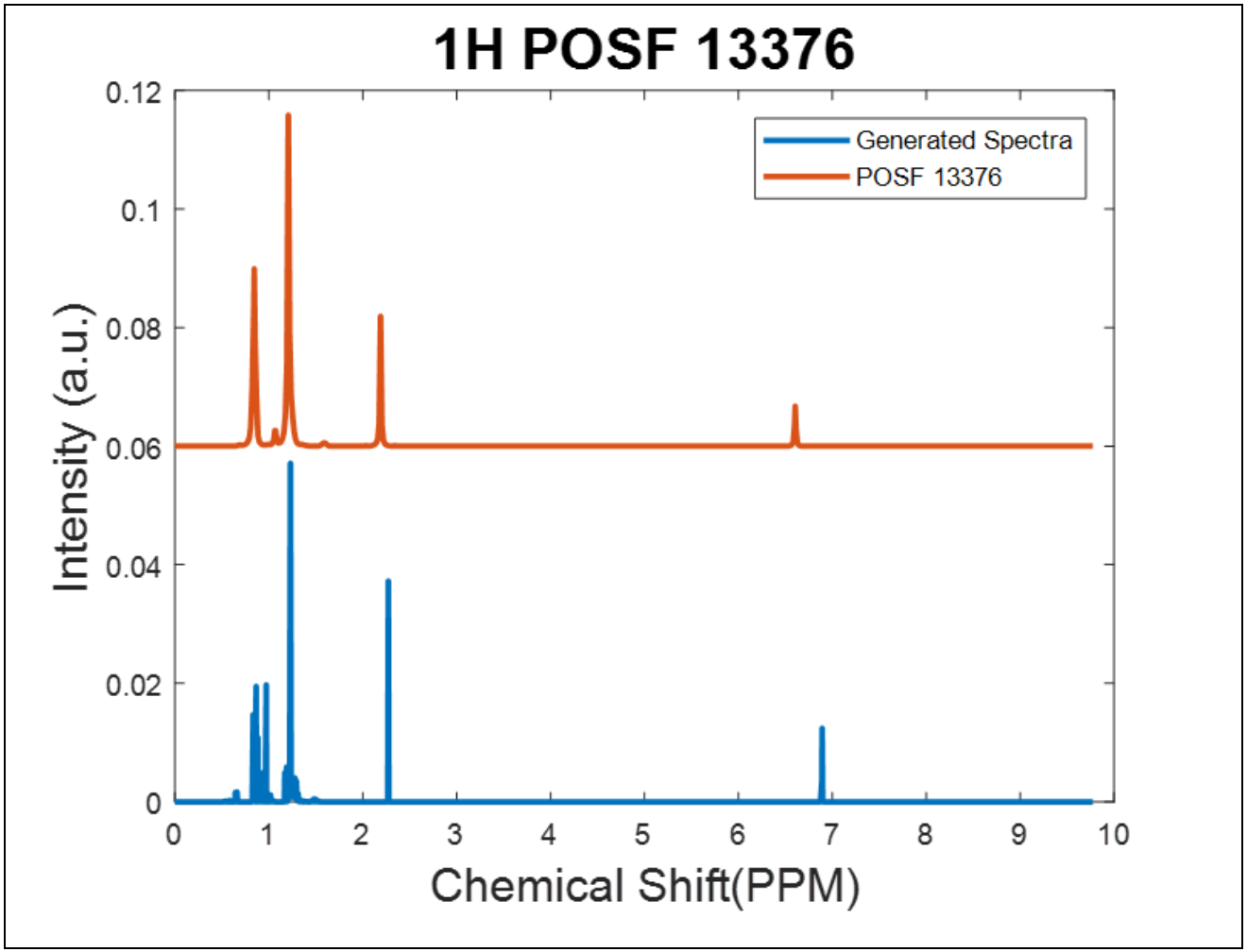

Figure 4.4: 1H NMR Spectra of Surrogate 1

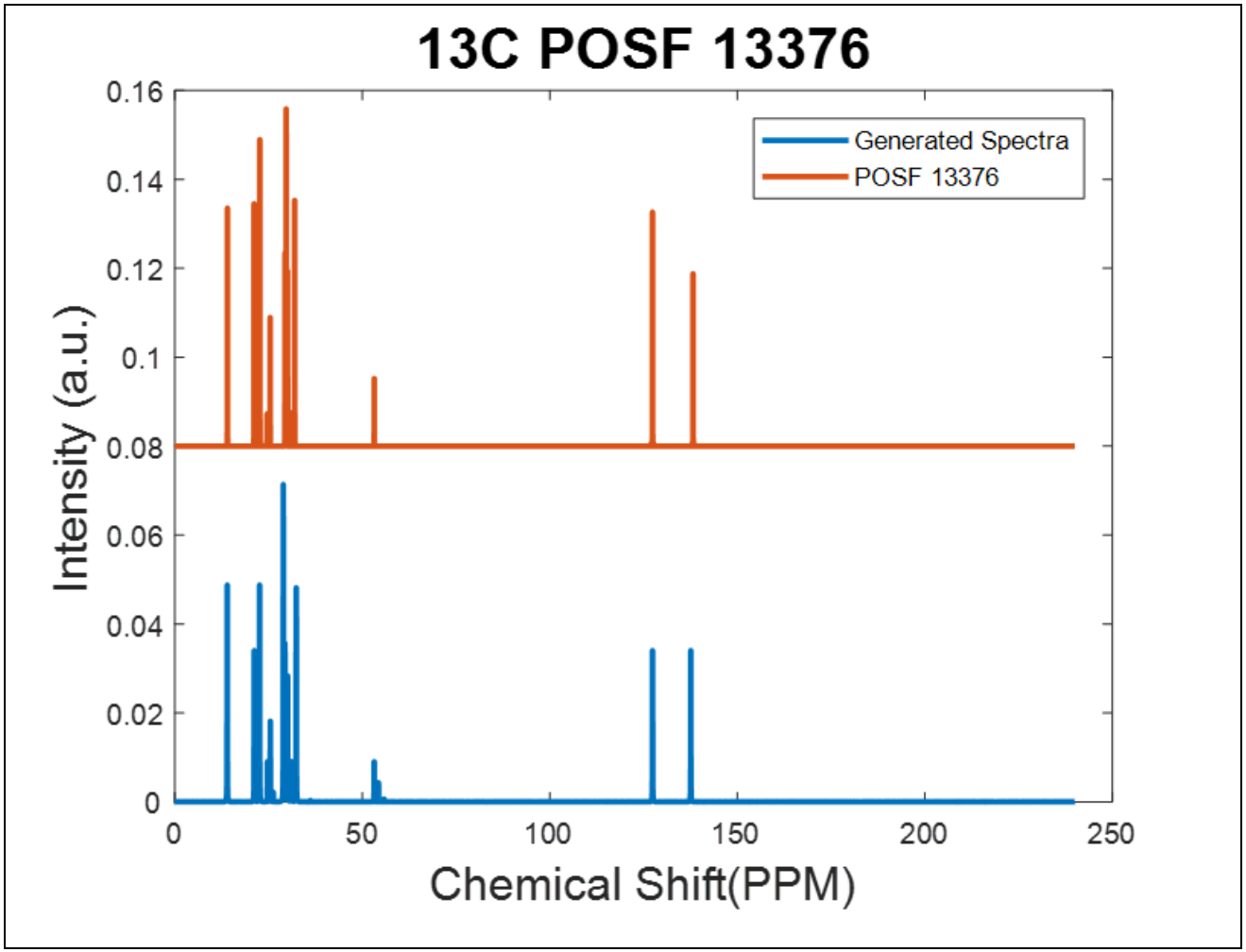

Figure 4.5: 13C NMR Spectra of Surrogate 1

peaks in the aromatic region which should be equal because of the chemicals present. The operating parameters of the tests were varied in an effort to observe all of these carbons. Since time is constrained on the machine, we could only increase the relaxation delay time to 90 seconds with very negligible benefits.

Table 4.1 shows the CPT values that were predicted using a QSPR method and compares them to those found from the mixture of Surrogate 1 POSF 13376. These values in Table 4.1 show that the surrogate properly matched the CPT values of the target fuel and that this method can accurately reconstruct the Surrogate 1 mixture. The DCN for this surrogate was found to be within 1 DCN value of the target fuel while the MW was within 4 g/mol. The H/C ratio differed from that of the target fuel by 0.021. This surrogate was formulated solely using the chemical functional group distribution and distillation curve and it was still able to predict the CPT values. Because the CPT values are almost identical with a maximum difference of 2.8 % error in the MW, it shows that this method can successfully formulate a surrogate fuel.

After Surrogate 1 was successfully recreated, the algorithm was used on Gevo ATJ POSF 10151 as it is a simple mixture that lacks both chemical diversity and preferential vaporization potential. All the results for the distillation curve along with both integrated and standard NMR spectra can be seen in Figures 4.6-4.10. The distillation curve, in Figure 4.6, is well fit and falls within 10 degrees of the actual measurements that were taken when distilling this fuel. Gevo ATJ is comprised primarily of highly branched isoalkanes that contain 12 and 16 carbons which exhibit unique placements in the NMR spectra.

Table 4.1: Generated Surrogate and CPT's of Surrogate 1

Components	Mole Fraction	Combustion Property Target	Model Fuel	Target Fuel
nC7	0.0671	DCN	50.5	49.8
nC8	0.0979	H/C ratio	2.008	1.987
nC10	0.0055	MW [g/mol]	139.1	143.1
nC12	0.2939	TSI	-	-
nC14	0.0514	Density at 15 °C [kg/m3]	757.9	763.9
nC16	0.0007	T_{10} [°C]	144	139
iC8	0.1909	T_{20} [°C]	151	
iC12	0.0454	T_{50} [°C]	186	194
iC16	0.0069	T_{90} [°C]	226	226
toluene	0			
nPB	0			
135TMB	0.2402			
MCH	0			
n-butylcyclohexane	0			

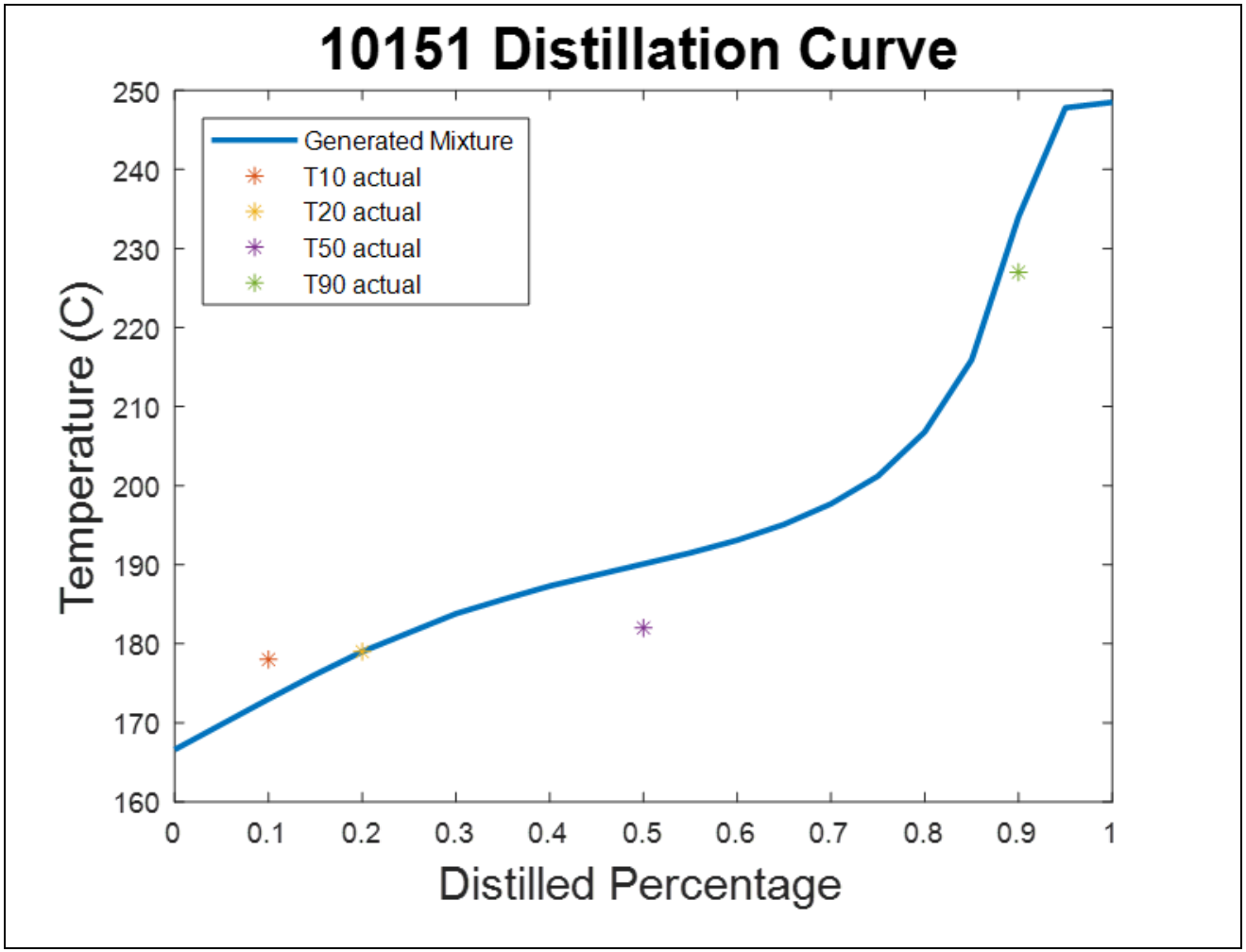

Figure 4.6: Distillation Curve of Gevo ATJ

From Figures 4.7 and 4.8, the integrated NMR spectra show that the very distinct chemical functional groups from the isoalkane structures are captured in the mixture. The fact that the algorithm successfully matched the structures from the NMR spectra is a very big step for proving how versatile this method can be. But because these are just the integrated spectra and may attribute some of the structures to similarly placed chemical functional groups, the standard NMR spectra must be inspected as well and these can be seen in Figures 4.9 and 4.10. Figure 4.9 shows the 1H spectra for the generated surrogate mixture and for the measured real fuel. Here it is clear that the basic structures are reproduced very well, with a 1.12 % error, but the 1H spectra only references the protons' environments. There is are similar intensities for all of the key functional groups that we are interested in, primarily the CH_3, CH_2, CH, and Aromatic groups which show that this method is providing a good foundation for many of the chemical properties that are of interest. The quaternary carbon functional group, C, which is a carbon that is connected to four other carbons, is found in the 13C NMR spectrum which is shown in Figure 4.10. Along with information about the number of quaternary carbons present, the 13C spectrum gives insight about how the chemical functional groups are connected as it shows the carbons' perspective which shows more overall structures. The 13C spectrum shown in Figure 4.10 has a 2.29 % error which shows that this method is viable for real fuels.

Figures 4.9 and 4.10 shows the traditional NMR spectrum of the generated surrogate for Gevo ATJ along with the measured spectrum of the real fuel and it is clear that it is almost an exact match which shows that this method can successfully reproduce the chemical functional groups of this fuel. Because the chemical functional group distribution

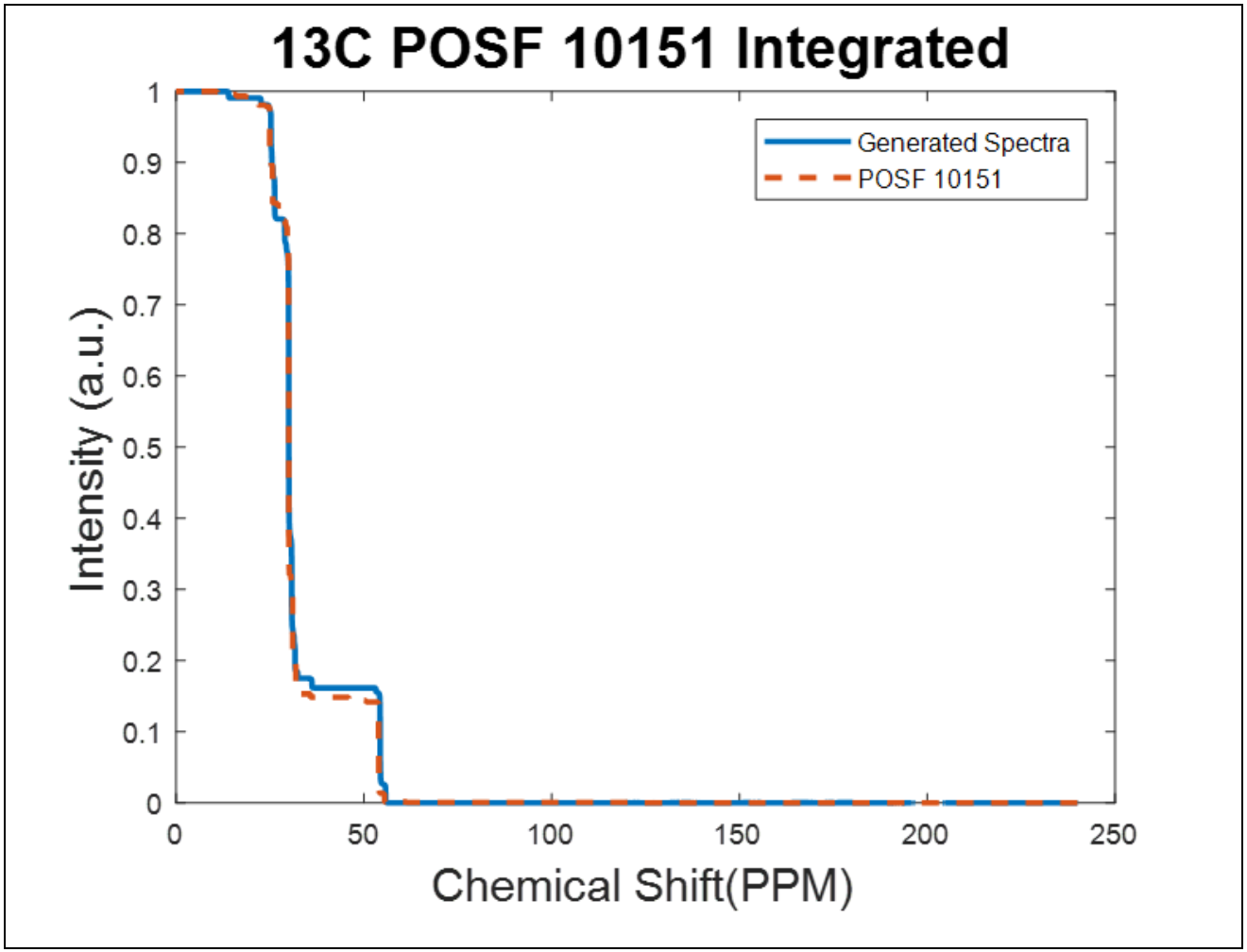

Figure 4.7: Integrated 13C NMR Spectra of Gevo ATJ

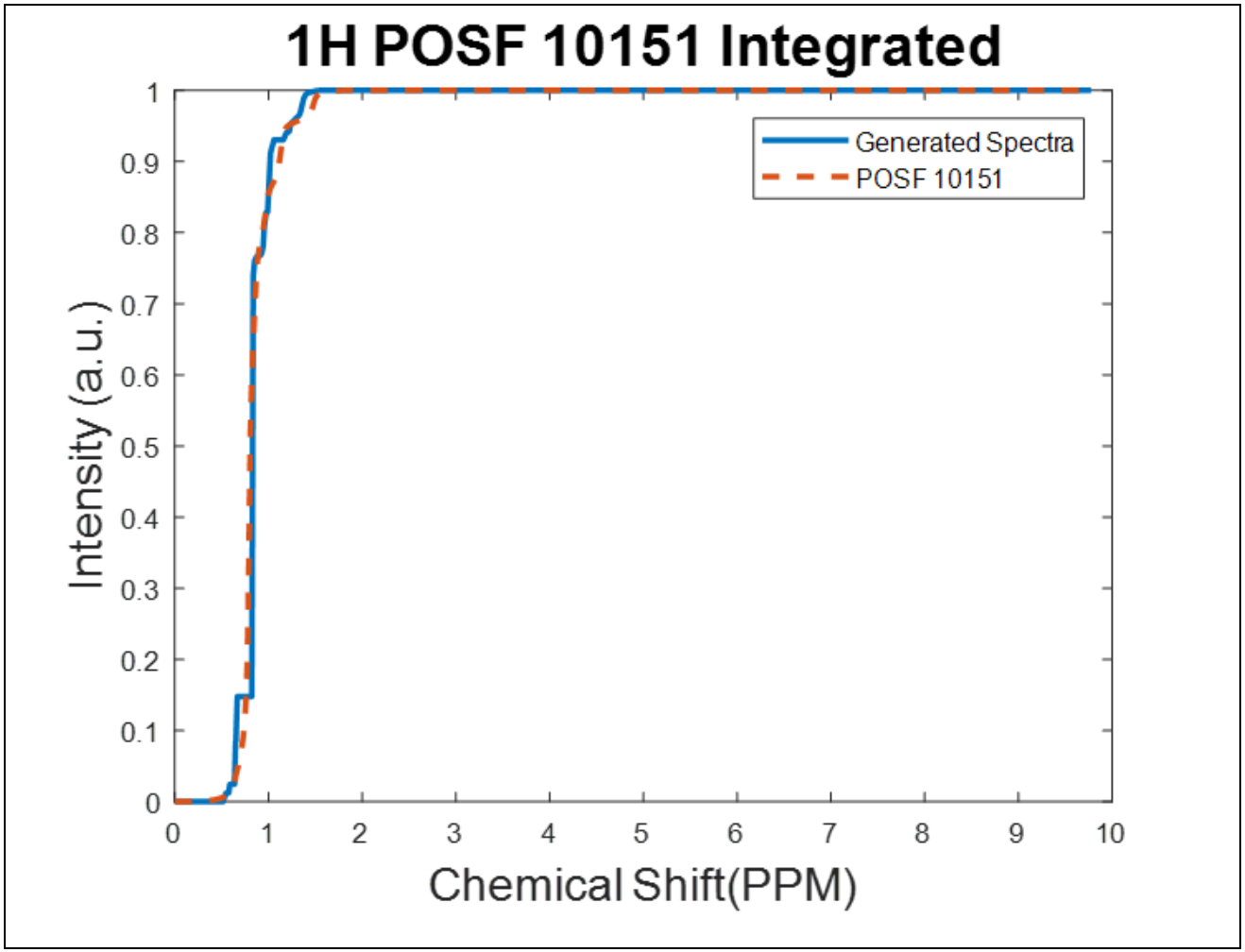

Figure 4.8: Integrated 1H NMR Spectra of Gevo ATJ

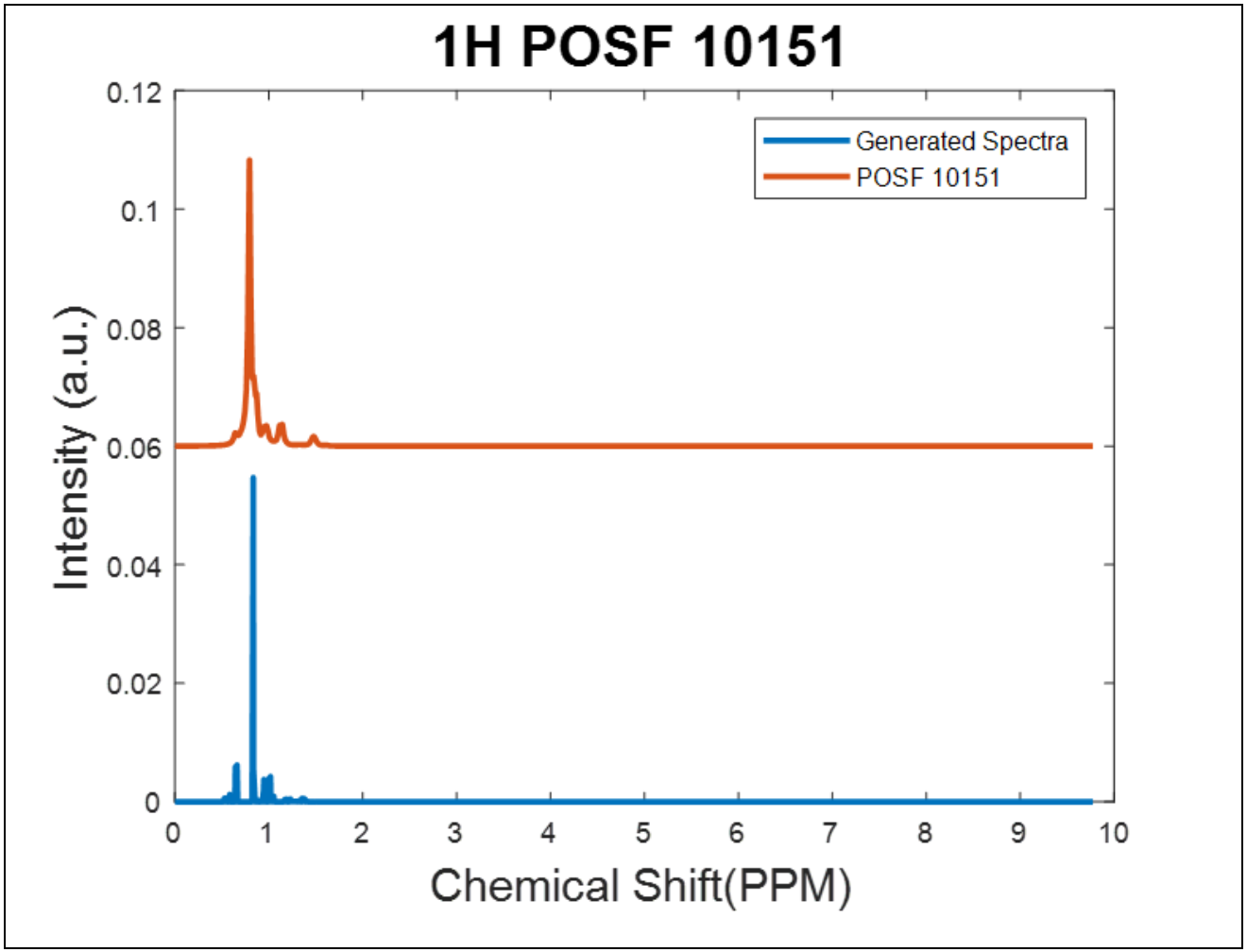

Figure 4.9: 1H NMR Spectra of Gevo ATJ

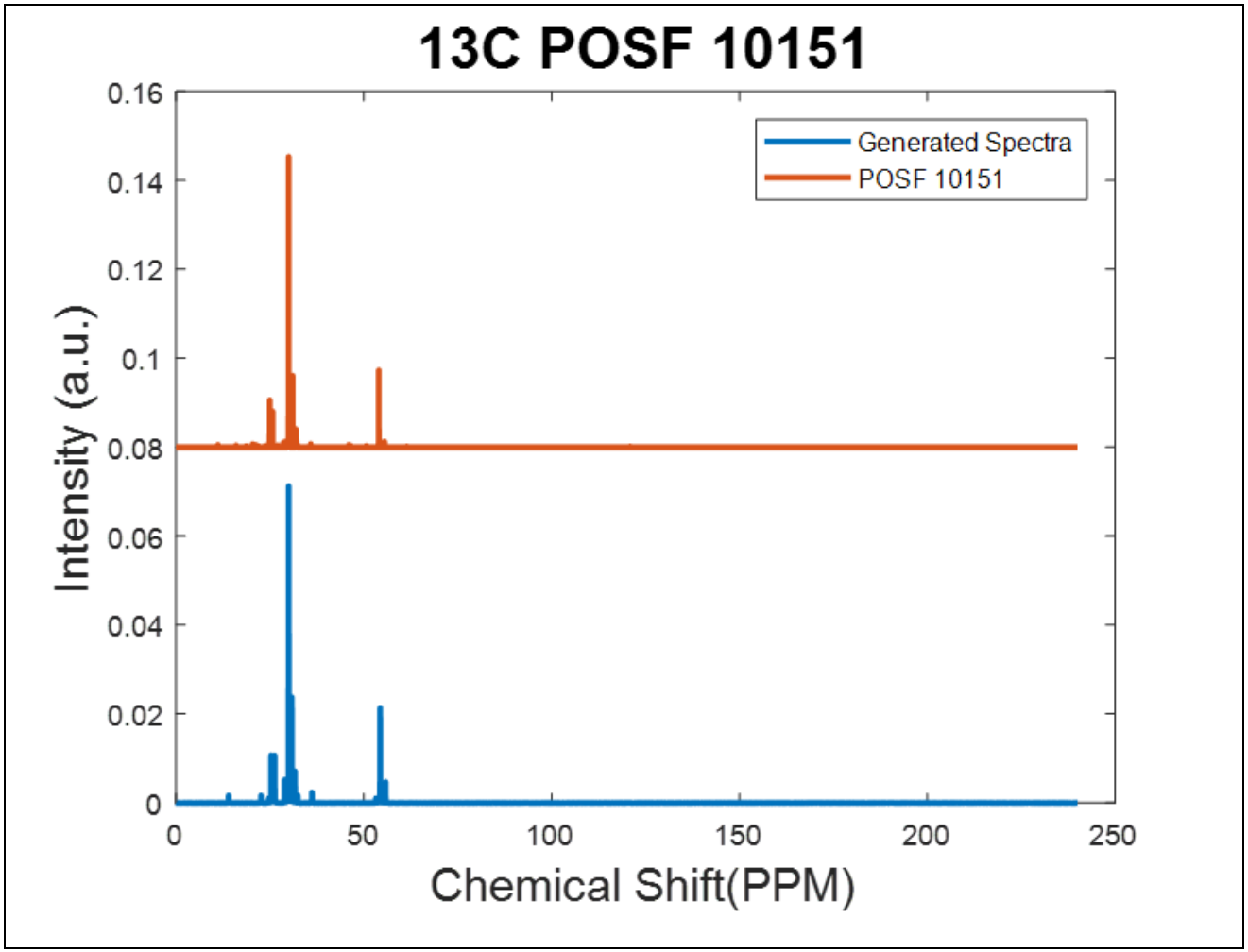

Figure 4.10: 13C NMR Spectra of Gevo ATJ

was adequately reproduced through the NMR spectra and the distillation curve, the CPT values needed to be compared to determine if it is indeed a match.

The predicted CPT's for the surrogate are shown in Table 4.2 along with the formulated surrogate. Except for the DCN, all of the CPT's are very well predicted. The Molecular Weight of the generated mixture is only 2.5 g/mol lighter than the real Gevo ATJ. The H/C ratio is within 0.005 of the target mixture which shows that the chemical functional groups are truly represented properly. The predicted DCN of this surrogate is substantially higher solely due to the lack of ability of the QSPR model that was used to properly predict the DCN value for the low DCN fuels such as iC12 and iC16 which comprise most of the mixture. This QSPR model over predicts the DCN for these two components by the same difference as that of the surrogate model and the target fuel. Taking the limitations of the QSPR into account, all of the CPT's match those of the target fuel within 1.43 % error not including DCN. These matched CPT's were predicted using only the chemical functional group distribution and the distillation curve which shows that this method will work even for unknown mixtures.

Now that this method has successfully generated surrogates for Surrogate 1 [21] and Gevo ATJ, the next step is to test with Shell SPK POSF 5729. Shell SPK is an alternative jet fuel that has substantially more chemical diversity than Gevo ATJ but still exhibits very little preferential vaporization potential. This was chosen as the next fuel to test as it will demonstrate whether or not this method will be able to simplify some chemical diversity while still constraining the preferential vaporization potential. The distillation curve for the surrogate that was generated can be seen in Figure 4.11. Because Shell SPK

Table 4.2: Generated Surrogate and CPT's of Gevo ATJ

Components	Mole Fraction	Combustion Property Target	Model Fuel	Target Fuel
nC7	0.001	DCN	27.4	15.1
nC8	0.0293	H/C ratio	2.163	2.168
nC10	0.0179	MW [g/mol]	173.1	175.6
nC12	0.0001	TSI	-	-
nC14	0.0074	Density at 15 °C [kg/m3]	753.9	759
nC16	0.0002	T_{10} [°C]	173	178
iC8	0.0684	T_{20} [°C]	179	179
iC12	0.7145	T_{50} [°C]	190	182
iC16	0.158	T_{90} [°C]	234	227
toluene	0			
nPB	0			
135TMB	0			
MCH	0.0031			
n-butylcyclohexane	0			

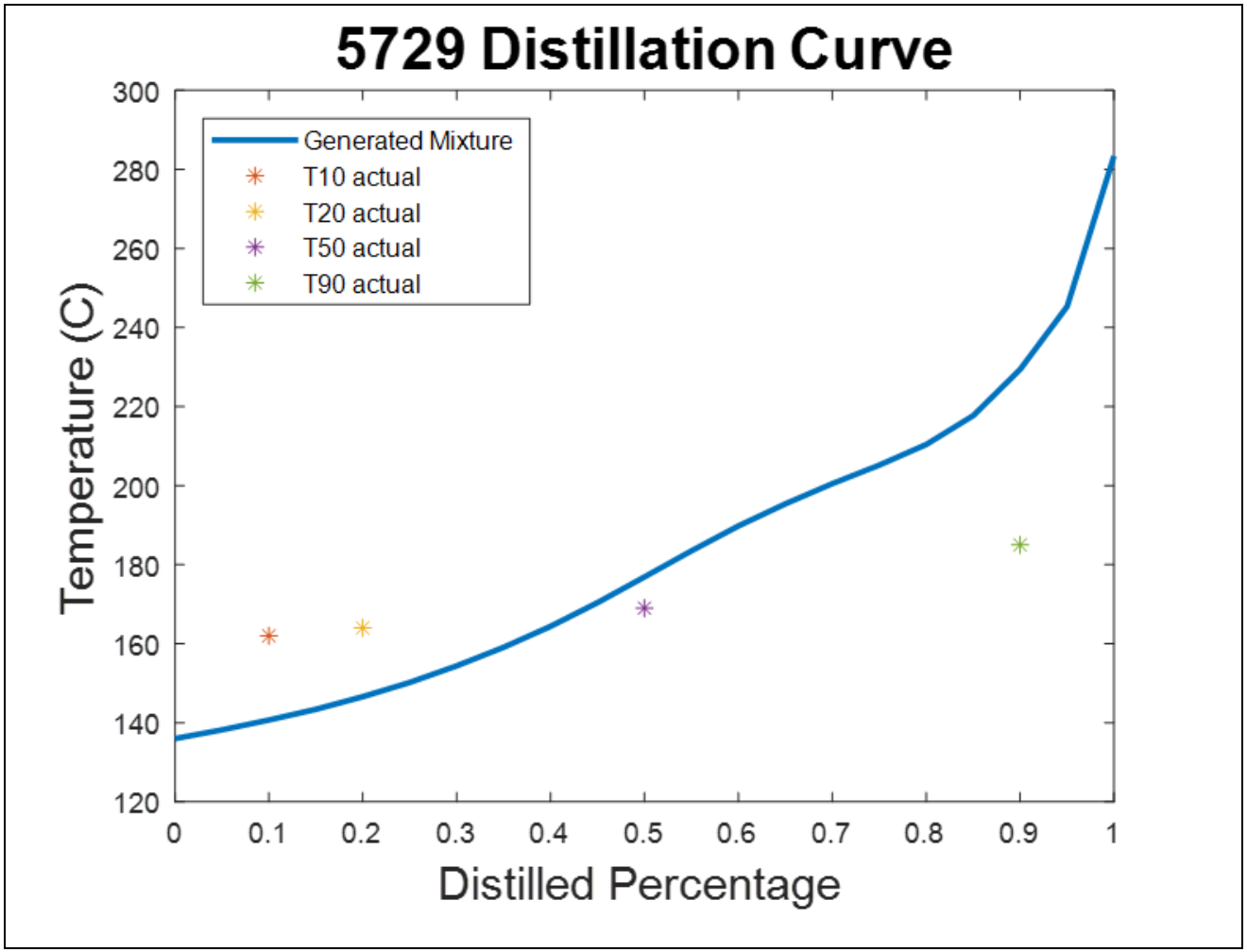

Figure 4.11: Distillation Curve of Shell SPK

is a synthetic parrafinic kerosene fuel it consists of very unique chemicals which may not be well represented by the chemical components that were used when testing this method. This lack of representation can be seen in the distillation curve where the generated mixture deviates significantly from the target fuel.

Figures 4.12 and 4.13 show the NMR spectra comparison between the generated surrogate and the real fuel. There is almost an exact match in the 1H spectrum which shows that the components are still well suited for capturing many of the chemical properties. From the 13C spectra comparison in Figure 4.13, it is clear that the key chemical functional groups are matched as well in the carbon environments. There is a 0.32 % error in the 1H spectrum in Figure 4.12. The carbon spectrum was not as well reproduced as the 1H spectrum was but the level of similarity between them gives strong support for this surrogate to reproduce the chemical properties. The 13C spectrum had a 5.61 % error.

These chemical properties were predicted using the same QSPR model as the previous fuels used and the results can be seen in Table 4.3. Table 4.3 also shows the formulated surrogate mixture and the CPT values of the target fuel for comparison. The DCN is almost identical between the two fuels which shows that this method once again captures the ignition properties of the target fuel from the chemical functional group distribution. The H/C ratio is matched to a difference of 0.042 which shows that the chemical functional groups of the surrogate are matching the chemical functional groups present in the target fuel. The MW of the target fuel is slightly lower than that of the surrogate mixture by 5 g/mol which shows that this method can even predict the physical properties of the fuels. Overall the CPT values matched within a 3.8 % error of the values

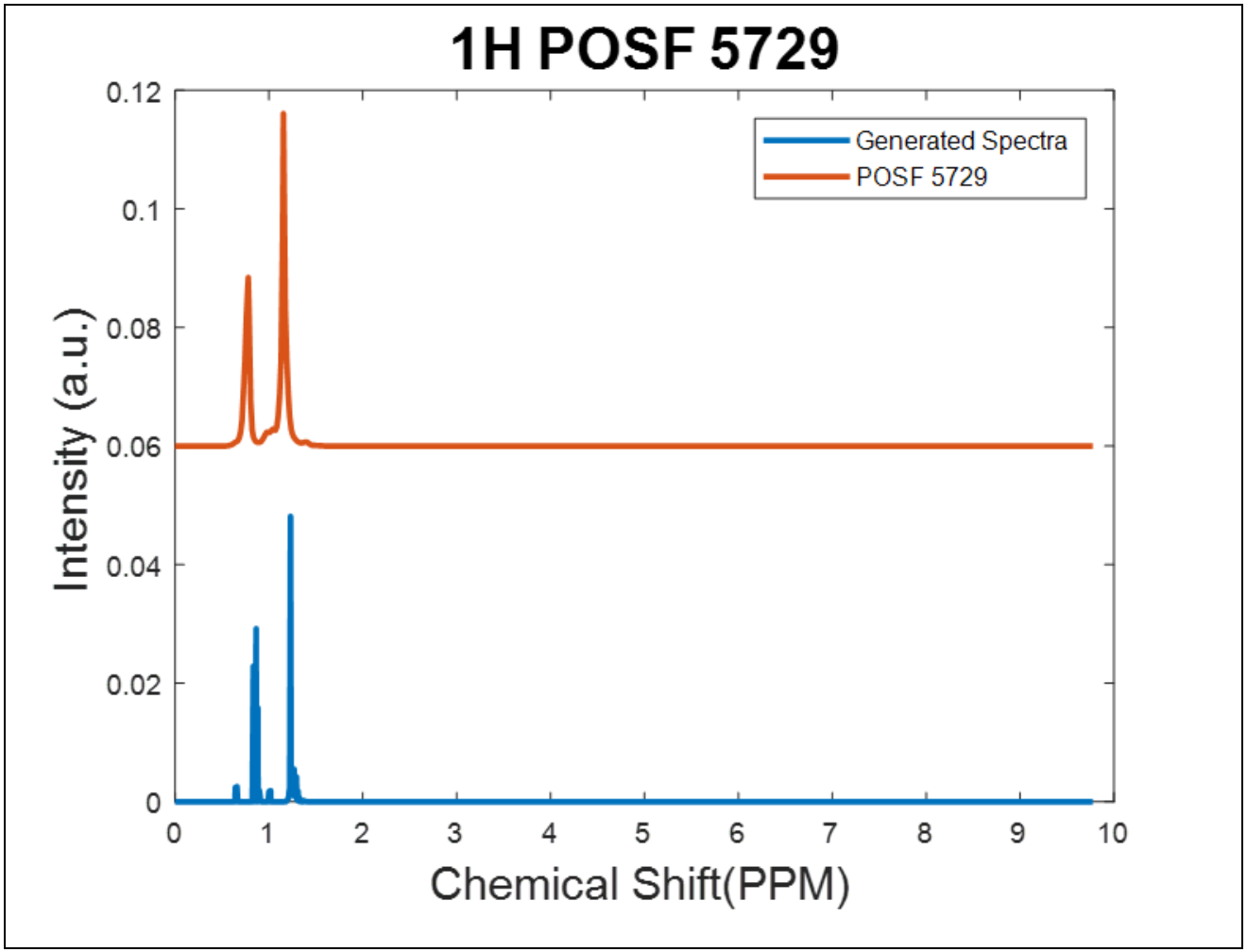

Figure 4.12: 1H NMR Spectra of Shell SPK

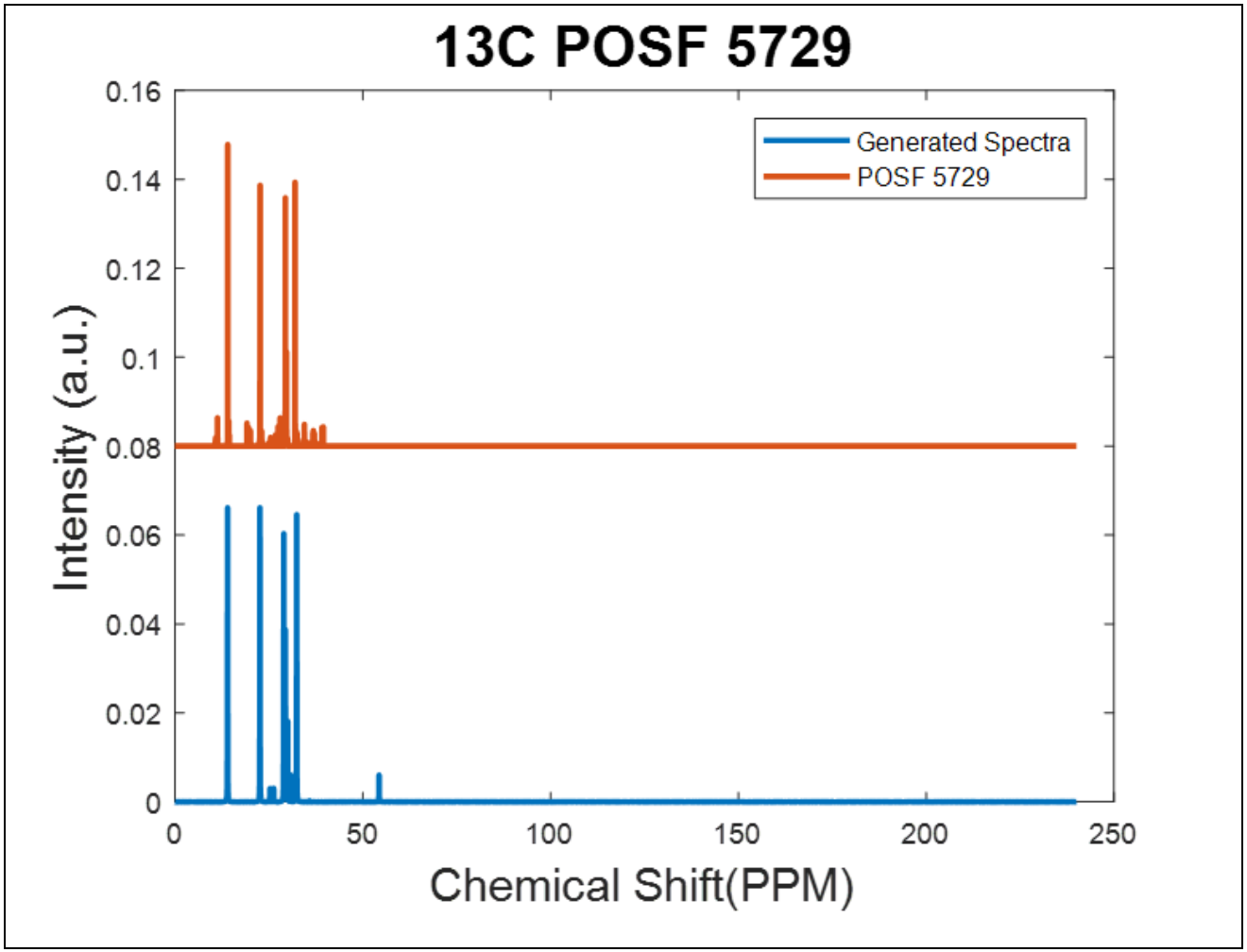

Figure 4.13: 13C NMR Spectra of Shell SPK

Table 4.3: Generated Surrogate and CPT's of Shell SPK

Components	Mole Fraction	Combustion Property Target	Model Fuel	Target Fuel
nC7	0.2162	DCN	59.99	58.4
nC8	0.2162	H/C ratio	2.198	2.24
nC10	0.2162	MW [g/mol]	143.6	138.3
nC12	0.2162	TSI	-	-
nC14	0.0146	Density at 15 °C [kg/m3]	733.9	-
nC16	0.0346	T_{10} [°C]	141	162
iC8	0	T_{20} [°C]	147	164
iC12	0.0829	T_{50} [°C]	177	169
iC16	0	T_{90} [°C]	229	185
toluene	0			
nPB	0			
135TMB	0			
MCH	0.0032			
n-butylcyclohexane	0			

for the real fuel. The comparison between the two NMR spectra and the distillation curve as well as the slight differences in CPT values show that this method can have sensitivity to the surrogate components which is to be expected as they should ideally be chosen to represent the fuel.

Because of the sensitivity to the surrogate components that was seen when using this method on Shell SPK, the next fuel that was tested was very similar. Sasol IPK is a synthetic jet fuel that is actually formed from coal and as such is an iso-parrafinic kerosene fuel. It is very similar to the Shell SPK in that it exhibits very low preferential vaporization potential while having significantly more chemical diversity than the Gevo ATJ fuel that was tested previously. Figure 4.14 shows the distillation curve from the generated surrogate and it shows that it is consistently 15°C low in the light end compared to the real fuel.

The 1H spectra that was generated matches the majority of the target spectra and is shown in Figure 4.15. The chemical functional groups are in the correct locations with the similar intensities which shows that the same chemical functional groups are present. In Figure 4.16 the 13C spectra comparison can be seen. The carbon spectrum of the real fuel is very broad with a large amount of diversity in the carbon structures present. The formulated surrogate matches the main functional group from the 13C spectrum but it does not capture the diversity of the other functional groups that are present. The predicted CPT values are shown in Table 4.4 to determine how much of an impact the fitting of the chemical functional group distribution can have on the CPT values of the surrogate.

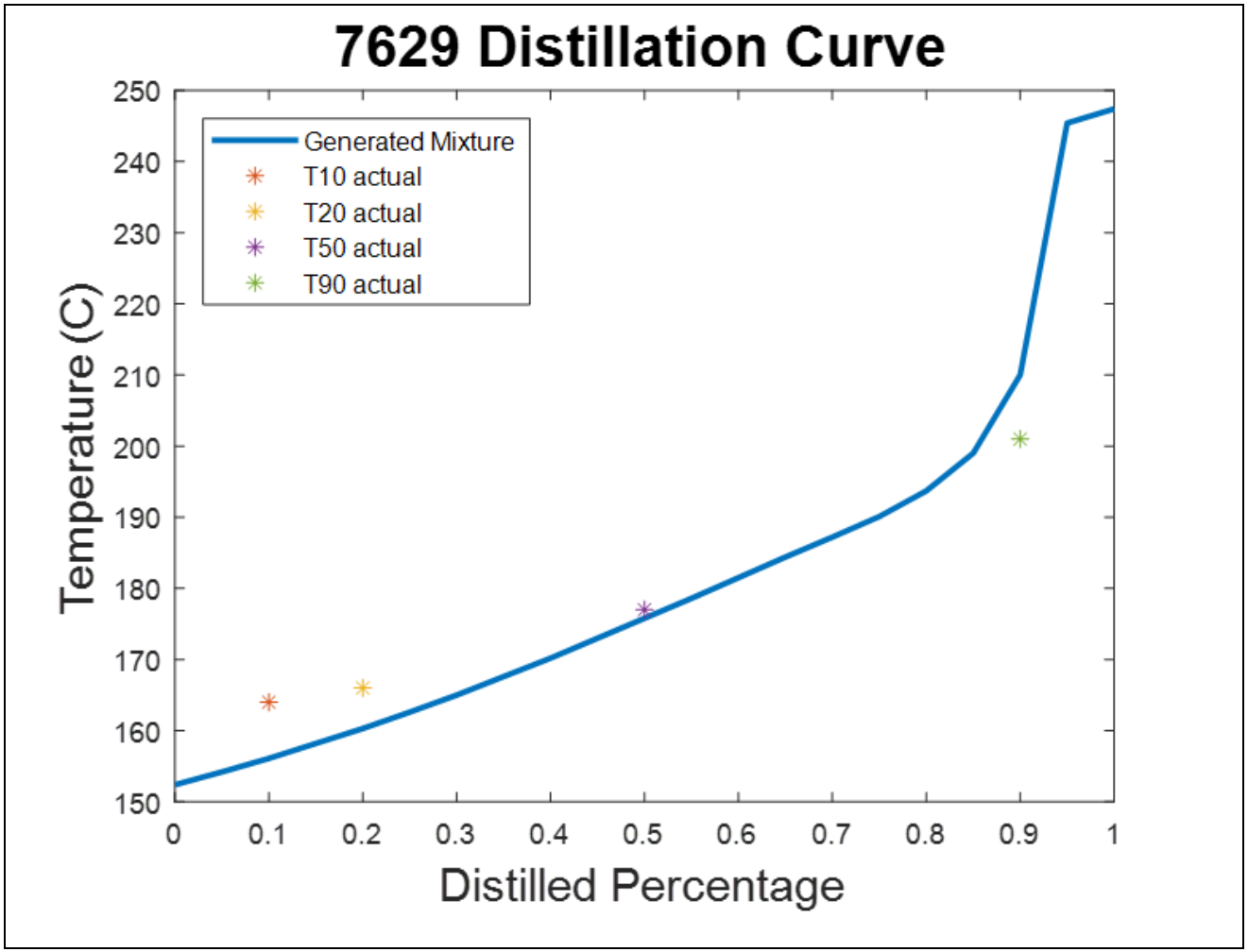

Figure 4.14: Distillation Curve of Sasol IPK

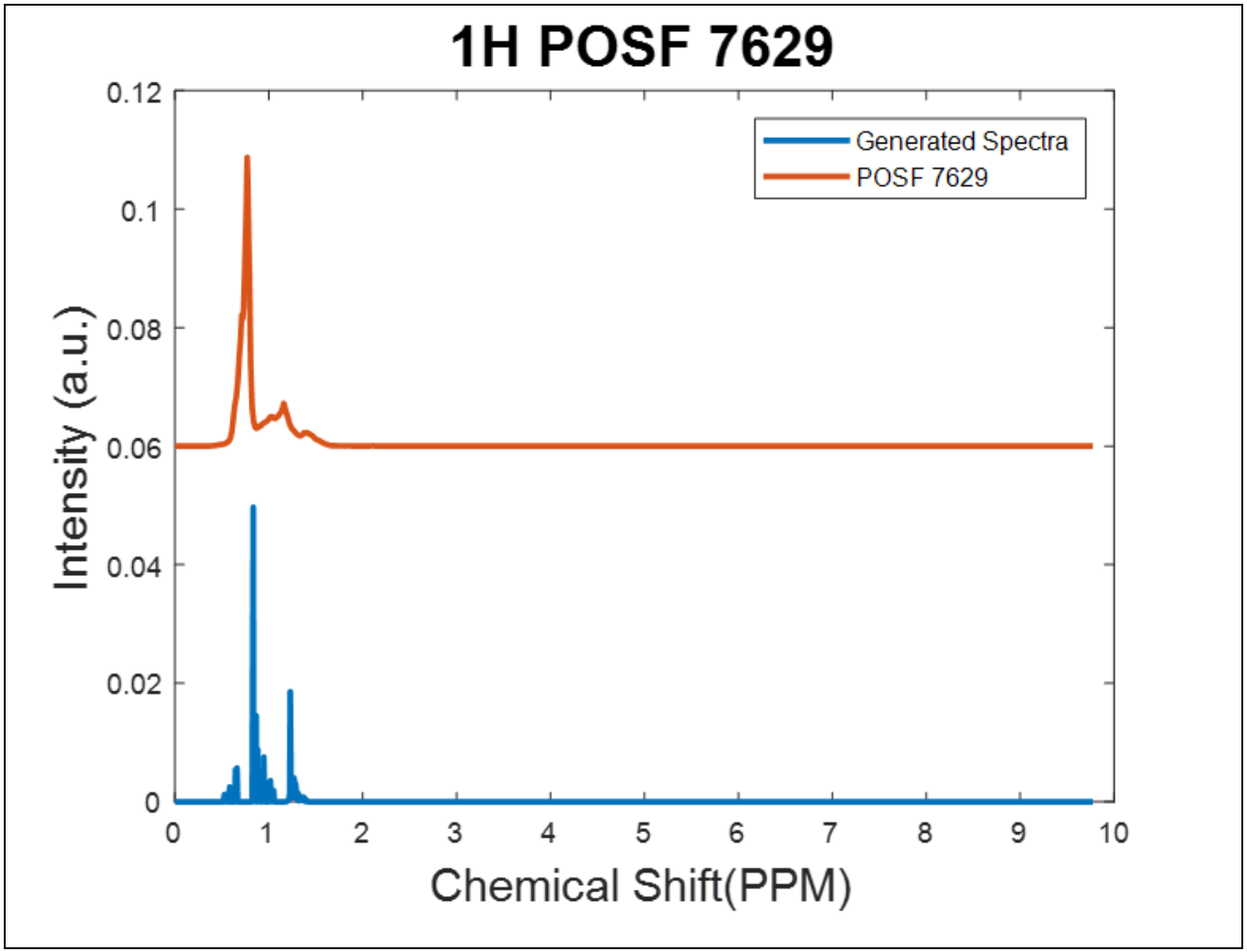

Figure 4.15: 1H NMR Spectra of Sasol IPK

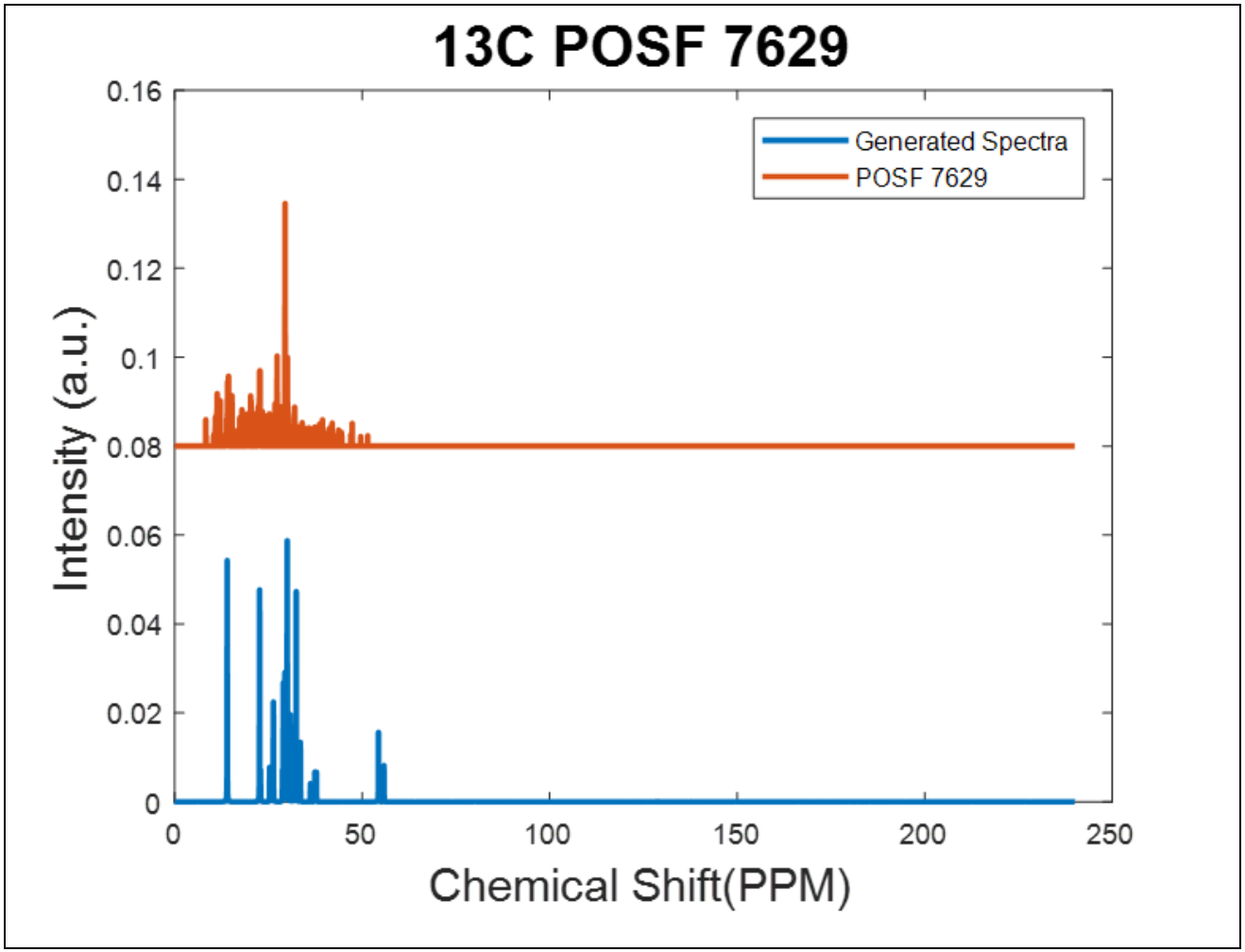

Figure 4.16: 13C NMR Spectra of Sasol IPK

Table 4.4: Generated Surrogate and CPT's of Sasol IPK

Components	Mole Fraction	Combustion Property Target	Model Fuel	Target Fuel
nC7	0.0392	DCN	52.4	31.3
nC8	0.2609	H/C ratio	2.163	2.195
nC10	0.2609	MW [g/mol]	146.1	148.5
nC12	0	TSI	-	-
nC14	0	Density at 15 °C [kg/m3]	748.2	-
nC16	0	T_{10} [°C]	156	164
iC8	0	T_{20} [°C]	160	166
iC12	0.1821	T_{50} [°C]	175	177
iC16	0.0965	T_{90} [°C]	210	201
toluene	0.0007			
nPB	0			
135TMB	0			
MCH	0.0021			
n-butylcyclohexane	0.1576			

From Table 4.4, it is clear that the DCN is not reproduced in the surrogate fuel which means that the mixtures could behave significantly differently in near limit conditions. The H/C ratio that is shown in Table 4.4 shows that the surrogate does match that of the target fuel to a difference of 0.032 and this is extremely useful in determining what the flame temperature of the fuel will be. The MW of the target fuel is also very close to the surrogate mixture with a 2.4 g/mol difference this allows the physical properties that are governed by the MW to be very similar. This lack of ability to capture the chemical functional groups, CPT's, or the boiling characteristics is primarily due to the fact that none of the surrogate components that were used can capture both.

Because of this, the algorithm was rerun using only the 1H NMR spectrum and distillation curve as it removes the constraints of the carbon structures which are so unique to Sasol IPK. The new distillation curve comparison can be seen in Figure 4.17 and it matches much better than the previous run with all temperatures being within 10°C of the target fuel. The new 1H spectrum is also a closer match than before with the location still being consistent and the relative intensities matching much better than previously.

This new 1H spectrum can be seen in Figure 4.18 and it is clear from these two comparisons that the surrogate is much better at reproducing both the chemical functional groups and the distillation curve when not constrained by the carbon structures. Figure 4.19 shows the 13C spectrum comparison which was not used as a surrogate formulation constraint. Even in this new comparison the most prominent functional groups and structures are the same between the two with slight differences in diversity and quantities.

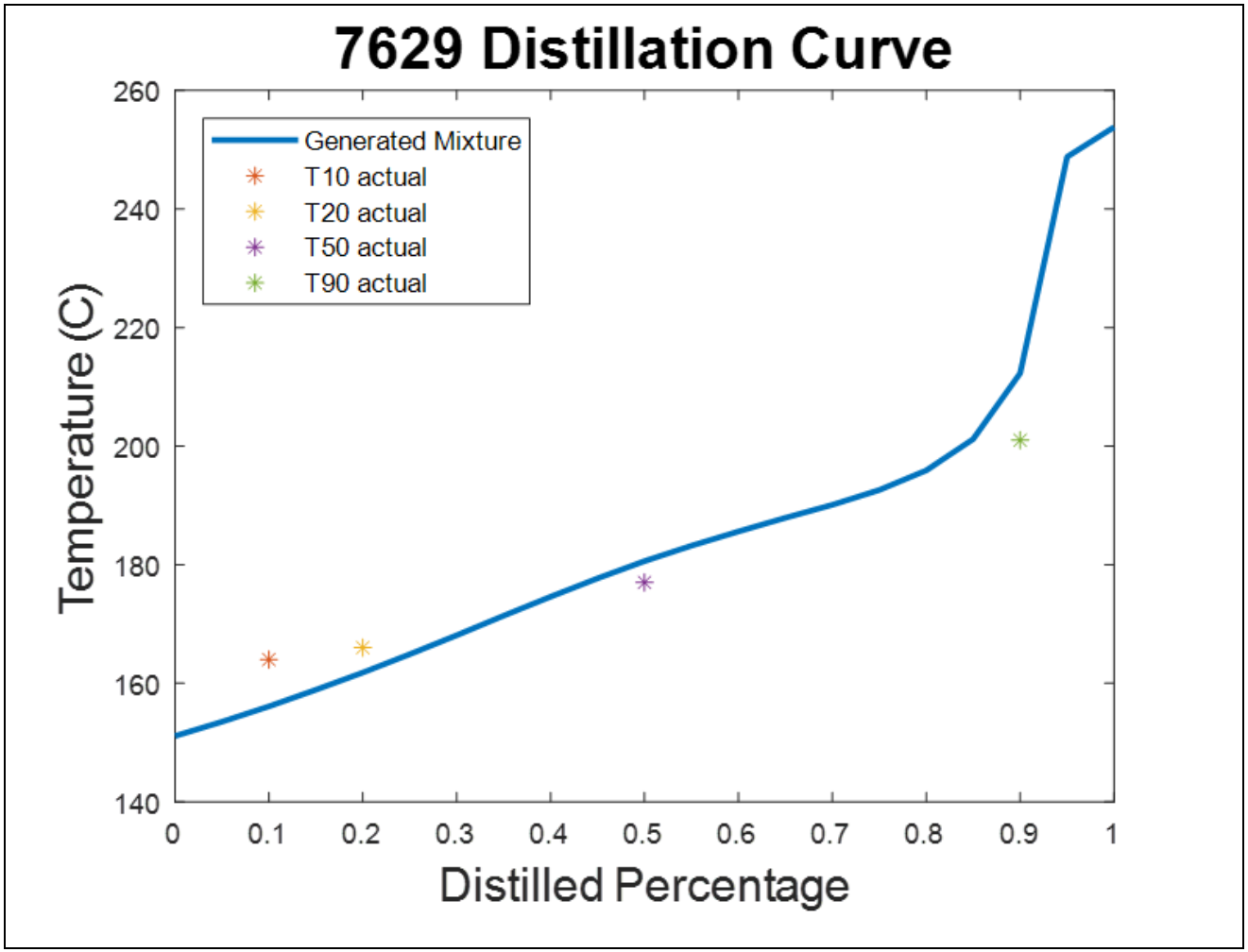

Figure 4.17: Distillation Curve of Sasol IPK (1H Only)

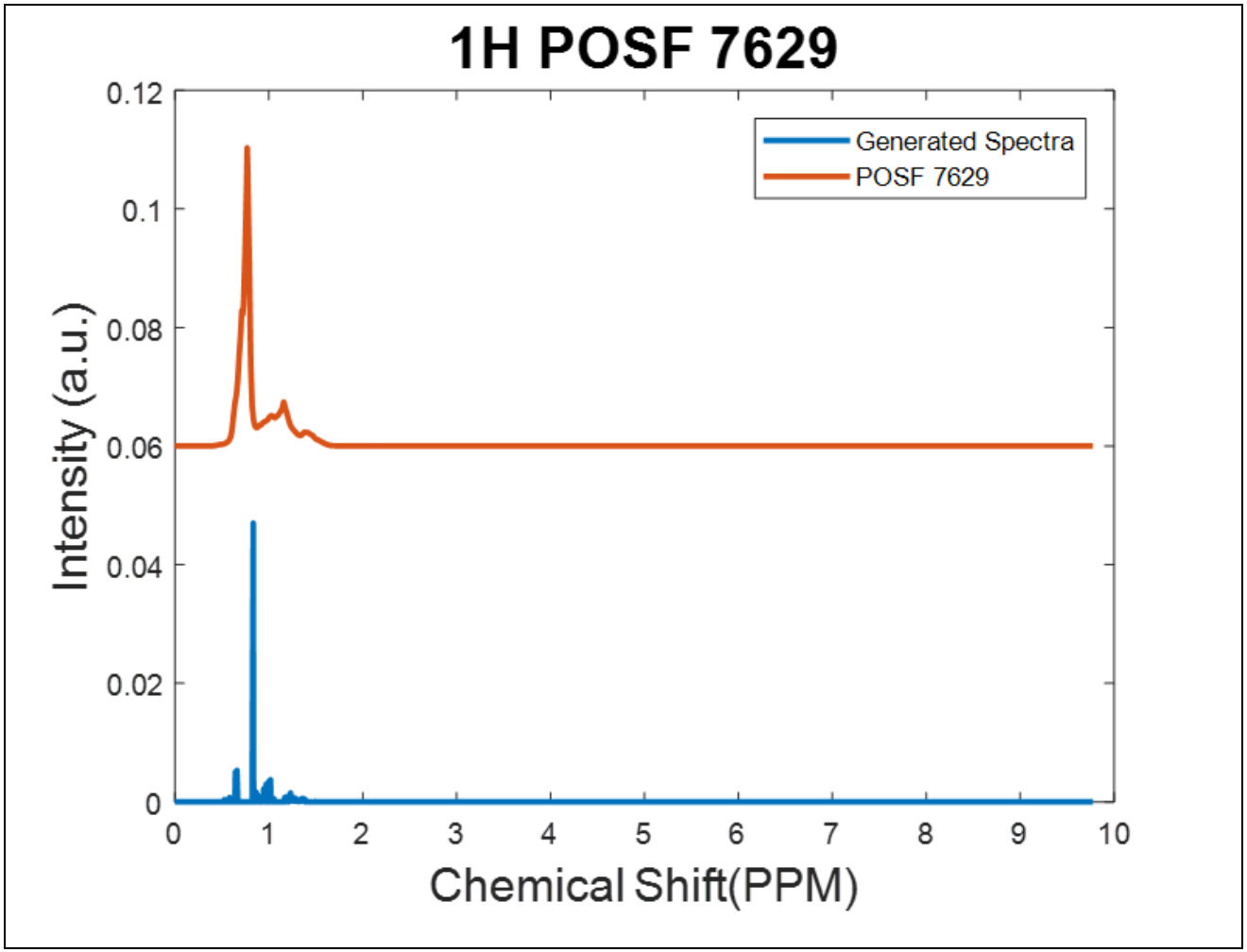

Figure 4.18: 1H NMR Spectra of Sasol IPK (1H Only)

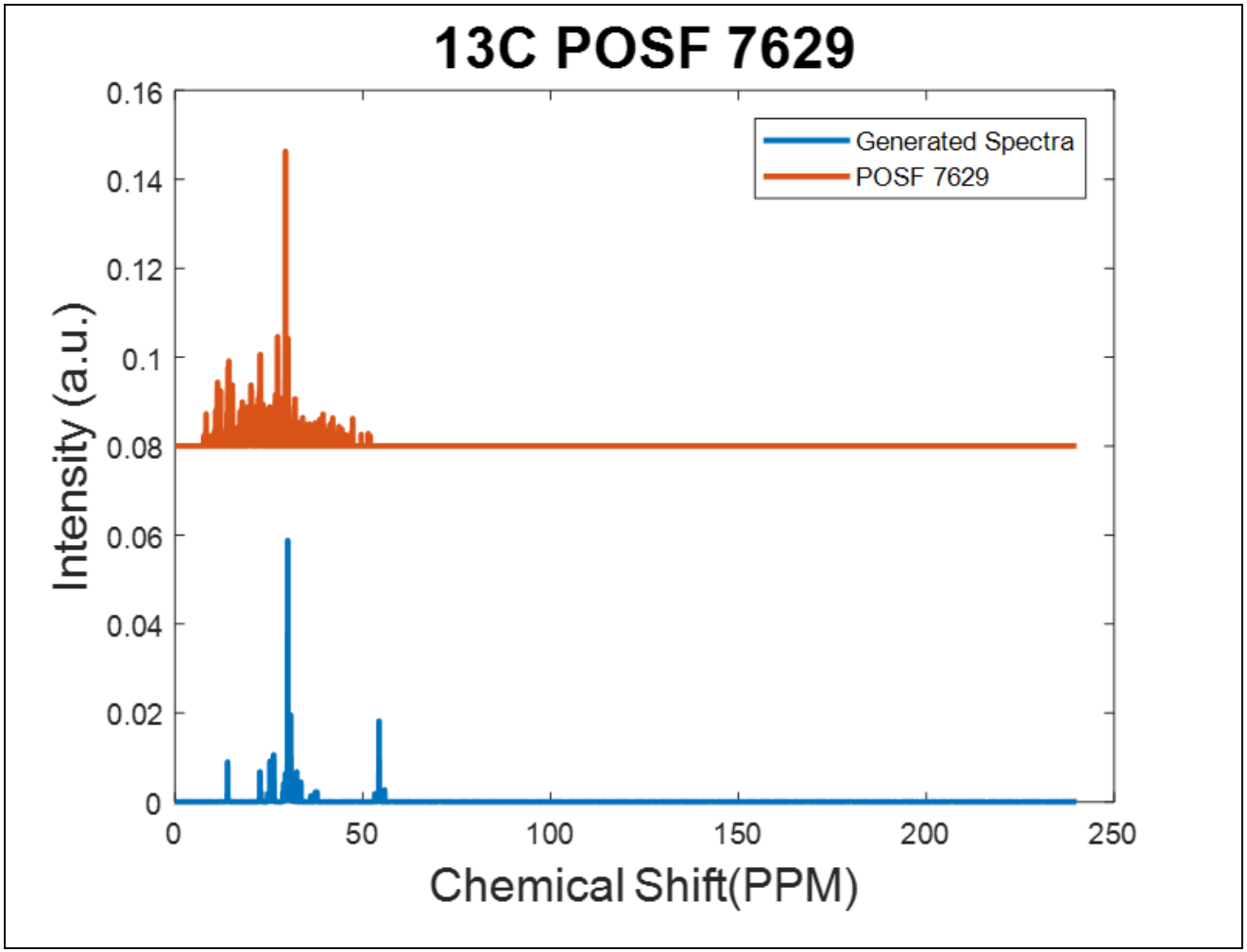

Figure 4.19: 13C NMR Spectra of Sasol IPK (1H Only)

Table 4.5: Generated Surrogate and CPT's of Sasol IPK (1H Only)

Components	Mole Fraction	Combustion Property Target	Model Fuel	Target Fuel
nC7	0.0005	DCN	36.8	31.3
nC8	0.1664	H/C ratio	2.159	2.195
nC10	0	MW [g/mol]	156.4	148.5
nC12	0	TSI	-	-
nC14	0.0227	Density at 15 °C [kg/m3]	750.6	-
nC16	0	T_{10} [°C]	156	164
iC8	0.1023	T_{20} [°C]	161	166
iC12	0.508	T_{50} [°C]	181	177
iC16	0.0759	T_{90} [°C]	212	201
toluene	0			
nPB	0			
135TMB	0.0001			
MCH	0			
n-butylcyclohexane	0.1242			

Because the goal of the surrogate is to match all of the CPT values the predicted values are shown for the new mixture in Table 4.5.

It is clear from Tables 4.4 and 4.5 that the new surrogate fits the target fuels CPT values better than the previous surrogate which was constrained using the 13C NMR spectrum. The DCN value of the new mixture is substantially closer than it was before and it within 5.5 DCN of the target fuel. This value being much closer means that the near limit behaviors that are influenced by the ignition properties will be similar as well as the fact that the ignition properties themselves will be the same. Both the H/C ratio and the MW that are predicted for the new surrogate are similar to the previous run and the slight differences are more than satisfactory for a substantially closer value for the DCN. Overall the CPT values for the new run matched within a 17.5% error of the values for the real fuel. Even with the lack of ability to capture the chemical functional group distribution, distillation curve, and carbon structures in the surrogate components, a surrogate can be formulated that matches the CPT values, distillation curve and chemical functional group distribution by using only the 1H NMR spectrum and distillation curve.

Because there is significant interest in producing surrogate fuels to simplify the extreme levels of chemical diversity in petroleum derived real fuels, the next set of fuels that were tested were Jet-A POSF 10325, JP-8 POSF 10264, and JP-5 POSF 10289. All three of these fuels are petroleum derived jet fuels and are widely used in many applications. Both Jet-A and JP-8 have a larger potential for preferential vaporization than JP-5 as it was formulated to have a substantially higher flash point, and this can be seen in Figure 2.2.

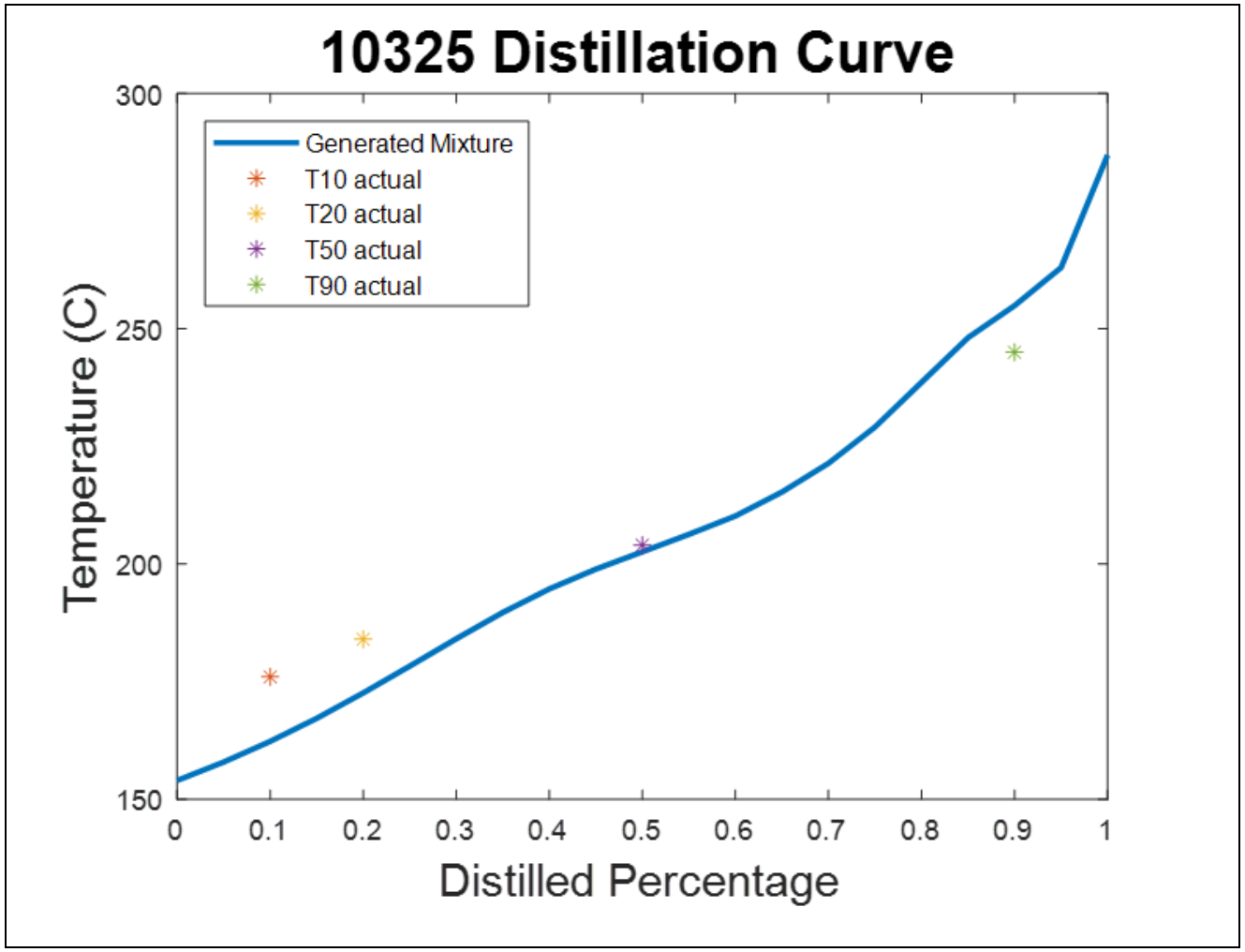

Figure 4.20: Distillation Curve of Jet-A

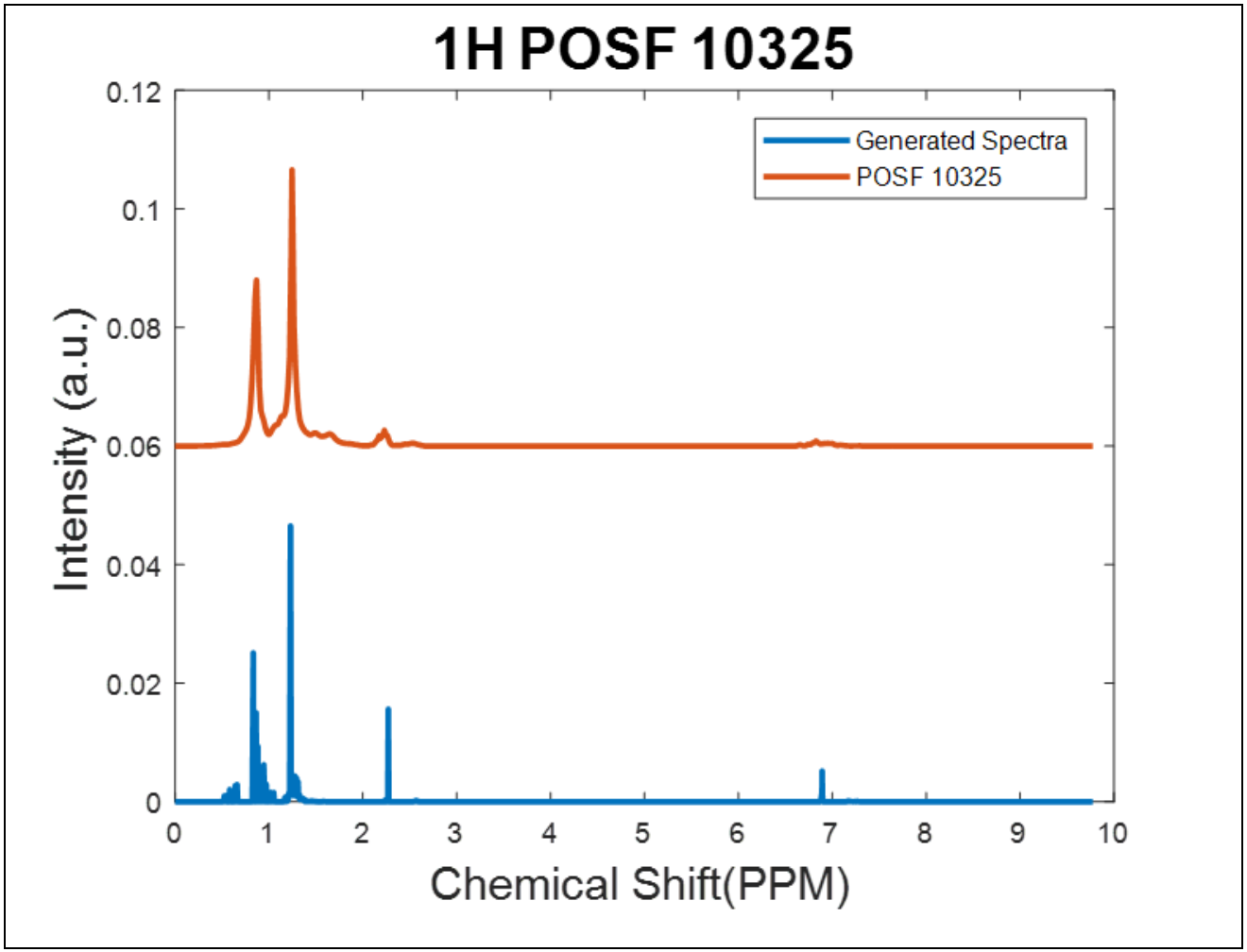

Figure 4.21: 1H NMR Spectra of Jet-A

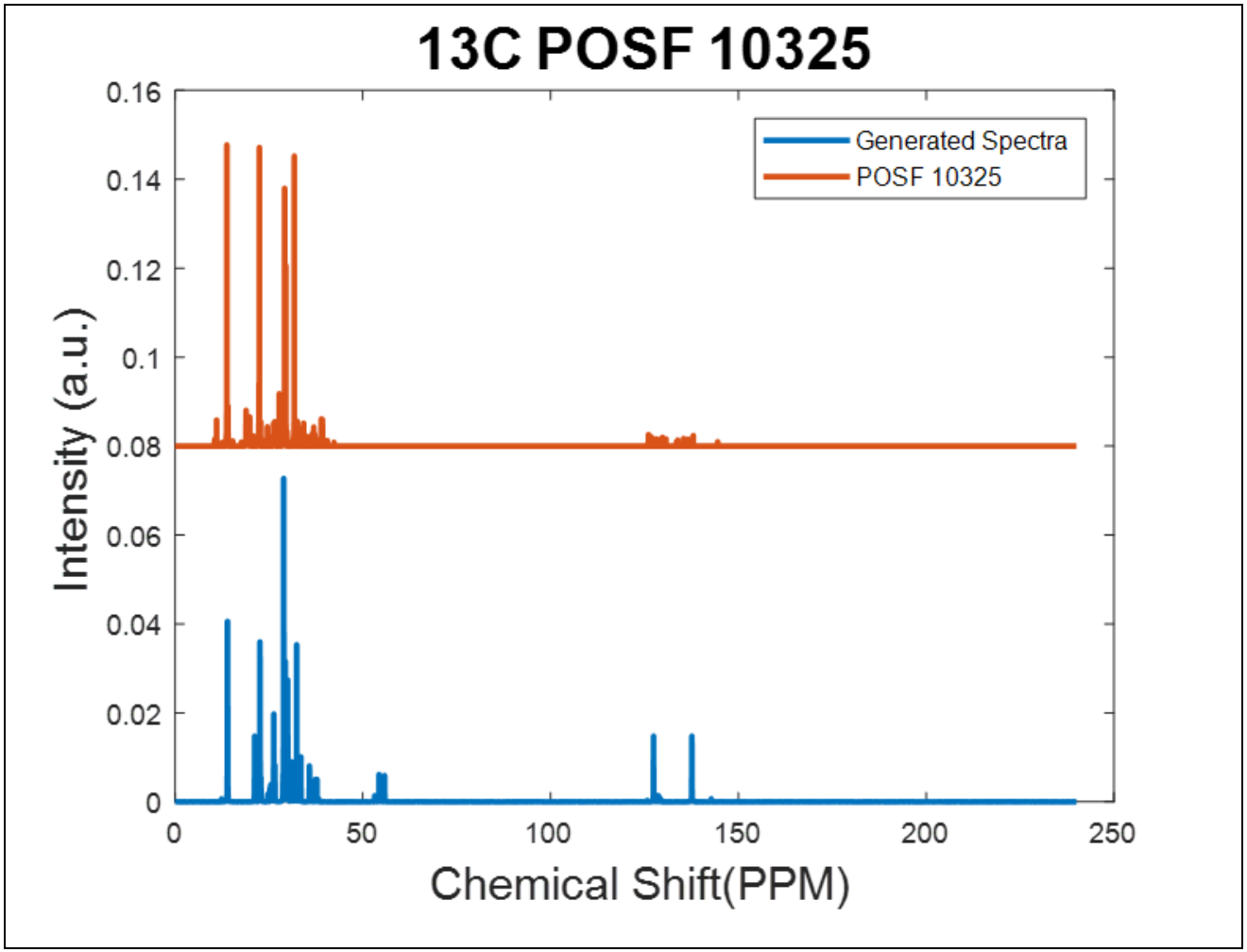

Figure 4.22: 13C NMR Spectra of Jet-A

Table 4.6: Generated Surrogate and CPT's of Jet-A

Components	Mole Fraction	Combustion Property Target	Model Fuel	Target Fuel
nC7	0.0298	DCN	53.3	50
nC8	0.0309	H/C ratio	2.034	1.961
nC10	0.0999	MW [g/mol]	152.8	160.8
nC12	0.1223	TSI	-	-
nC14	0.1195	Density at 15 °C [kg/m3]	773	804
nC16	0.04	T_{10} [°C]	162	176
iC8	0.0348	T_{20} [°C]	173	184
iC12	0.0751	T_{50} [°C]	203	204
iC16	0.0738	T_{90} [°C]	255	245
toluene	0.0083			
nPB	0.0168			
135TMB	0.1226			
MCH	0.1007			
n-butylcyclohexane	0.1256			

When formulating a surrogate for Jet-A POSF 10325, the results are shown in Figures 4.20-4.22 with the predicted CPT values in Table 4.6. From the 1H spectrum, the largest functional groups are reproduced with the appearance of substantial deviation from the aromatic groups and the aromatic CH group. This deviation is not nearly as significant as it appears because the simulated spectrum is much sharper and the area under the curve is equal for both.

Similarly, in the 13C spectra shown in Figure 4.22, the key functional groups are all present with the biggest difference in the 3rd largest peak from the left. This peak is present in both but in the real fuel's NMR spectrum it is actually a doublet and another singlet peak in close proximity and has the same integrated value as the singlet peak on the simulated spectrum. The distillation curve of the formulated surrogate reproduces that of the real fuel to within 10 degrees C which is within a believable uncertainty for the measured data from the distillation tests.

Table 4.6 shows the formulated surrogate mixture for Jet-A as well as the CPT values for both the surrogate and real fuel. By comparing the predicted DCN of the surrogate to the DCN of the real fuel, there is a difference of 3.3 DCN which is close enough to be well within the limitations of the QSPR model to accurately predict. The H/C ratio and MW are also shown for both fuels in Table 4.6 and there is a difference of 0.073 and 8.0 g/mol between the two. While this is not quite as well of a match as hoped for, with a max of 6.6% error, the nature of the extreme chemical diversity is influencing the real fuel values. Because of this chemical diversity, the surrogate can approximate the CPT values for the target fuel but they are not as precise of a match as the alternative fuels.

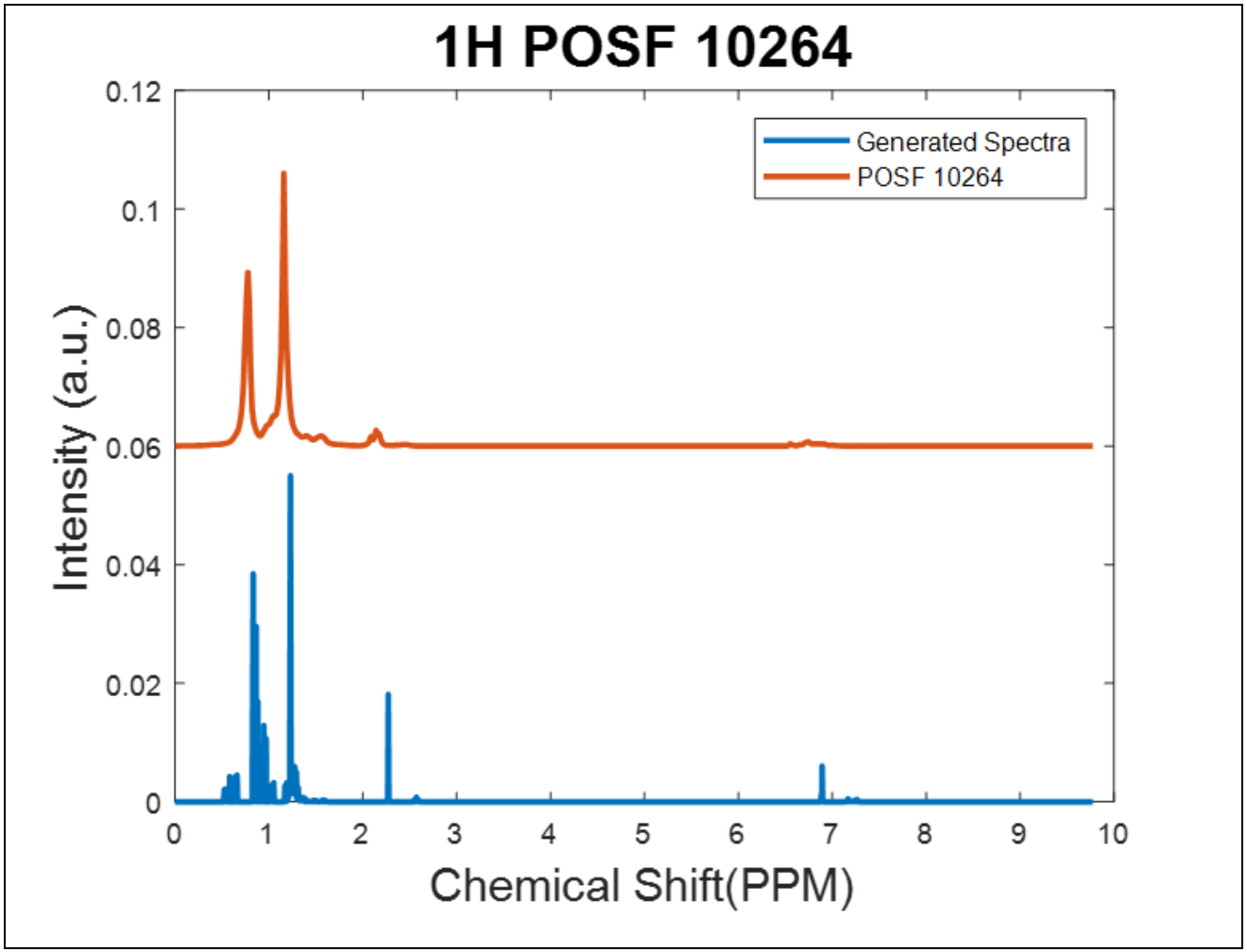

Figure 4.23: 1H NMR Spectra of JP8

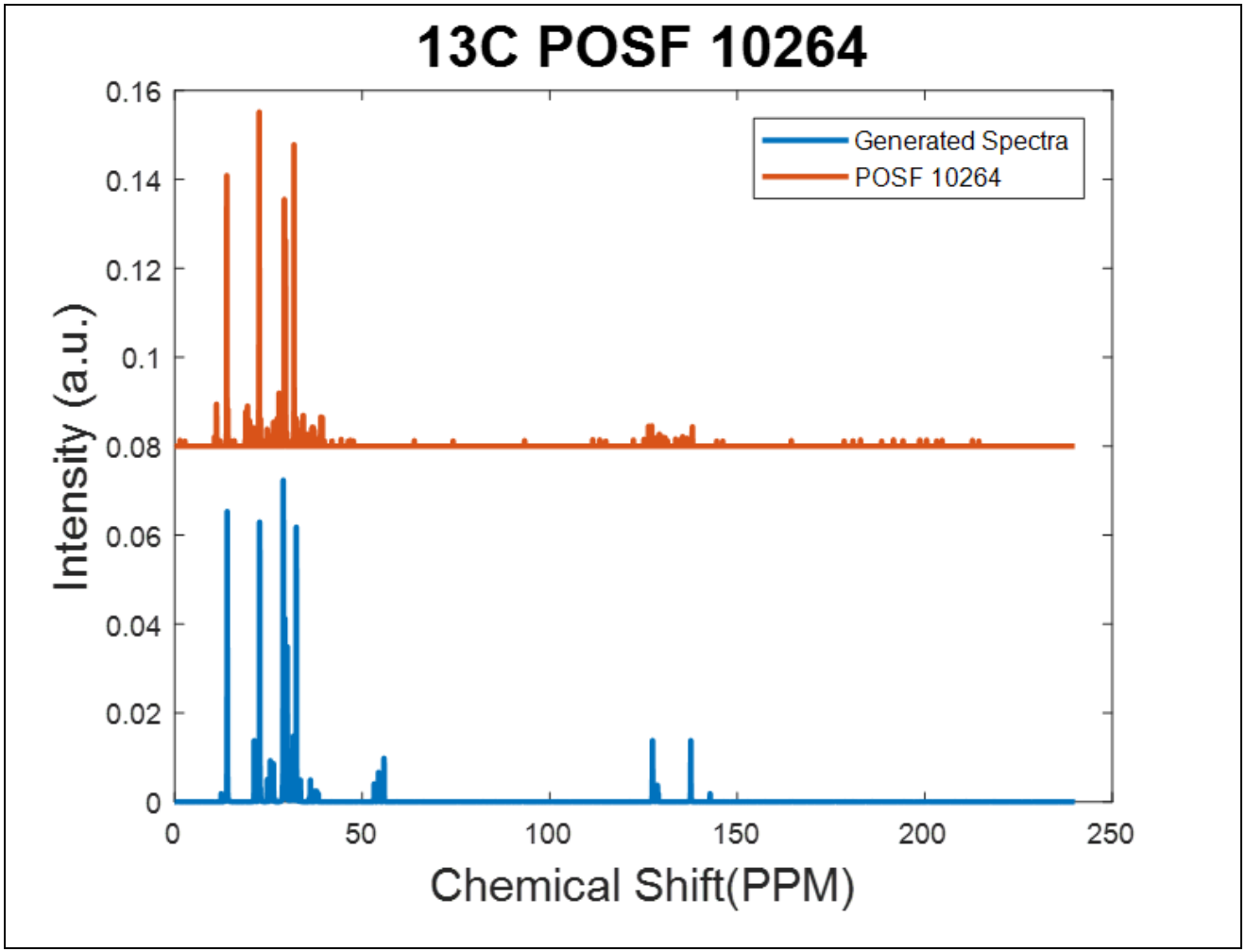

Figure 4.24: 13C NMR Spectra of JP8

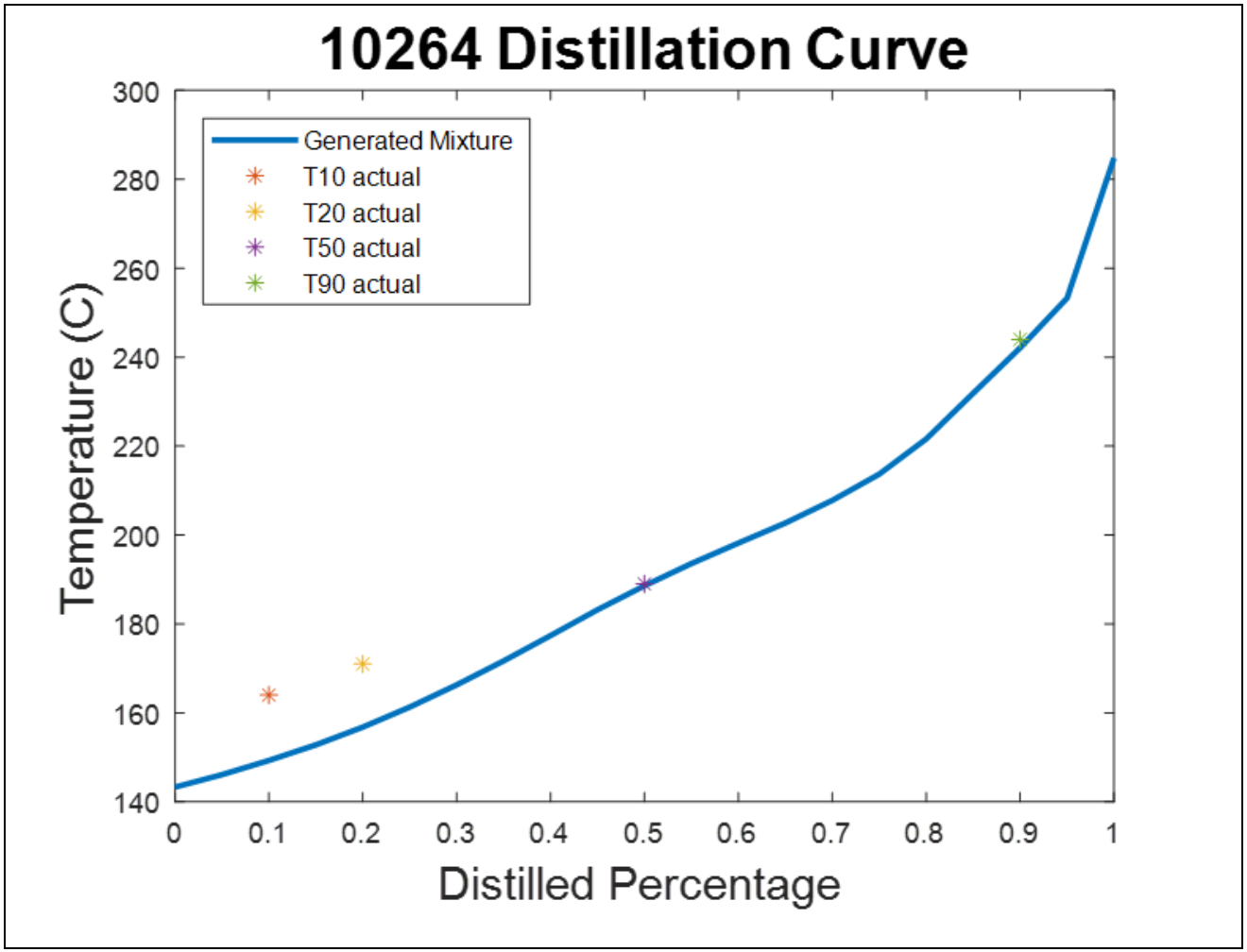

Figure 4.25: Distillation Curve of JP8

Table 4.7: Generated Surrogate and CPT's of JP8

Components	Mole Fraction	Combustion Property Target	Model Fuel	Target Fuel
nC7	0.1073	DCN	54.7	49.6
nC8	0.1313	H/C ratio	2.089	2.02
nC10	0.155	MW [g/mol]	146.1	152
nC12	0.1467	TSI	-	-
nC14	0.0371	Density at 15 °C [kg/m3]	754	780
nC16	0.0185	T_{10} [°C]	149	164
iC8	0.0766	T_{20} [°C]	157	171
iC12	0.0606	T_{50} [°C]	189	189
iC16	0.0928	T_{90} [°C]	242	234
toluene	0			
nPB	0.0345			
135TMB	0.087			
MCH	0.0064			
n-butylcyclohexane	0.0461			

Just as with the Jet-A, the results for JP-8 are shown in Figures 4.23-4.25 and the predicted values for the various CPT's are shown in Table 4.7. The 1H NMR spectra comparison between the formulated surrogate and the real fuel that is shown in Figure 4.23 accounts for all of the key functional group species that are present. There is a similar amount of CH_3, CH_2, CH, and aromatic groups in all once the resolution of the real fuel's NMR measurements is taken into account.

The real fuel's NMR spectrum is by nature substantially broader than that of the simulated spectrum because the NMR records the real-world response of the nuclei to the electromagnetic field. In Figure 4.24 the 13C NMR comparison can be seen and just as the NMR spectrum is broader in the proton domain, it is broader in the 13C domain as well for the real fuels. The formulated surrogate does contain the same chemical functional groups in similar quantities to that of the real fuel in the standard NMR spectrum and the inconsistencies can be explained by the broader resolution of the real-world measurements.

The distillation curve for the formulated surrogate is shown in Figure 4.25 along with the 4 known measurements of the target fuel. The distillation curve of the surrogate follows the trend of the target fuel and is within 15 degrees C of the real fuel. This deviation from the real fuel could be due to errors in the measurements of the real fuel, the fact that the bubble point calculation overestimates the real boiling temperature, or the chemical diversity in the real fuel may not be entirely accounted for in the surrogate components.

Table 4.7 shows the surrogate mixture as well as the various CPT's for both the real and surrogate fuels. Comparing the DCN values between the two shows that there is a 5 DCN difference between the two which falls within an acceptable range of the target

because of the limits of how accurately the QSPR can predict. The H/C ratio and MW are also shown in Table 4.7 and are both within an acceptable range similar to the Jet-A that was run previously. Overall the CPT values matched within a 10.3% error of the values for the real fuel. Because of the large chemical diversity, the chemical properties of the surrogate will only be able to give a good approximation for the real fuel.

The last petroleum derived fuel this method was used to determine a surrogate mixture for is JP-5 POSF 10289. JP-5 is a real-world fuel that is like Jet-A and JP-8 but has a substantially higher flash point and consequently features higher temperatures in the beginning of the distillation curve. JP-5 has a large amount of chemical diversity since it is refined from petroleum products. The large amount of chemical diversity that comes from petroleum products is limited in JP-5 because it is specifically created to have a higher flash point than other jet fuels. This higher flash point is achieved by boiling off the light end of the fuel which leaves the heavier molecules behind and these molecules are less likely to spontaneously react as they are less volatile. The distillation curve for the surrogate that was formulated for JP-5 is shown in Figure 4.26 along with the known boiling temperatures for the real fuel. Because the light end of this fuel is boiled off to create a higher flash point, the distillation curve begins at a higher temperature which is consistent with the real fuel and the surrogate fuel in Figure 4.26. The distillation curve of the surrogate reproduces that of the target fuel for the T10, T20, and T50 temperatures very well but deviates significantly for the T90 value and these can be seen in Table 4.8. The first 3 temperatures all fall within 6 degrees Celsius while the T90 difference is 25 degrees Celsius. This large difference could be due to the lack of heavier molecules than hexadecane and may be a factor of the sensitivity to the surrogate components.

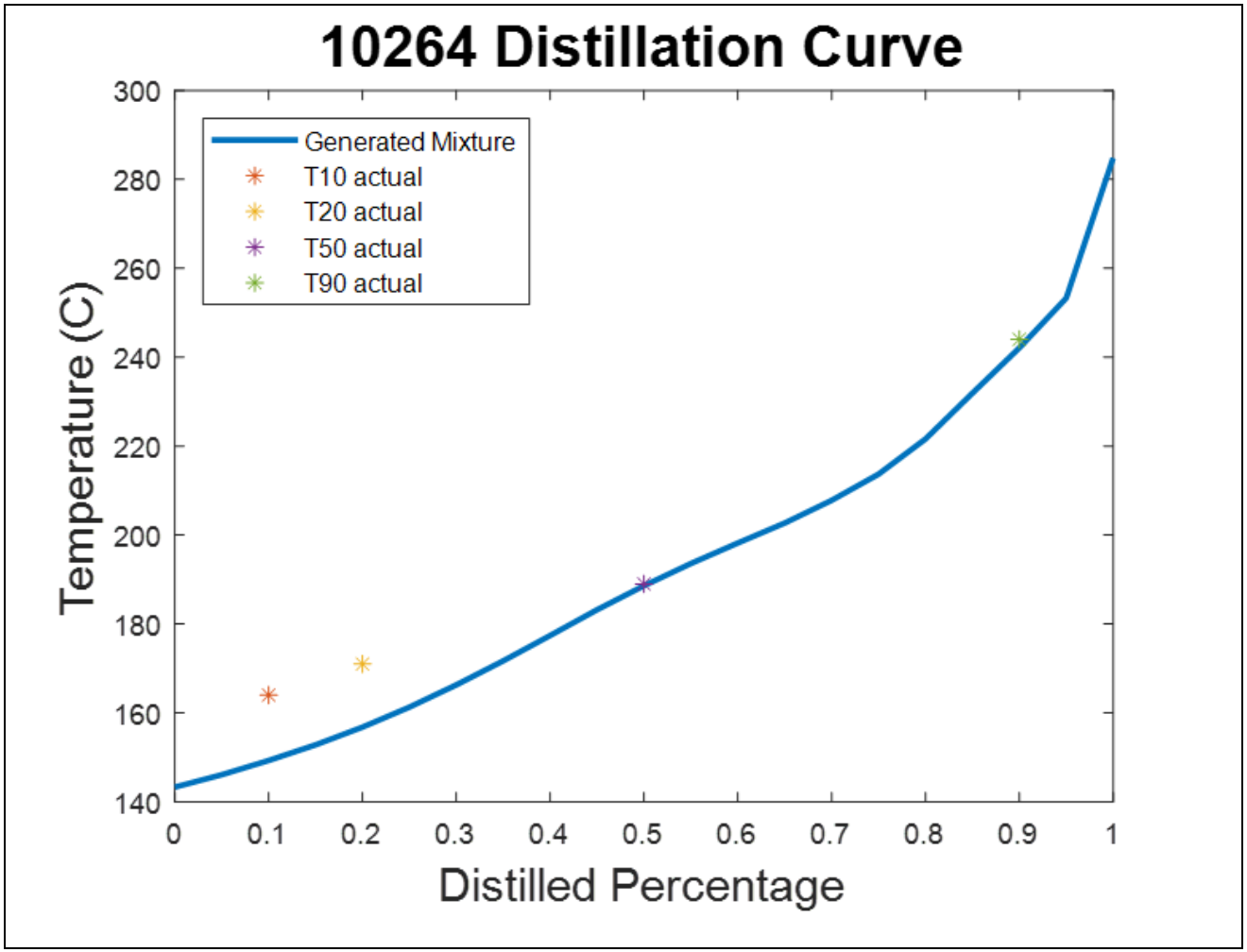

Figure 4.26: Distillation Curve of JP5

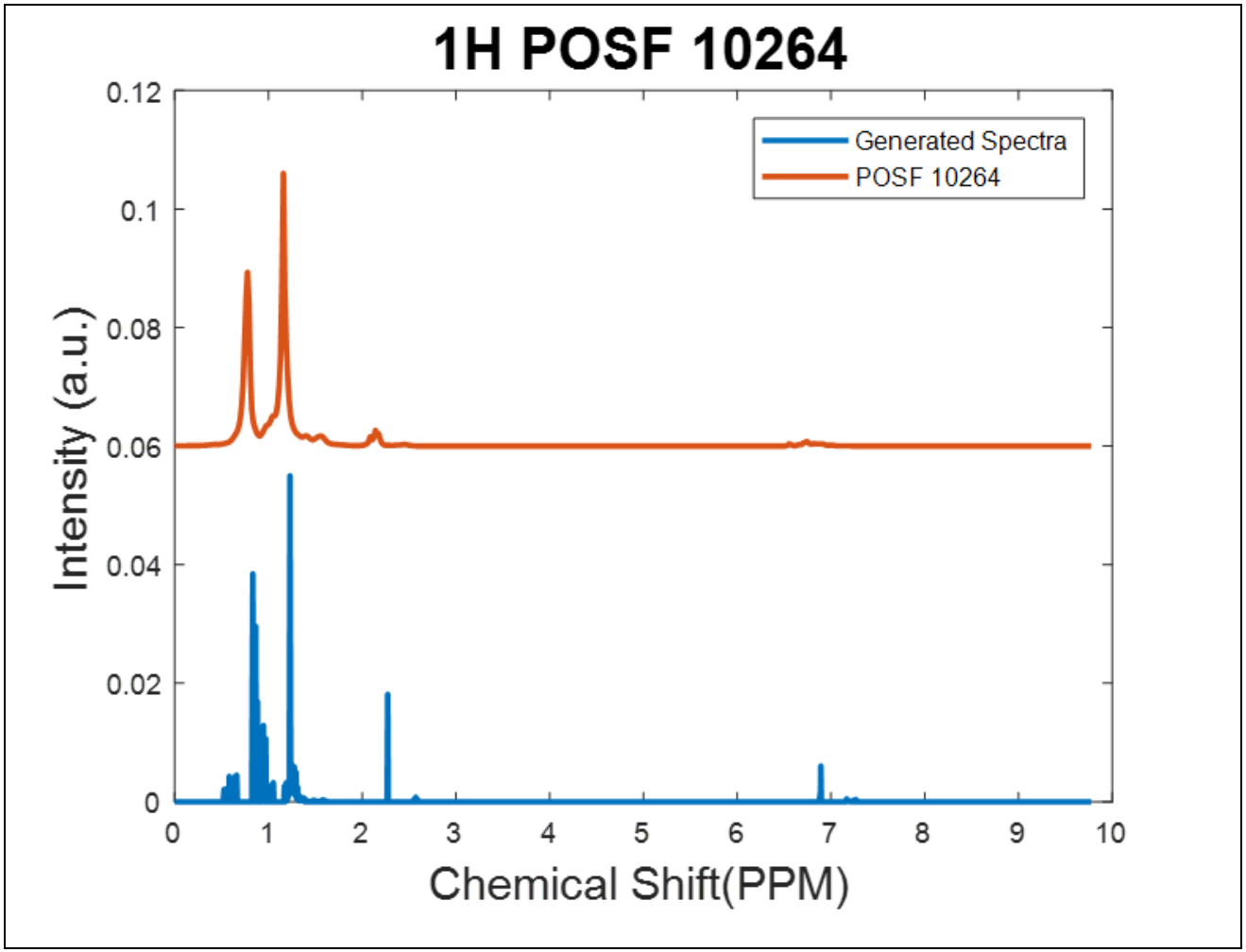

Figure 4.27: 1H NMR Spectra of JP5

The 1H NMR spectra comparison between the generated surrogate and JP-5 is shown in Figure 4.27. From this comparison, the CH_2 and CH_3 peaks have very similar intensities and are the located in the correct location to confirm that they are the same chemical functional groups. The CH peak has a very low intensity relative to the CH_2 and CH_3 groups which is consistent between the two spectra. The aromatics functional group is also in very low quantity in both spectra which means that all functional groups are consistent between the two spectra. When considering the 13C spectra that are shown in Figure 4.28, the largest four peaks are the same in both the surrogate and the target fuel. These four peaks are in the location that is consistent with n-alkanes but the quantities that are present lead to the belief that the differences between this surrogate and real-fuel combination are due to the sensitivity to the surrogate components. This sensitivity to surrogate components can be seen further in Table 4.8 where the CPT values are predicted.

The CPT values that are shown in Table 4.8 are the DCN, MW, and H/C ratio of both the target fuel and the formulated surrogate mixture. Overall the CPT values matched within a 46.5 error of the values for the real fuel. The surrogate model failed to adequately predict the DCN of the real fuel and the two have a difference of 19 DCN. This shows that the surrogate cannot predict the ignition behaviors of the JP-5, this is because JP-5 was specifically formulated to have very unique ignition behaviors. These unique ignition behaviors are a result of the desire for a higher flash point for fuel and the surrogate components may not be optimally selected to account for this. Excluding the DCN, the highest error was the H/C ratio with a 8.27% error. The H/C ratio prediction for the surrogate model also varies from the target fuels measured value by 0.157 which is the largest difference out of all of the fuels that were tested but this could also stem from the

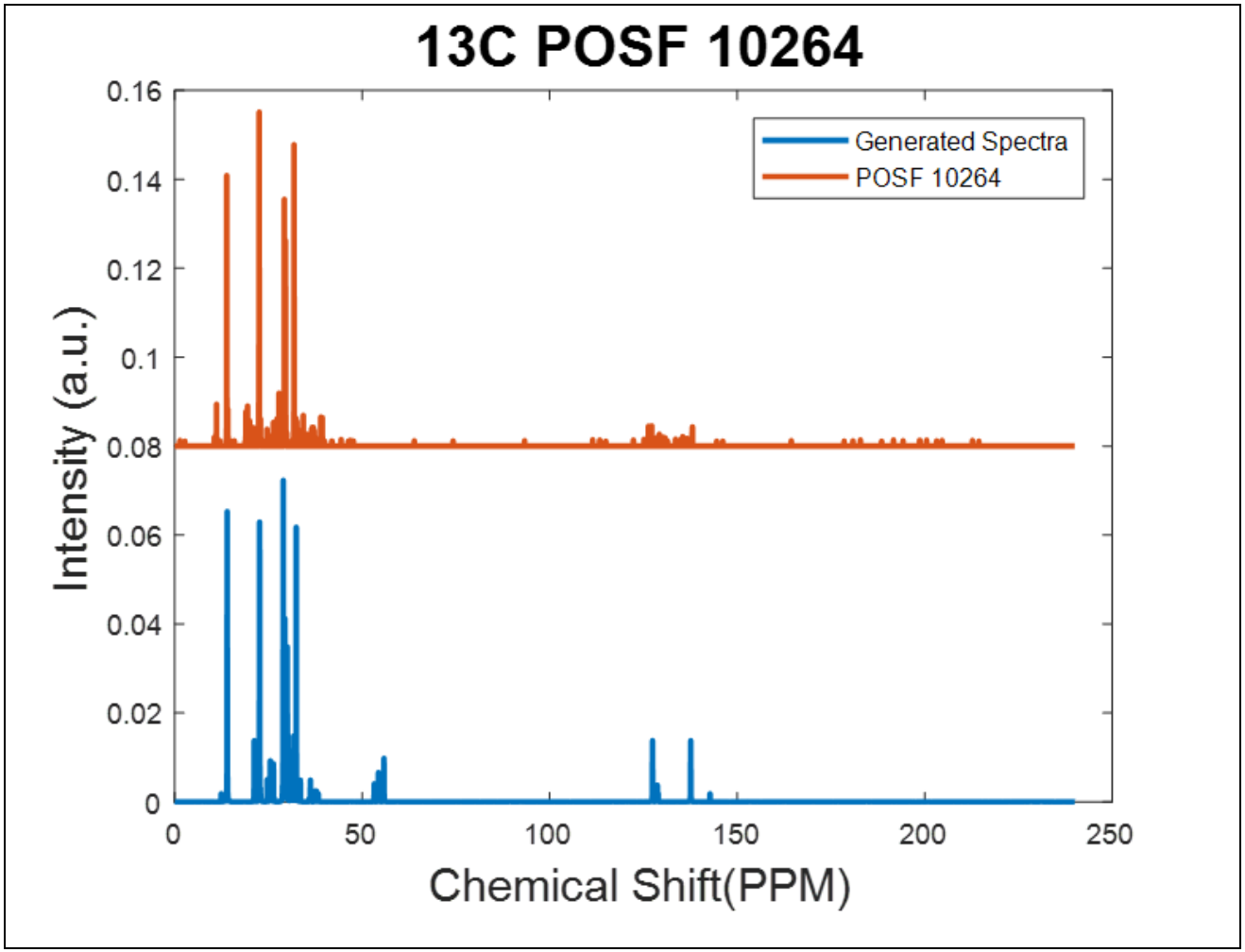

Figure 4.28: 13C NMR Spectra of JP5

Table 4.8: Generated Surrogate and CPT's of JP5

Components	Mole Fraction	Combustion Property Target	Model Fuel	Target Fuel
nC7	0.0274	DCN	59.9	40.9
nC8	0.0259	H/C ratio	2.055	1.898
nC10	0.1132	MW [g/mol]	168.3	166
nC12	0.1132	TSI	-	-
nC14	0.1132	Density at 15 °C [kg/m3]	773.7	827
nC16	0.1132	T_{10} [°C]	187	192
iC8	0.012	T_{20} [°C]	194	199
iC12	0.1132	T_{50} [°C]	216	218
iC16	0.1132	T_{90} [°C]	269	244
toluene	0.0023			
nPB	0.1037			
135TMB	0.0317			
MCH	0.0048			
n-butylcyclohexane	0.1132			

desire for a high flash point in the real fuel. The MW for the surrogate mixture is very well fitted to the target fuel with a difference of 2.3 g/mol which shows that the many of the physical properties will be very similar. The unique properties of JP-5 POSF 10289 and the sensitivity to the choice of surrogate components shows that for this fuel, an acceptable surrogate could not be found with these components.

The last two surrogates that were formulated to test this method were for HRJ Camelina, POSF 7720, and HRJ Tallow, POSF 6308. These two fuels are both alternative jet fuels that are created from various fats and oils. Both fuels exhibit much higher potential for preferential vaporization than any of the other fuels that have been tested; this can be seen in Figures 2.1 and 2.2. Because these fuels are both processed using specific chemical reaction methods, they have much less chemical diversity than the petroleum fuels that were previously run. These fuels may not be as diverse in terms of chemical species, but they do have unique molecular structures as they are formed from fats and oils stocks.[4]

HRJ Tallow POSF 6308 was tested first as it has less preferential vaporization potential and a similar amount of chemical diversity. HRJ Tallow was used to formulate the surrogate that is shown in Figures 4.29-4.31. The 1H spectra comparison is shown in Figure 4.29 and the surrogate matches the target fuel very well. The CH_2 and CH_3 functional groups are the dominant peaks in both and they appear in very similar relative intensities to each other. The functional groups that are present in substantially smaller quantities in the generated surrogate are in low enough quantities and in the proper location to be included with the two major peaks in the measured spectrum due to the resolution issues.

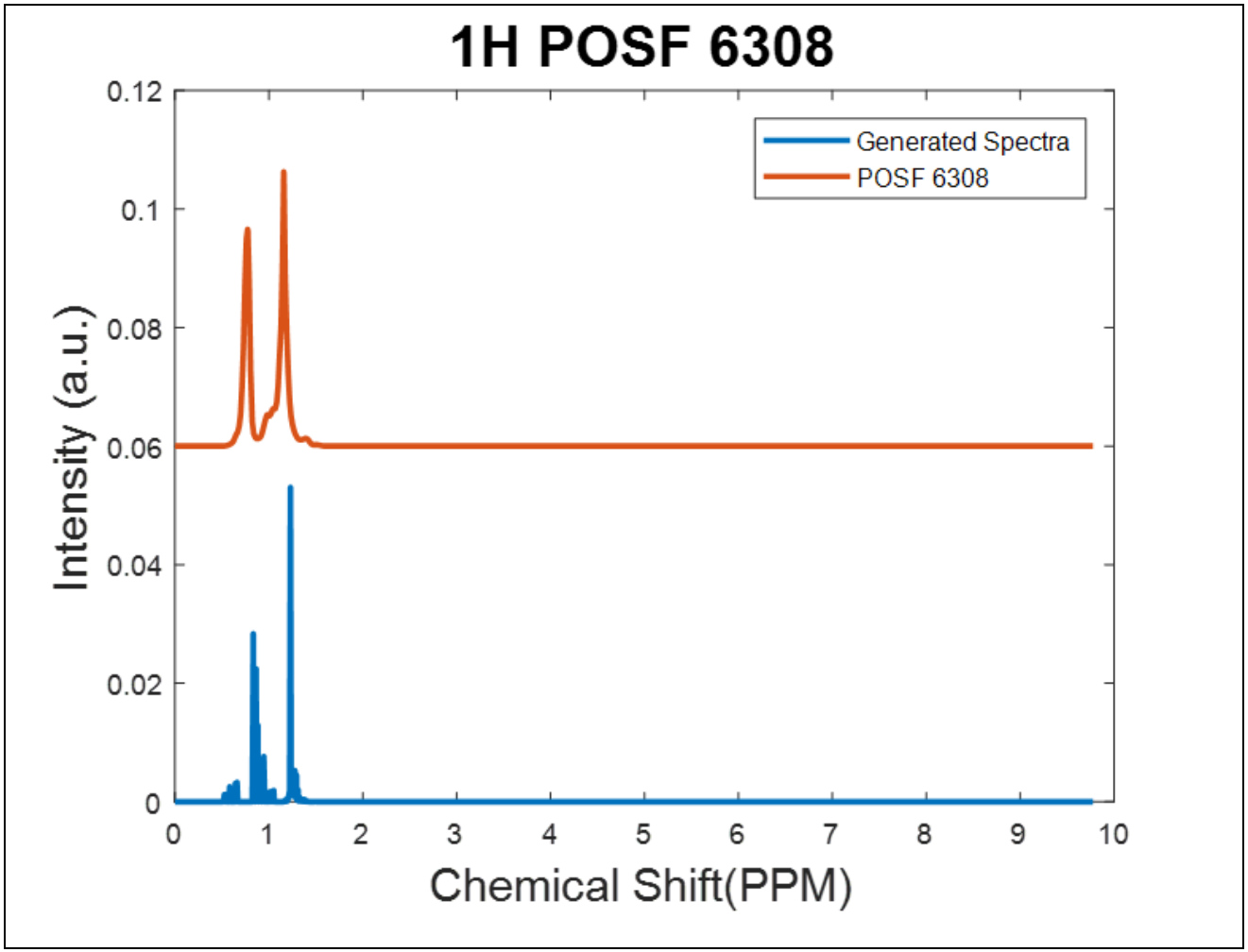

Figure 4.29: 1H NMR Spectra of HRJ Tallow

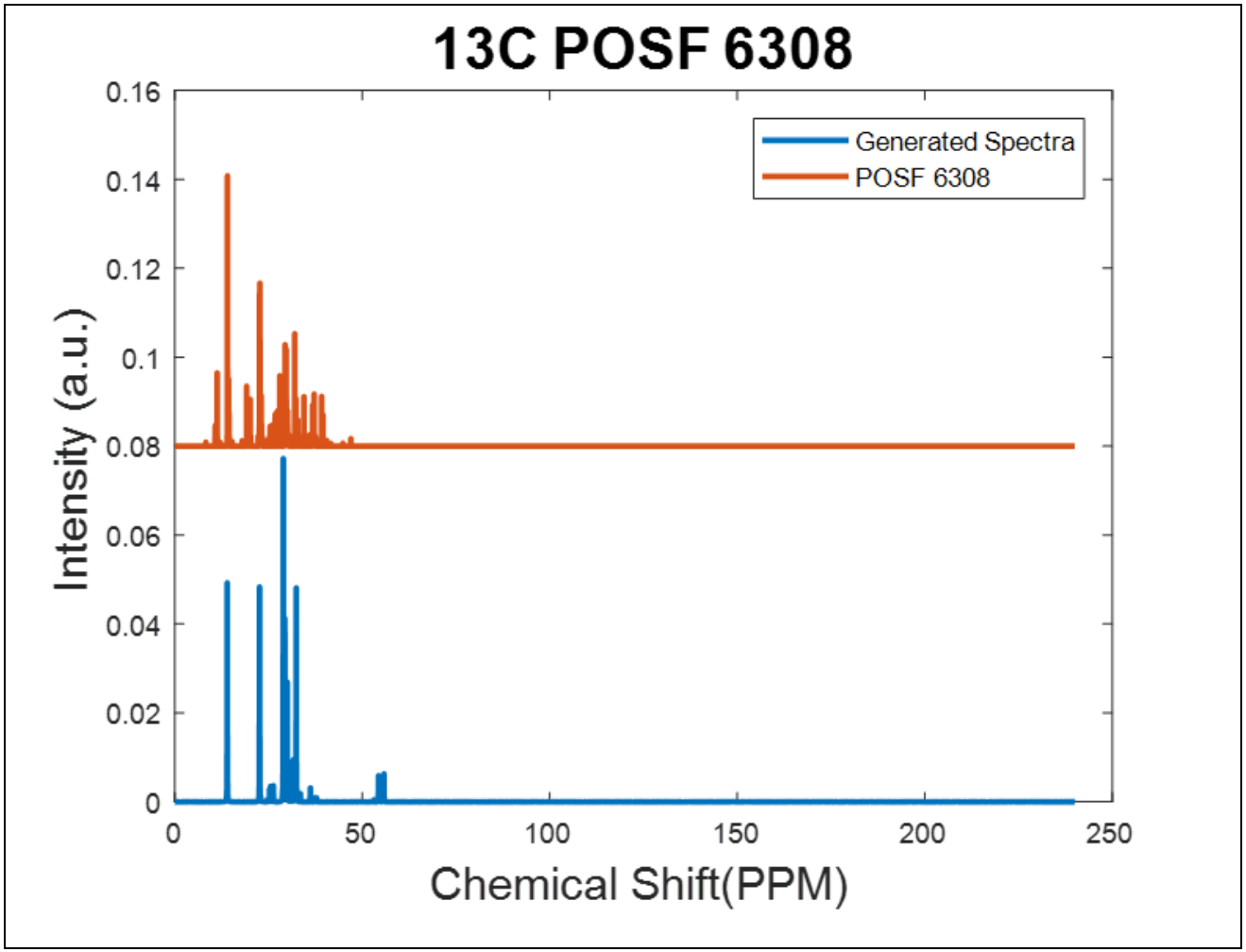

Figure 4.30: 13C NMR Spectra of HRJ Tallow

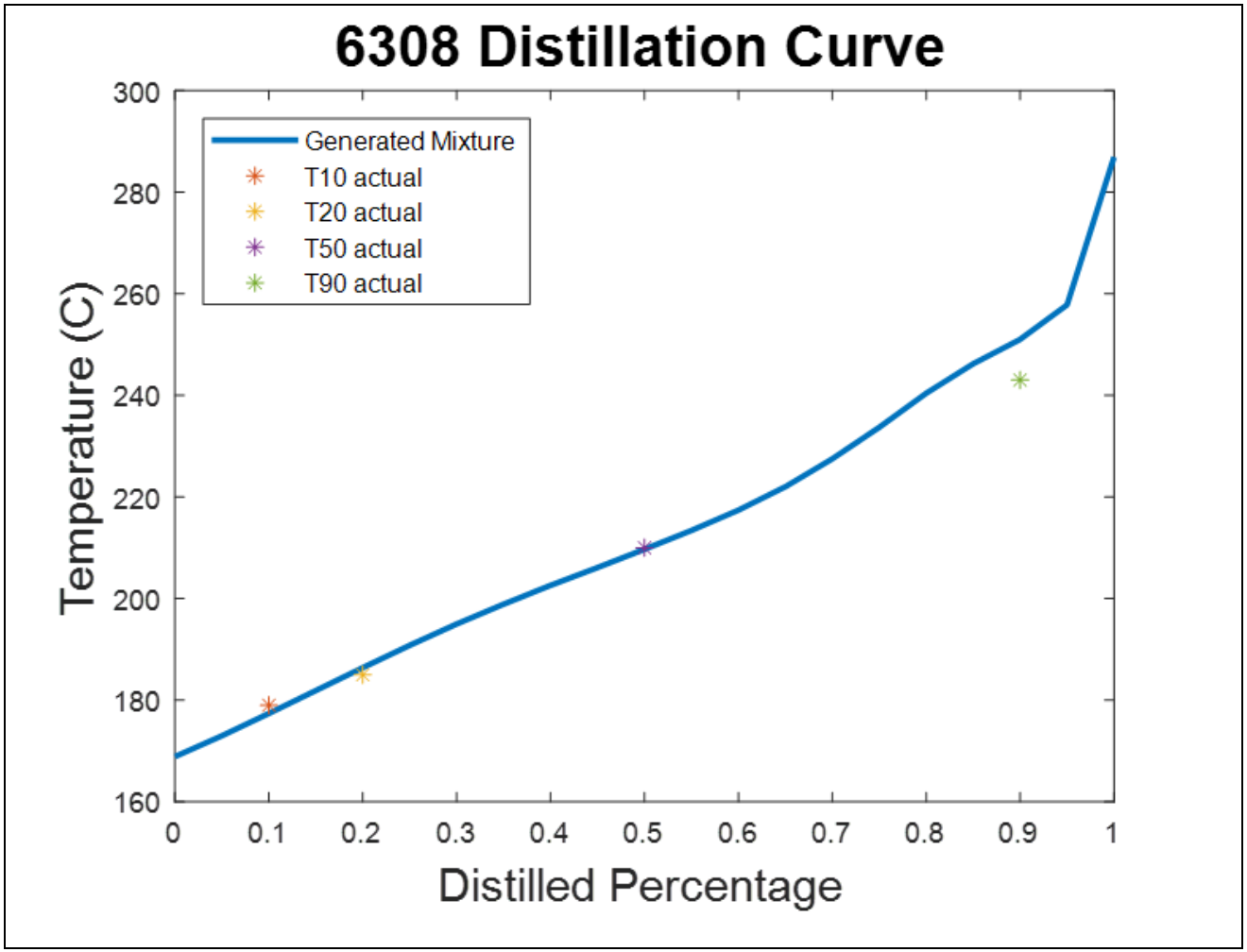

Figure 4.31: Distillation Curve of HRJ Tallow

From the 13C spectra comparison that is shown in Figure 4.30 there is a substantial diversity in the carbon structures that is not truly captured by the formulated surrogate. The surrogate does contain for the two largest peaks in the real fuel and it deals with the carbon diversity by lumping most of it into a two CH_2 peak that is in the region. There is a peak, located at 54 ppm, in the generated surrogate but not from the that is from the CH_2 groups in the highly branched iso-alkane surrogate components. If there were more surrogate components that were varying levels of branched alkanes than the diversity in the carbon structures may have been reproduced without any extra peaks on the spectrum.

Figure 4.31 shows the distillation curve for this surrogate as well as the known values for the HRJ Tallow fuel. The distillation curve of this surrogate mixture matches all of the known points very well with the only difference that is larger than 2 degrees Celsius being at the T90 point which had a difference of 8 degrees. This is very much within the possible error for the real-world distillation experiments and therefor considered successful.

Table 4.9 shows the formulated surrogate as well as the predicted CPT values and how they compare to those of the target fuel. The CPT values are predicted using a QSPR regression model method that was previously used to predict surrogate fuels. The predicted DCN of the surrogate is almost 8 DCN higher than that of the target fuel. This is largely due to the QSPR that was used predicting several of the key surrogate components 7 DCN higher than their actual values. The components iC12, iC16, and nC10 are all predicted between 5 and 8 DCN high and these make up a sizeable portion of this surrogate mixture. The H/C ratio predicted is only 0.011 higher than that of the target fuel which is a sign that this is a valid surrogate for HRJ Tallow. The MW is also only 0.3 g/mol higher than that

Table 4.9: Generated Surrogate and CPT's of HRJ Tallow

Components	Mole Fraction	Combustion Property Target	Model Fuel	Target Fuel
nC7	0.039	DCN	65.97	58.1
nC8	0.1014	H/C ratio	2.169	2.18
nC10	0.2767	MW [g/mol]	163.4	163.7
nC12	0.1769	TSI	-	-
nC14	0.1478	Density at 15 °C [kg/m3]	751.1	758
nC16	0.0228	T_{10} [°C]	177	179
iC8	0.0153	T_{20} [°C]	186	185
iC12	0.0908	T_{50} [°C]	210	210
iC16	0.0999	T_{90} [°C]	251	243
toluene	0.0001			
nPB	0			
135TMB	0			
MCH	0			
n-butylcyclohexane	0.0293			

of the target which shows that this surrogate does fit all of the CPT's that currently have the capability of being predicted within a 13.5% error. The density which was compared as an extra validation point was also very close to that of the target fuel. This data shows that this surrogate is indeed a good fit for HRJ Tallow as it reproduces all of the CPT's and the density.

HRJ Camelina has a much higher potential for preferential vaporization but the chemical structures are very similar to those found in HRJ Tallow. Using this method to generate a surrogate for HRJ Camelina POSF 7720 yields the results shown in Figures 4.32-4.34 and Table 4.10. The 1H spectrum is very well reproduced here as well and can be seen in Figure 4.32. In this figure, the chemical functional groups have the same relative intensities as well as the same location which shows that this surrogate successfully captured all of the chemical functional groups that are accounted for in the 1H spectrum.

Figure 4.33 shows the simulated 13C NMR spectrum of the formulated surrogate and compares it with that of the target fuel. Similar to several of the other fuels tested in this paper, the carbon spectrum has a lot more diversity in the chemical functional groups than what is represented in the surrogate components. This difference in chemical diversity causes many of these carbon structures to be lumped into the functional groups that are available. This is a great example of the goal of this method which is to simplify the chemical diversity and account for the preferential vaporization of the fuel.

The distillation curve can be seen in Figure 4.34 and it is also compared to the known temperatures for the target fuel. All of the temperatures are reproduced to within 6 degrees Celsius which is well within the acceptable error values of the real fuel. The

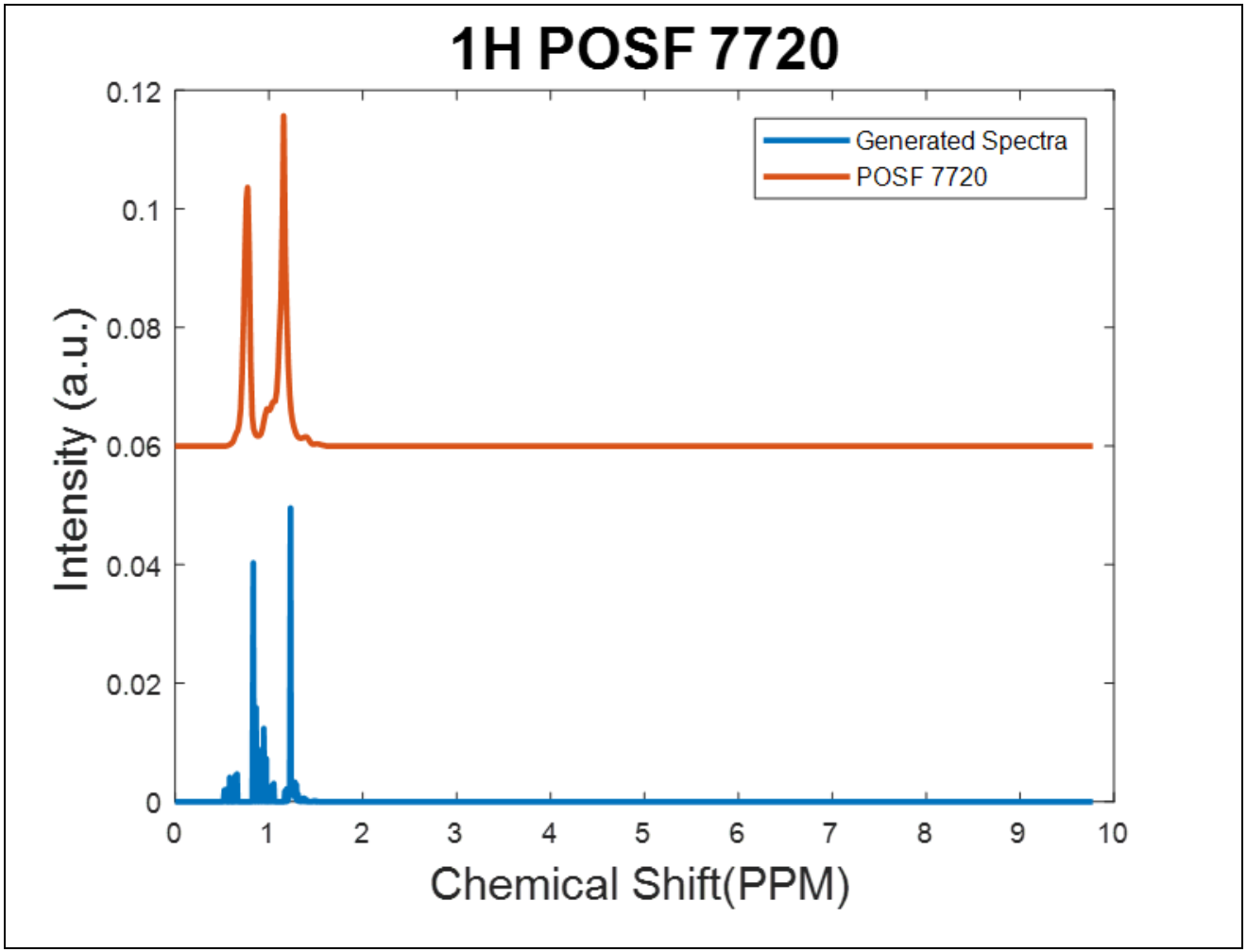

Figure 4.32: 1H NMR Spectra of HRJ Camelina

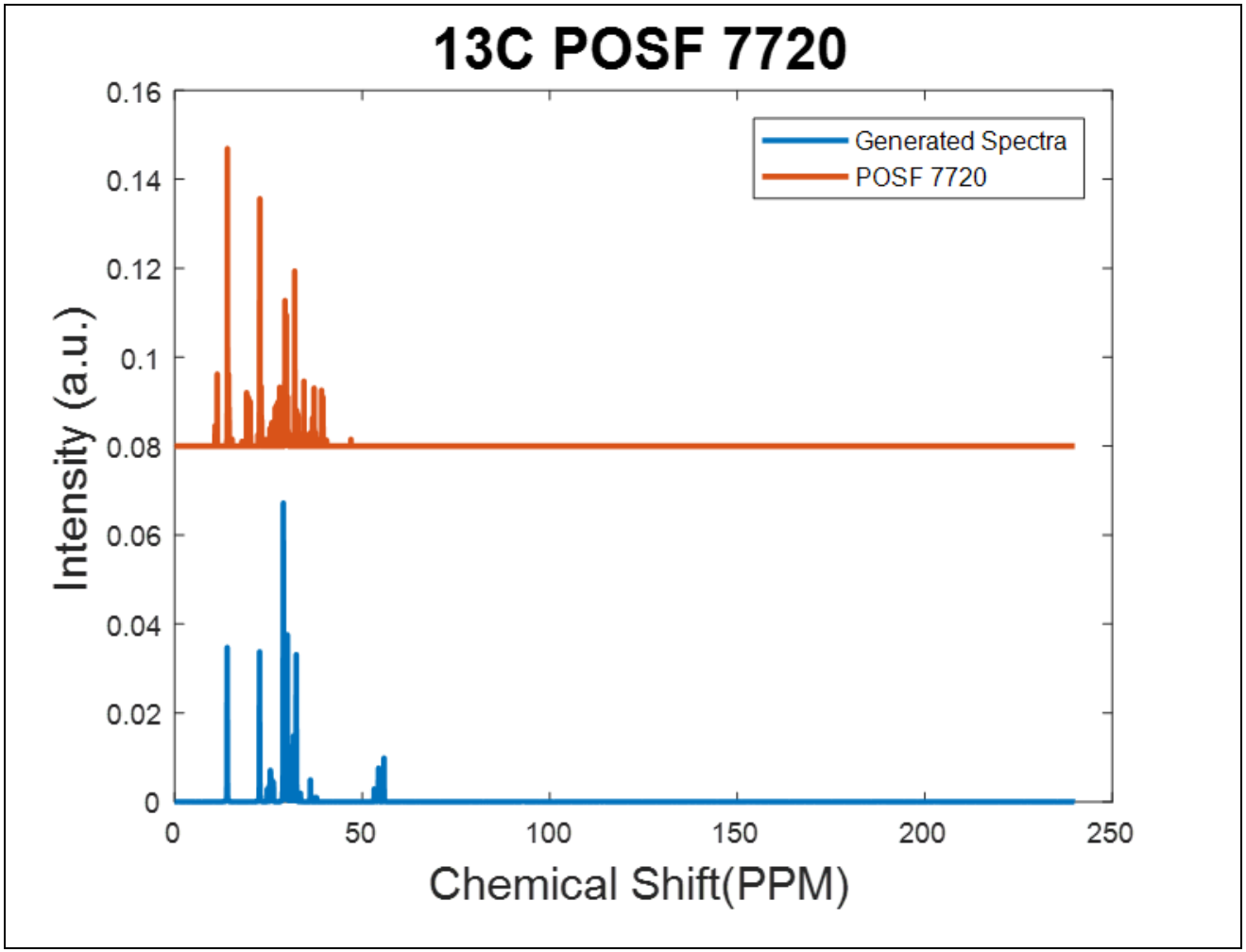

Figure 4.33: 13C NMR Spectra of HRJ Camelina

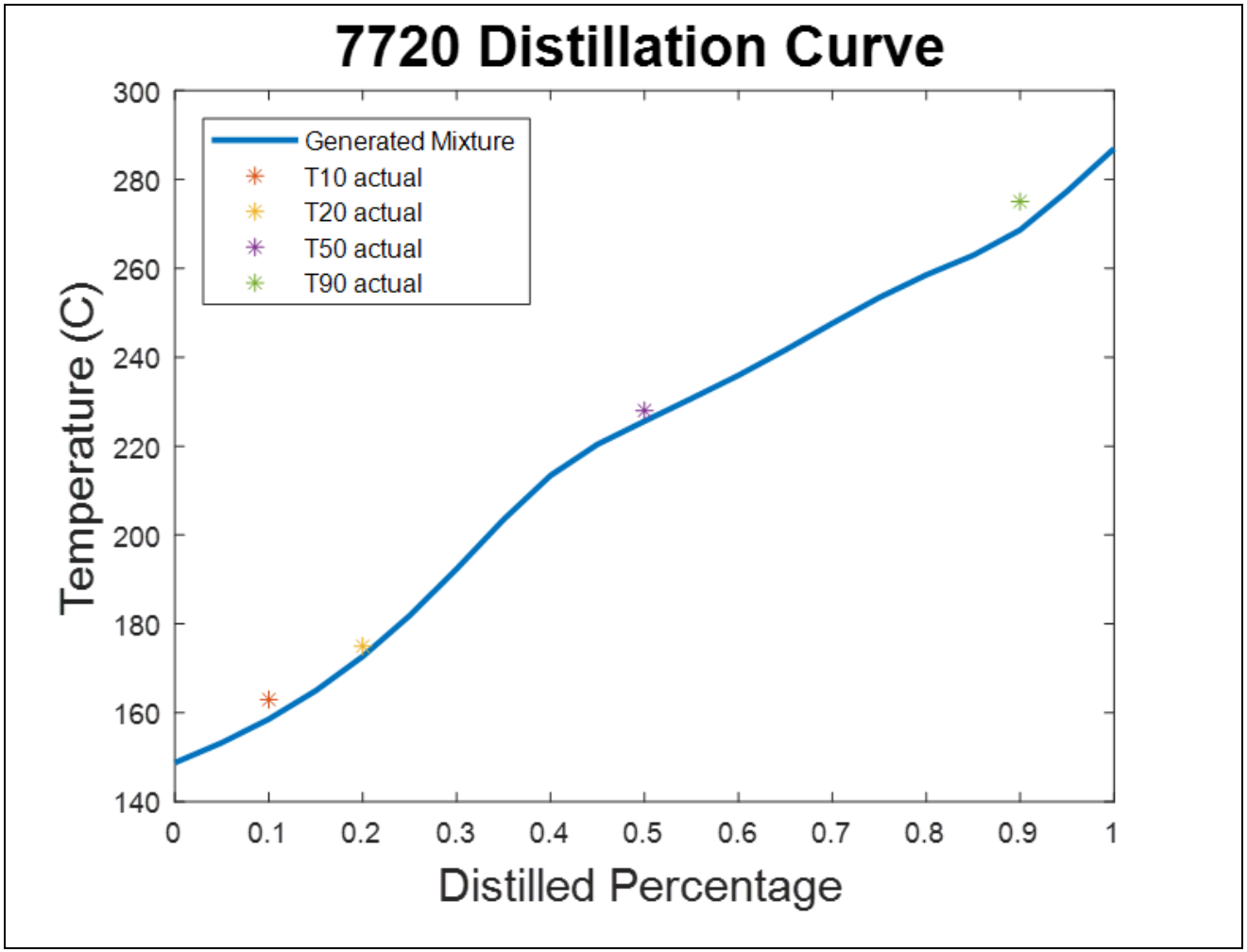

Figure 4.34: Distillation Curve of HRJ Camelina

Table 4.10: Generated Surrogate and CPT's of HRJ Camelina

Components	Mole Fraction	Combustion Property Target	Model Fuel	Target Fuel
nC7	0.1102	DCN	59.6	58.9
nC8	0.0666	H/C ratio	2.162	2.202
nC10	0.0752	MW [g/mol]	168.9	167.6
nC12	0.111	TSI	-	-
nC14	0.0918	Density at 15 °C [kg/m3]	754.5	-
nC16	0.1202	T_{10} [°C]	159	163
iC8	0.0985	T_{20} [°C]	173	175
iC12	0.1254	T_{50} [°C]	226	228
iC16	0.1678	T_{90} [°C]	269	275
toluene	0			
nPB	0			
135TMB	0			
MCH	0			
n-butylcyclohexane	0.0332			

surrogate also follows the trend of the real fuel very well and is considered a successful reproduction because of how close the temperatures are to each other. Table 4.10 shows the predicted CPT values for this surrogate mixture as well as the known values for the real fuel. The DCN is predicted to be within 1 DCN value of the target fuel and the MW is predicted within 2 g/mol as well. The H/C ratio has the largest difference with a difference of 0.04. These values show that this surrogate properly matches the CPT values for the real fuel within a 1.8% error and that this is indeed a valid surrogate.

CHAPTER 5

CONCLUSION

The goal of surrogate fuels is to simplify the extremely complex chemistry that governs real fuel processes. Typically, surrogate fuels have been formulated using a CPT approach, but recently experiments have shown that CPT's are governed by the chemical functional group distribution of the real fuels.[10] This realization led to the creation of a new method to formulate surrogate fuels from the chemical functional group distribution and the distillation curve that is not constrained to the empirical testing. This hypothesis was tested using NMR spectra to measure the chemical functional group distribution of the real fuels and an optimization algorithm to reproduce the spectra, with the results being shown previously.

The fuels that were tested in this work are a variety of alternative jet fuels along with petroleum derived fuels. These fuels not only contained varying levels of chemical diversity but also varying amounts of preferential vaporization potential. Using the NMR along with the distillation curve produced very good surrogate mixtures for their respective target fuels that reproduced the values within 13% error when not considering JP5. The surrogate fuels produced using this method were used in a QSPR regression model to predict the CPT values of the surrogates that were then compared to the target fuels. Because the DCN was predicted using the QSPR method, the limitations of the QSPR

effect the error for the DCN. When not considering DCN, the highest error for the H/C ratio was 3.7% and for the MW it was 5%.

Because the alternative fuels were reconstructed better, the highest errors for these was 1.9% for the H/C ratio and 3.8% for the MW. These results showed that this method of surrogate formulation does work and that the chemical functional group distribution along with the distillation curve is sufficient to constrain a surrogate formulation method.

The surrogate components that were used in this testing were selected due to their abundance in petroleum derived jet fuels and their widely understood kinetic models. This allows for the development of a highly reduced kinetic model for the target fuel based on these components. This method did reveal that there is a significant sensitivity to what surrogate components are used and they should ideally be tailored to suit the target fuel. This sensitivity could be mitigated in some cases by only considering the 1H NMR spectrum and distillation curve at cost to precision of the surrogate.

These results showed that alternative fuels can be easily characterized using this method and validates that the surrogate will reproduce the chemical and physical properties of a target fuel. When considering the petroleum derived fuels, the results were good estimates of the chemical and mechanical properties, but the extreme chemical diversity caused the results to not be as precise as the alternative fuels. This reveals a necessity to further categorize the roles surrogate components can play on the validity of the surrogate mixture as well as a need to consider increasing the total number of components overall or in certain functional group areas.

REFERENCES

[1] Renewable Energy Explained.
https://www.eia.gov/energyexplained/?page=renewable_home (accessed June 2019).
[2] US Energy Facts Explained.
https://www.eia.gov/energyexplained/?page=us_energy_home (accessed June 2019).
[3] http://www.caafi.org/information/pdf/D4054_Users_Guide_V6_2.pdf (accessed June 2019).
[4] C. Allen, D. Valco, E. Toulson, T. Edwards, T. Lee, Ignition behavior and surrogate modeling of JP-8 and of camelina and tallow hydrotreated renewable jet fuels at low temperatures, Combustion and Flame 160 (2013) 232-239.
[5] A.Y. Cooney, S.L. Singer, A hybrid droplet vaporization-chemical surrogate approach for emulating vaporization, physical properties, and chemical combustion behavior of multicomponent fuels, Proceedings of the Combustion Institute 37 (2019) 3229-3236.
[6] P. Dagaut, A. El Bakali, A. Ristori, The combustion of kerosene: Experimental results and kinetic modelling using 1- to 3-component surrogate model fuels, Fuel 85 (2006) 944-956.
[7] S. Dooley, S.H. Won, M. Chaos, J. Heyne, Y. Ju, F.L. Dryer, K. Kumar, C.-J. Sung, H. Wang, M.A. Oehlschlaeger, R.J. Santoro, T.A. Litzinger, A jet fuel surrogate formulated by real fuel properties, Combustion and Flame 157 (2010) 2333-2339.
[8] S. Dooley, S.H. Won, J. Heyne, T.I. Farouk, Y. Ju, F.L. Dryer, K. Kumar, X. Hui, C.-J. Sung, H. Wang, M.A. Oehlschlaeger, V. Iyer, S. Iyer, T.A. Litzinger, R.J. Santoro, T. Malewicki, K. Brezinsky, The experimental evaluation of a methodology for surrogate fuel formulation to emulate gas phase combustion kinetic phenomena, Combustion and Flame 159 (2012) 1444-1466.
[9] S. Dooley, S.H. Won, S. Jahangirian, Y. Ju, F.L. Dryer, H. Wang, M.A. Oehlschlaeger, The combustion kinetics of a synthetic paraffinic jet aviation fuel and a fundamentally formulated, experimentally validated surrogate fuel, Combustion and Flame 159 (2012) 3014-3020.
[10] F.L. Dryer, Chemical kinetic and combustion characteristics of transportation fuels, Proceedings of the Combustion Institute 35 (2015) 117-144.
[11] F.L. Dryer, S. Jahangirian, S. Dooley, S.H. Won, J. Heyne, V.R. Iyer, T.A. Litzinger, R.J. Santoro, Emulating the Combustion Behavior of Real Jet Aviation Fuels by Surrogate Mixtures of Hydrocarbon Fluid Blends: Implications for Science and Engineering, Energy & Fuels 28 (2014) 3474-3485.
[12] E.G. Eddings, S. Yan, W. Ciro, A.F. Sarofim, FORMULATION OF A SURROGATE FOR THE SIMULATION OF JET FUEL POOL FIRES, Combustion Science and Technology 177 (2005) 715-739.
[13] T. Edwards, L.Q. Maurice, Surrogate Mixtures to Represent Complex Aviation and Rocket Fuels, Journal of Propulsion and Power 17 (2001) 461-466.

[14] S. Honnet, K. Seshadri, U. Niemann, N. Peters, A surrogate fuel for kerosene, Proceedings of the Combustion Institute 32 (2009) 485-492.
[15] M.L. Huber, E.W. Lemmon, T.J. Bruno, Surrogate Mixture Models for the Thermophysical Properties of Aviation Fuel Jet-A, Energy & Fuels 24 (2010) 3565-3571.
[16] S. Humer, A. Frassoldati, S. Granata, T. Faravelli, E. Ranzi, R. Seiser, K. Seshadri, Experimental and kinetic modeling study of combustion of JP-8, its surrogates and reference components in laminar nonpremixed flows, Proceedings of the Combustion Institute 31 (2007) 393-400.
[17] D. Kim, J. Martz, A. Violi, A surrogate for emulating the physical and chemical properties of conventional jet fuel, Combustion and Flame 161 (2014) 1489-1498.
[18] C.J. Mueller, W.J. Cannella, T.J. Bruno, B. Bunting, H.D. Dettman, J.A. Franz, M.L. Huber, M. Natarajan, W.J. Pitz, M.A. Ratcliff, K. Wright, Methodology for Formulating Diesel Surrogate Fuels with Accurate Compositional, Ignition-Quality, and Volatility Characteristics, Energy & Fuels 26 (2012) 3284-3303.
[19] C. Pera, V. Knop, Methodology to define gasoline surrogates dedicated to auto-ignition in engines, Fuel 96 (2012) 59-69.
[20] W.J. Pitz, C.J. Mueller, Recent progress in the development of diesel surrogate fuels, Progress in Energy and Combustion Science 37 (2011) 330-350.
[21] S.H. Won, F.M. Haas, S. Dooley, T. Edwards, F.L. Dryer, Reconstruction of chemical structure of real fuel by surrogate formulation based upon combustion property targets, Combustion and Flame 183 (2017) 39-49.
[22] K. Dussan, S.H. Won, A.D. Ure, F.L. Dryer, S. Dooley, Chemical functional group descriptor for ignition propensity of large hydrocarbon liquid fuels, Proceedings of the Combustion Institute 37 (2019) 5083-5093.
[23] S. Dooley, J. Heyne, S.H. Won, P. Dievart, Y. Ju, F.L. Dryer, Importance of a Cycloalkane Functionality in the Oxidation of a Real Fuel, Energy & Fuels 28 (2014) 7649-7661.
[24] W. Lyu, L. Zhang, K. Li, G. Wang, Q. Shi, S. Zhao, C. Xu, Average Molecule Construction of Petroleum Fractions Based on 1H-NMR, AIChE Journal 65 (2019) 270-280.
[25] S.H. Won, P.S. Veloo, S. Dooley, J. Santner, F.M. Haas, Y. Ju, F.L. Dryer, Predicting the global combustion behaviors of petroleum-derived and alternative jet fuels by simple fuel property measurements, Fuel 168 (2016) 34-46.
[26] D.C. Bell, J.S. Heyne, S.H. Won, F.L. Dryer, The Impact of Preferential Vaporization on Lean Blowout in a Referee Combustor at Figure of Merit Conditions, doi:10.1115/POWER2018-7432(2018) V001T001A011.
[27] N. Rock, I. Chterev, B. Emerson, S.H. Won, J. Seitzman, T. Lieuwen, Liquid Fuel Property Effects on Lean Blowout in an Aircraft Relevant Combustor, Journal of Engineering for Gas Turbines and Power 141 (2019) 071005-071005-071013.
[28] S.H. Won, N. Rock, S.J. Lim, S. Nates, D. Carpenter, B. Emerson, T. Lieuwen, T. Edwards, F.L. Dryer, Preferential vaporization impacts on lean blow-out of liquid fueled combustors, Combustion and Flame 205 (2019) 295-304.
[29] J.T. Bays, D.L. King, A NMR-Based Carbon-Type Analysis of Diesel Fuel Blends From Various Sources, United States, 2013-05-10, 2013.
[30] A.M. Castillo, L. Patiny, J. Wist, Fast and accurate algorithm for the simulation of NMR spectra of large spin systems, Journal of Magnetic Resonance 209 (2011) 123-130.

[31] G.F. Pauli, B.U. Jaki, D.C. Lankin, Quantitative 1H NMR: Development and Potential of a Method for Natural Products Analysis, Journal of Natural Products 68 (2005) 133-149.

APPENDIX A
OPTIMIZATION CODE

```
clear, clc
%% Inputs
chems=
{'nC7';'nC8';'nC10';'nC12';'nC14';'nC16';'iC8';'iC12';'iC16';'Toluene';'nPropylBenzene';'13
5TMB';'MCH';'BCH'};
Ho=xlsread('H5729.xlsx'); %------ This is the 1H NMR Spectrum of the Real Fuel
Co=xlsread('C5729.xlsx'); %------ This is the 13C NMR Spectrum of the Real Fuel

Ptot=100; %---------------------- This is the Atmospheric Pressure in kPa
T0=298; %-------------------------- This is the Atmospheric Temperature in K
%Distillation Temperatures ------- need to code to read from file?
T10a=162;
T20a=164;
T50a=169;
T90a=185;
iter=1;
d=0.05; %----------------------- This is the distillation percentage
% moles0=[1 9 11 12 10 1 5 19 6 1 5 18 0 0];
% moles0matrix=[0 0 0 0 0 0 0 80 20 0 0 0];
moles0matrix=randi([0 iter],[iter,length(chems)]);
%% Antoine Table
% this section creates a table(Antoine_Table) in Matlab which contains the
% Antoine Values for Distillation (A,B,and C) of the chemicals that are
% selected
[Antoine_Values,Antoine_Text]=xlsread('Antoine_Coefficients');
A=Antoine_Values(1,:)';
B=Antoine_Values(2,:)';
C=Antoine_Values(3,:)';
Antoine_Tablefull=table(A,B,C,'RowNames',Antoine_Text');
Antoine_Table=Antoine_Tablefull(chems,:);
A=Antoine_Table{:,1};
B=Antoine_Table{:,2};
C=Antoine_Table{:,3};
clear Antoine_Tablefull Antoine_Values Antoine_Text

%% find distillation percentages and locations
% This section creates the distilled percents and the locations in the
% Temperature matrix (T) to compare to the actual values
% (T10a,T20a,T50a,T90a)
```

```
del=0:d:1;
[~,d10]=min(abs(del-.1));
[~,d20]=min(abs(del-.2));
[~,d50]=min(abs(del-.5));
[~,d90]=min(abs(del-.9));
Tempsa=[T10a;T20a;T50a;T90a];
Pv10=exp(A+(B./(T10a+273+C)))';
Pv20=exp(A+(B./(T20a+273+C)))';
Pv50=exp(A+(B./(T50a+C+273)))';
Pv90=exp(A+(B./(T90a+C+273)))';
%% Preparing the 1H NMR Spectrum
HSpec=zeros(32768,2);
[~,xstart]=min(abs(Ho(:,1)));%-0.100025)); %-----------------------Figure out how to
remove -.100025
for i=1:length(HSpec)
   HSpec(i,2)=Ho(xstart-i+1,2);
   a=abs(HSpec(i,2));
   b=HSpec(i,2);
   if a<100
      HSpec(i,2)=0;
   elseif b<0
      HSpec(i,2)=0;
   end
end
clear Ho
Ho=(HSpec/max(cumtrapz(HSpec)))';
HIo=cumtrapz(Ho);
HIo=HIo/max(HIo);
%% Preparing the 13C NMR Spectrum
[~,xstop]=min(abs(Co(:,1)-0));
shift=length(Co(:,2))/2-xstop;
shift=round(shift,0);
CSpec=zeros(16384,2);
% Removing the solvent (The X axis is backwards)
[~,solventstart]=min(abs(Co(:,1)-76)); % Identifies where the solvent starts (This is
CDCL3 so triple peak)
[~,solventstop]=min(abs(Co(:,1)-78));  % Identifies where the solvent stops
for i=solventstop:solventstart
   Co(i,2)=0;
end
% The solvent has been Removed in the for loop above this
CS=zeros(1,length(Co));
for i=1:xstop
  CS(i+(length(CS)-xstop))=Co(i,2);
end
for i=1:length(CSpec)
```

```
    CSpec(i,1)=Co(2*i,1);
    CSpec(i,2)=CS(2*i);
end
clear Co
cox=CSpec(:,1);
Co=CSpec(:,2)';
Co(Co<1000)=0;
CIo=cumtrapz(Co);
CIo=CIo/max(CIo);
clear HSpec CSpec solventstart solventstop xstart xstop xv Tempscos shift

%% Preparing the Individual Spectra
for i=1:length(chems)
   Hfilenames{i}=strcat('H',chems{i},'.jdx');
   Hf(i)=jcampread(Hfilenames{i});
   HF(i,:)=Hf(i).Blocks.YData;
   Cfilenames{i}=strcat('C',chems{i},'.jdx');
   Cf(i)=jcampread(Cfilenames{i});
   CF(i,:)=Cf(i).Blocks.YData;
end


T=T0:600;
Pvapa=exp(A+B./(T+C));


G=@(moles)NMR_Optimizer(moles,chems,d,HF,CF,CIo,HIo,Ptot,Pvapa,T10a,T20a,T50
a,T90a,T0);
[m,~]=size(moles0matrix);
for zz=1:m
   moles0(1,:)=moles0matrix(zz,:);

mix(zz,:)=fminimax(G,moles0,[],[],[],[],zeros(1,length(chems)),100*ones(1,length(chems
)),[],optimoptions('fminimax','MaxFunctionEvaluations',10000));
   Gvals(zz,:)=G(mix(zz,:));
end

[aa,bb]=min(Gvals);
moles1=mix(bb,:);
x=moles1/sum(moles1);
T=T0:318;
mol=zeros(length(T),length(chems));
Pvap=exp(A+(B./(T+C)))';
for j=1:length(T)
   for i=1:length(chems)
      if j==1
```

```
            mol(1,:)=x;
        else
            mol(j,i)=mol(j-1,i)-d*xg(j-1,i);
        end
    end

    xl=mol./sum(mol,2);
    Ppx=Pvap.*xl;
    Ppxtot=sum(Ppx,2);
    xg=Ppx./Ppxtot;
    Res=(Ptot-Ppxtot).^2;
end
for k=1:length(T)
countr=0;
a=Res(k);
    while a>0.01 && countr<8000
        Pvap=exp(A+(B./(T+C)))';
        for j=1:length(T)
            for i=1:length(chems)
                if j==1
                    mol(1,:)=x;
                else
                    mol(j,i)=mol(j-1,i)-d*xg(j-1,i);
                end
                bb=mol(j,i);
                if bb<=0
                    mol(j,i)=0;
                end
            end
            xl=mol./sum(mol,2);
            Ppx=Pvap.*xl;
            Ppxtot=sum(Ppx,2);
            xg=Ppx./Ppxtot;
            Res=(Ptot-Ppxtot).^2;
        end
    atry=Res(k);
    if atry<=a
        T(k)=T(k)+0.1;
    elseif atry>a
        T(k)=T(k)-0.1;
    end
    a=atry;
    countr=countr+1;
    end
end
T1=T(d10)-273
```

```
T2=T(d20)-273
T3=T(d50)-273
T4=T(d90)-273
figure,plot(del,T-273,'LineWidth',2)
hold on
plot(0.1,Tempsa(1),'*')
% plot(0.2,Tempsa(2),'*')
plot(0.5,Tempsa(3),'*')
plot(0.9,Tempsa(4),'*')
box on
xlabel('Distilled Percentage','FontSize',16)
ylabel('Temperature (C)','FontSize',16)
title('5729 Distillation Curve','FontSize',20)
% legend('Generated Mixture','T10 actual','T20 actual','T50 actual','T90
actual','Location','northwest')
legend('Generated Mixture','T10 actual','T50 actual','T90 actual','Location','northwest')

HSpectraSolutiontry=x*HF;
HSpectraSolutiontry=HSpectraSolutiontry/max(cumtrapz(HSpectraSolutiontry));
HSpectraSolutiontryI=cumtrapz(HSpectraSolutiontry);

CSpectraSolutiontry=x*CF;
CSpectraSolutiontry=CSpectraSolutiontry/max(cumtrapz(CSpectraSolutiontry));
CSpectraSolutiontryI=cumtrapz(CSpectraSolutiontry);

Ho=Ho/max(cumtrapz(Ho));
HoI=cumtrapz(Ho);

Co=Co/max(cumtrapz(Co));
CoI=cumtrapz(Co);

Hxx=Hf(1).Blocks.XData;
Cxx=Cf(1).Blocks.XData;


figure,plot(Hxx,2.3*HSpectraSolutiontry,'LineWidth',2)
hold on
plot(Hxx,0.5*0.8*1.2*24*Ho+0.06,'LineWidth',2)
box on
xlabel('Chemical Shift(PPM)','FontSize',16)
ylabel('Intensity (a.u.)','FontSize',16)
legend('Generated Spectra','POSF 5729')
title('1H POSF 5729','FontSize',20)

figure,plot(Cxx,CSpectraSolutiontry,'LineWidth',2)
hold on
```

```
plot(Cxx,0.1*1.6*2*Co+0.08,'LineWidth',2)
box on
xlabel('Chemical Shift(PPM)','FontSize',16)
ylabel('Intensity (a.u.)','FontSize',16)
legend('Generated Spectra','POSF 5729')
title('13C POSF 5729','FontSize',20)

figure,plot(Hxx,HSpectraSolutiontryI,'LineWidth',2)
hold on
plot(Hxx,HoI,'--','LineWidth',2)
box on
xlabel('Chemical Shift(PPM)','FontSize',16)
ylabel('Intensity (a.u.)','FontSize',16)
legend('Generated Spectra','POSF 5729')
title('1H POSF 5729 Integrated','FontSize',20)

figure,plot(Cxx,CSpectraSolutiontryI,'LineWidth',2)
hold on
plot(Cxx,CoI,'--','LineWidth',2)
box on
xlabel('Chemical Shift(PPM)','FontSize',16)
ylabel('Intensity (a.u.)','FontSize',16)
legend('Generated Spectra','POSF 5729')
title('13C POSF 5729 Integrated','FontSize',20)

function
[G]=NMR_Optimizer(moles,chems,d,HF,CF,CIo,HIo,Ptot,Pvapa,T10a,T20a,T50a,T90a,
T0)
   MOLES=zeros(1/d,length(chems));
   kk=zeros(1/d,length(Pvapa));
   minkk=zeros(1/d,1);
   Pvap_i=zeros(1/d,1);
   Pvap=zeros(1/d,length(chems));
   xg=zeros(1/d,length(chems));
   for j=1:1/d
      if j==1
         MOLES(1,:)=moles/sum(moles);
      else
         MOLES(j,:)=MOLES(j-1,:)-d*xg(j-1,:);
      end
      MOLES(j,MOLES(j,:)<0)=0;
      kk(j,:)= abs((MOLES(j,:)/sum(MOLES(j,:)))*Pvapa-Ptot);
      minkk(j)= min(kk(j,:));
      Pvap_i(j)= find(kk(j,:)==minkk(j));
      Pvap(j,:)= Pvapa(:,Pvap_i(j));
      xg(j,:)= ((MOLES(j,:).*Pvap(j,:))/sum(MOLES(j,:)*Pvap(j,:)'));
```

```
    end
    T10=T0+Pvap_i(3)-1-273;
    T20=T0+Pvap_i(5)-1-273;
    T50=T0+Pvap_i(11)-1-273;
    T90=T0+Pvap_i(19)-1-273;

    x=moles/sum(moles);
    H=x*HF;
    C=x*CF;
    HI=cumtrapz(H);
    HI=HI/max(HI);
    CI=cumtrapz(C);
    CI=CI/max(CI);
%     eq1=sum(abs(HI-HIo));
%     eq2=sum(abs(CI-CIo));
    eq1=abs(HIo-HI)*HIo';
    eq2=abs(CIo-CI)*CIo';
    eq3=(T10-T10a)/T10a*1000;
    eq4=(T20-T20a)/T20a*1000;
    eq5=(T50-T50a)/T50a*1000;
    eq6=(T90-T90a)/T90a*1000;
    G=abs(eq1)+abs(eq2)+abs(eq3)+abs(eq4)+abs(eq5)+abs(eq6);
end
```